

EP&S TECHNICAL NOTE 119

APPENDIX

G-2 Meeting (4 pages) 3/28/85
Danby/Jackson

Tactical Decision - (Prior to June)

① Set aside vertical injection and superconducting magnets until Proposal Draft work on "CERN-85" complete

② Priority to improvements that can be demonstrated "on paper" in next few months:
i.e. plausible but not experimentally verified.

examples

(i) reduce "ends" of magnet blocks

(ii) " " of coils

(iii) computed perturbations to Cern Fe? (small improvements)

(iv) Feedback from field monitoring to passive
XXXX
→ shimming (ferromagnetic).

(v) Feedback from field monitoring to
X.XXX
→ active shimming (currents).

③ "Cern 85": Magnet review and Cost Estimate

→ Principally MIT

(Complemented by BNL; CERN; others.)

④ NMR monitoring for feedback

principally Yale; Michigan; BNL; others.

● Principle Premise

① People will not (nor should) believe that a priori we can build magnet 10 → 20x more uniform than Cern.

② Cern stated, at their precision, $\frac{\Delta B}{B} \approx 1 \times 10^{-6}$; knowledge of field integrals for muons ~~the~~ major error was control of each

of 40 magnet blocks by NMR monitor feedback from one point

② Much more elaborate monitoring, affecting our ability both for feedback to field correction and our ability to calculate orbit fBds is principle means to large improvement

→ BNL approach

① To do computations (in collaboration with MIT & others) that throw light on required monitoring for given knowledge of field, and devise illustrative passive and active shimming.

⑤ To use above, in concert with magnet design and NMR monitor efforts, to do quantitative improvement for Proposal draft.

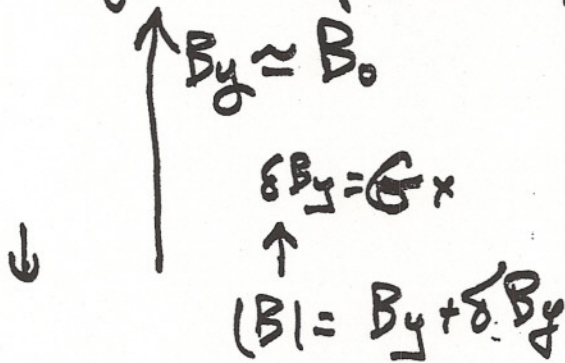
Example of Monitoring

4

- (1) NMR reads |B| only (scalar)
- (2) Cannot say anything about orientation.
- (3) However, normal & skew multipoles can be found from magnitude

Example Dipole B_y + quadrupole.

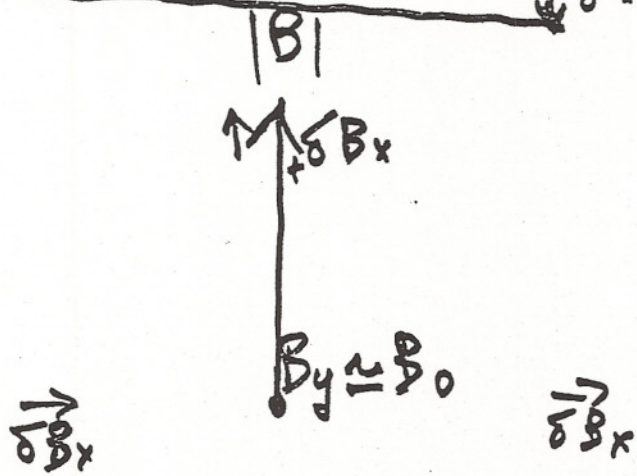
$$\begin{cases} \delta B_y = Gx \\ \delta B_x = Gy \\ \text{normal} \end{cases}$$



δB_x is negligible



$$\begin{cases} \delta B_y = Gy \\ \delta B_x = Gx \\ \text{skew} \end{cases}$$



(Reading the magnitude gives both quadrupole and dipole magnitude but not direction.

POISSON MAGNET CODE

+ ILLUSTRATIVE EXAMPLE OF

CERN $g-2$ RING MAGNET

G.T. DANBY

J.W. JACKSON

3/28/85

POISSON

GENERAL PURPOSE CODE (MAGNETOSTATIC)

TWO DIMENSIONAL (X, Y or R, θ)

FINITE PERMEABILITY (6 TABLES)

MESH OF IRREGULAR TRIANGLES

VARIABLE TRIANGULAR MESH WHICH SPECIFIE

GEOMETRY OF MAGNET

CDC	6000	PTS.
VAX	20000	"

MAY CONSIDER SYMMETRIC OR ASYMMETRIC

GEOMETRY (W. FRAME, C, H, ...)

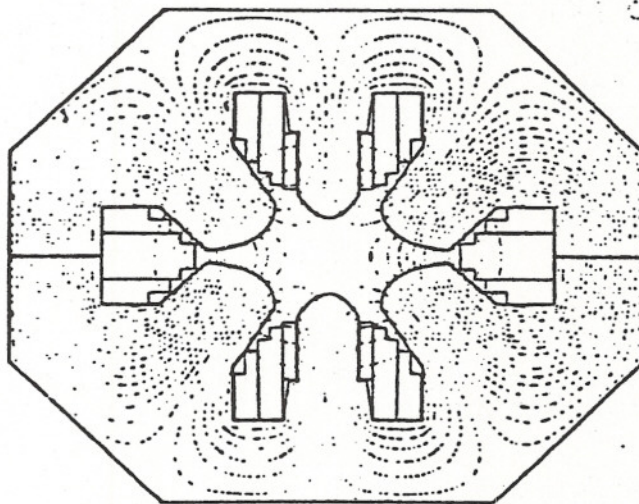
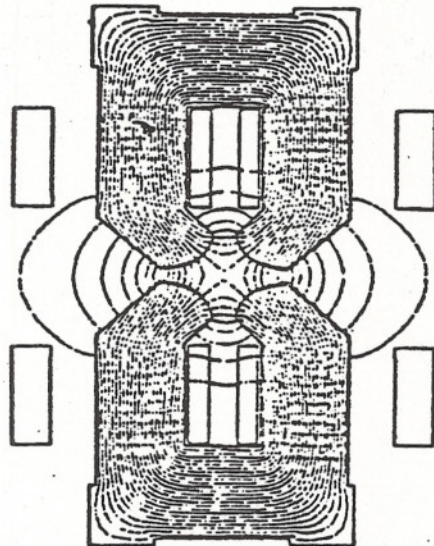


Figure 3. Outline and flux distribution of (top) Collins quadrupole and (bottom) sextupole magnet.

OUTPUT INCLUDES: VECTOR POTENTIAL, FIELDS,
FIELD GRADIENTS, ETC.

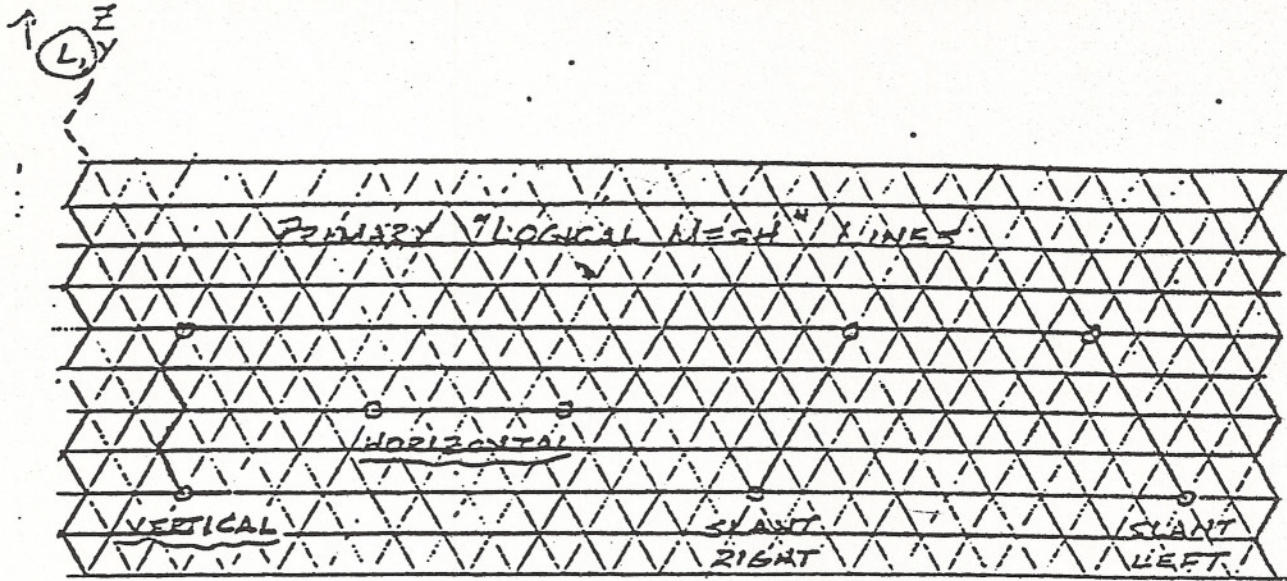
ALSO INCLUDES HARMONIC ANALYSIS OPTION

1.1 A LIST OF THE POISSON GROUP PROGRAMS AND THEIR FUNCTIONS

===

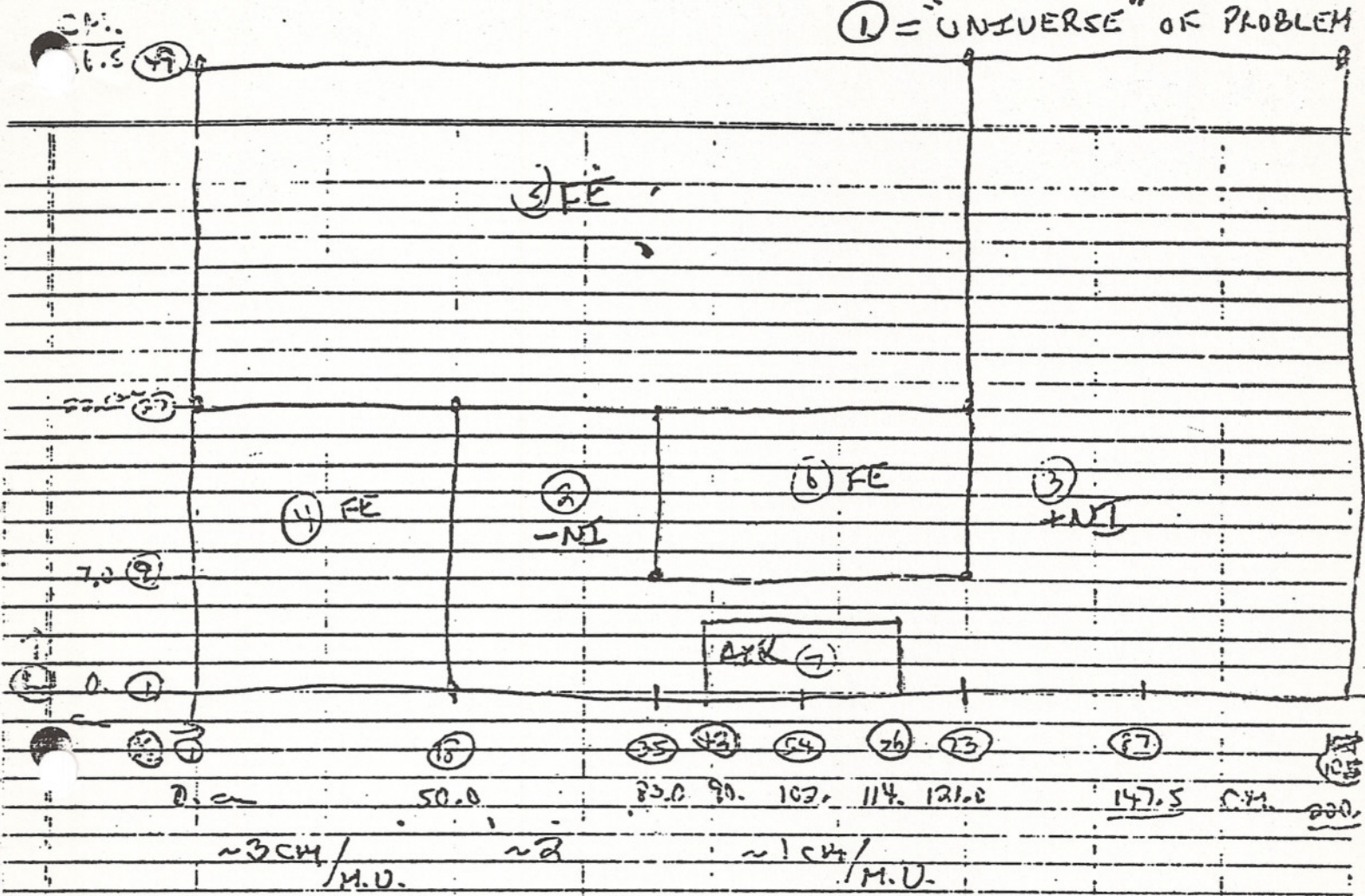
- (1) LATTICE - GENERATES AN IRREGULAR TRIANGULAR MESH FROM INPUT DATA FOR THE "LOGICAL" AND PHYSICAL COORDINATES DESCRIBING THE PROBLEM, CALCULATES POINT CURRENT TERMS IN REGIONS WITH DISTRIBUTED CURRENT DENSITY, SETS UP MESH, POINT RELAXATION ORDER, AND WRITES THE INFORMATION NEEDED TO SOLVE THE PROBLEM ON THE "TAPE35" FILE (DUMP NUMBER 0).
- (2) POISSON - SOLVES BY SUCCESSIVE POINT OVER-RELAXATION POISSON'S (OR LAPLACE'S) EQUATION FOR THE VECTOR (SCALAR) POTENTIAL, WITH NON-LINEAR IRON (DIAGNOSTIC) FOR TWO-DIMENSIONAL OR CYLINDRICAL PROBLEMS, CALCULATES THE DERIVATIVES OF THE POTENTIAL (FIELDS AND GRADIENTS), CALCULATES THE STORED ENERGY, AND PERFORMS HARMONIC (MULTIPOLE) ANALYSIS OF THE POTENTIAL.
- X(2A) DIRECT - SAME AS POISSON EXCEPT SOLVES BY A "DIRECT" METHOD, I.E. A DIRECT SOLUTION OF THE BLOCK TRIDIAGONAL SYSTEM OF DIFFERENCE EQUATIONS. WITH THIS PROGRAM "PERMANENT" MAGNET PROBLEMS MAY BE SOLVED.
- (4) (3) TEKPLOT - PLOTS PHYSICAL MESHES AND EQUIPOTENTIAL LINES.
- (3) (4) FORCE - CALCULATES FORCES AND TORQUES ON COILS AND IRON REGIONS FROM POISSON POTENTIAL SOLUTIONS.
- (5) AUTOMESH - PREPARES THE INPUT DATA FOR LATTICE FROM PHYSICAL GEOMETRY DATA DESCRIBING THE PROBLEM, I.E. CONSTRUCTS THE "LOGICAL" MESH AND GENERATES (X,Y) COORDINATE DATA FOR STRAIGHT LINES, ARCS OF CIRCLES, AND SEGMENTS OF HYPERBOLAS.
- (6) MIRT - OPTIMIZES POISSON PROBLEMS IN TERMS OF MINIMIZING FIELD ERRORS BY ADJUSTING POLE PROFILES, CURRENTS, COIL SHAPES, ETC.
- X(7) REFINE - RESOLVES ALL OR PART OF A POISSON PROBLEM WITH ONE HALF THE ORIGINAL MESH SPACING.
- (8) SUPERFISH - SOLVES FOR THE "TEM" RESONANT MODES (FUNDAMENTAL AND ALL HIGHER FREQUENCIES) INCLUDING FIELD DISTRIBUTIONS IN CYLINDRICALLY SYMMETRIC RADIO FREQUENCY CAVITIES.

EQUILATERAL TRIANGLE "LOGICAL" MESH



IT IS NECESSARY TO GIVE DATA FOR ONLY THE END POINTS "O" ALONG THESE LINES. INTERMEDIATE POINTS WILL THEN BE LINEARLY INTERPOLATED FOR (X, Y).

① = "UNIVERSE" OF PROBLEM



[5457]

DRUMM, ET AL. (NIMF, 1979)

ZONING

①

④
1115

②
-NI

⑥
FE

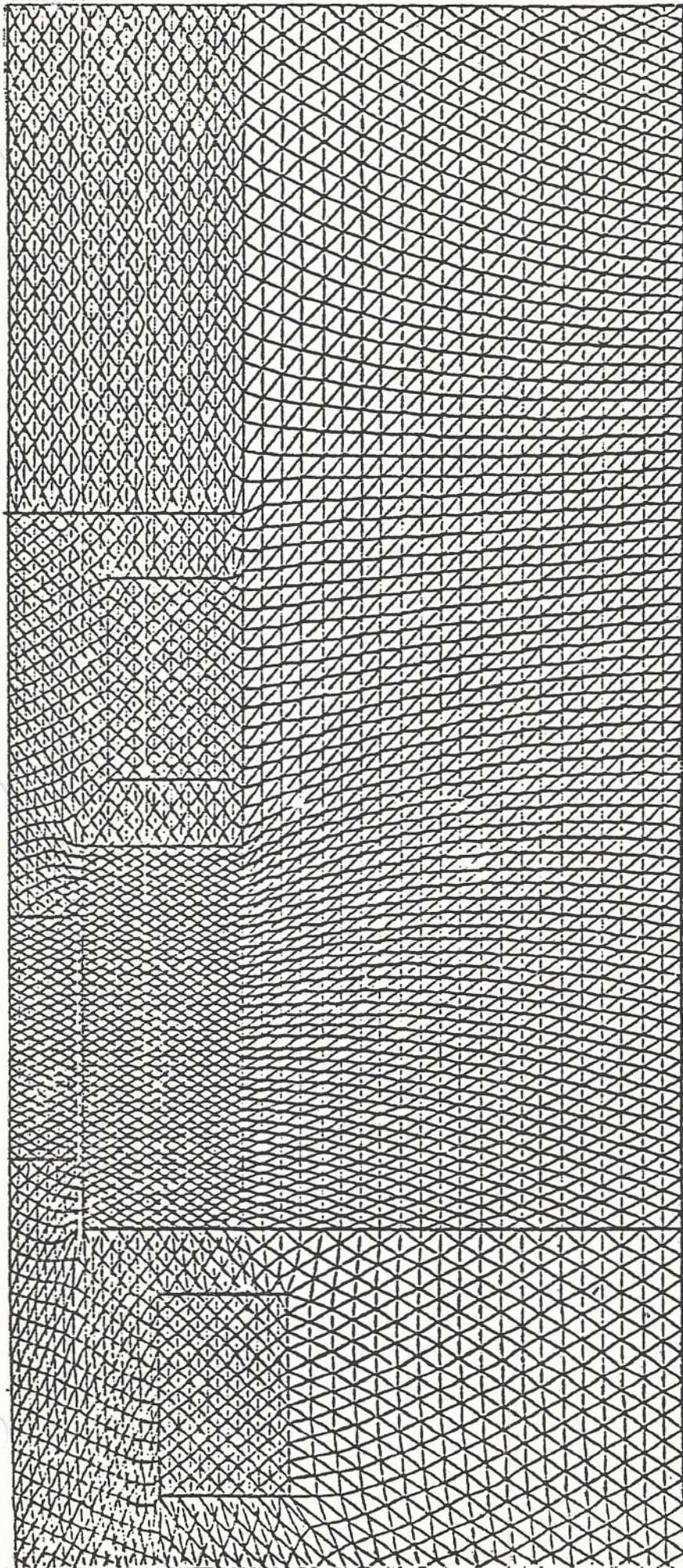
③
+NI

⑤
FE

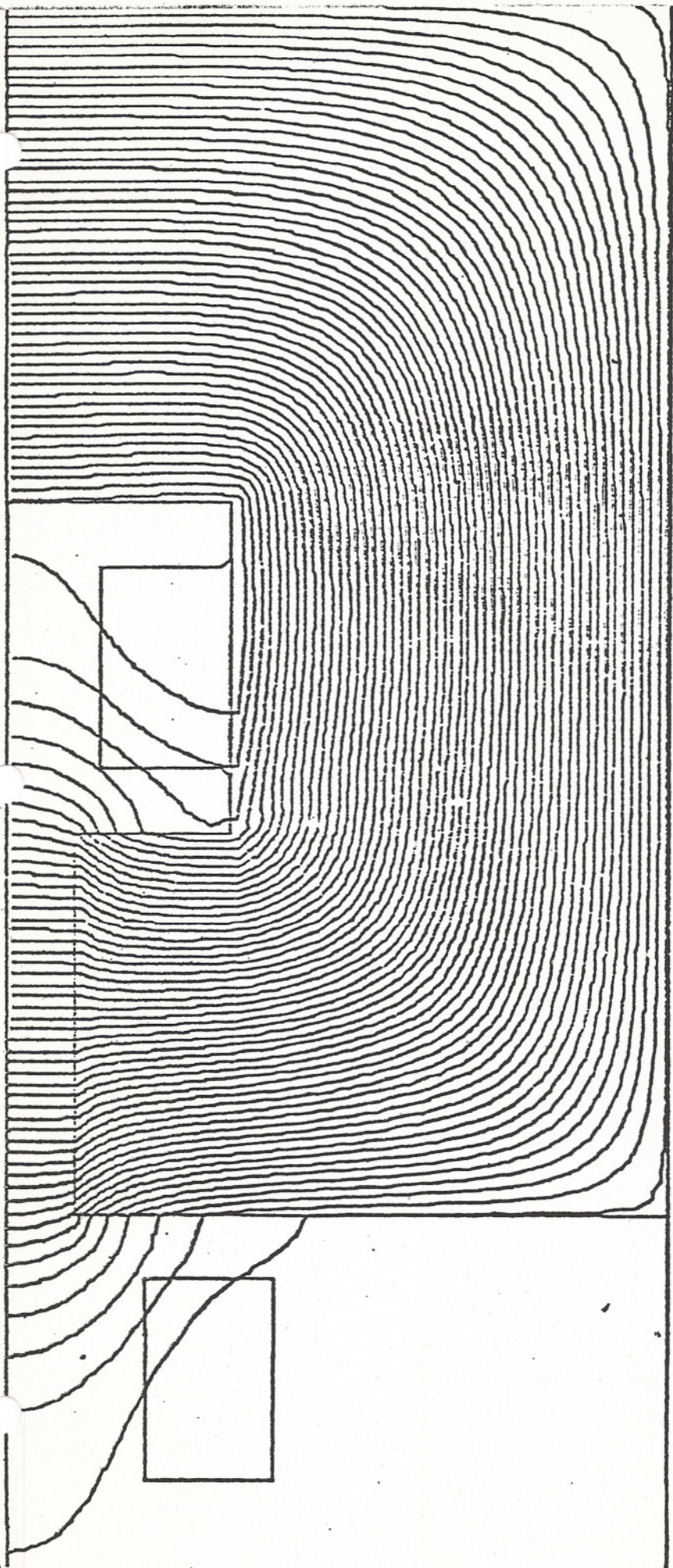
⑧

⑨

⑦
AIR



(2)



FIELD BUMPS / TOLERANCES

$$\mu = \infty$$

<u>B_N</u>	<u>(A)</u>	<u>(B)</u>	<u>(C)</u>	<u>(D)</u>
N= 0	17,053.	17,054.	17,054.	17,054. GAUSS
1	-.125	-.135	-.075	.000
2	-1.274	.027	.027	.026
3	-.143	-.153	-.103	-.040
4	-.543	-.004	-.005	-.005
5	.	.	.	-.000
6	.	.	.	-.013

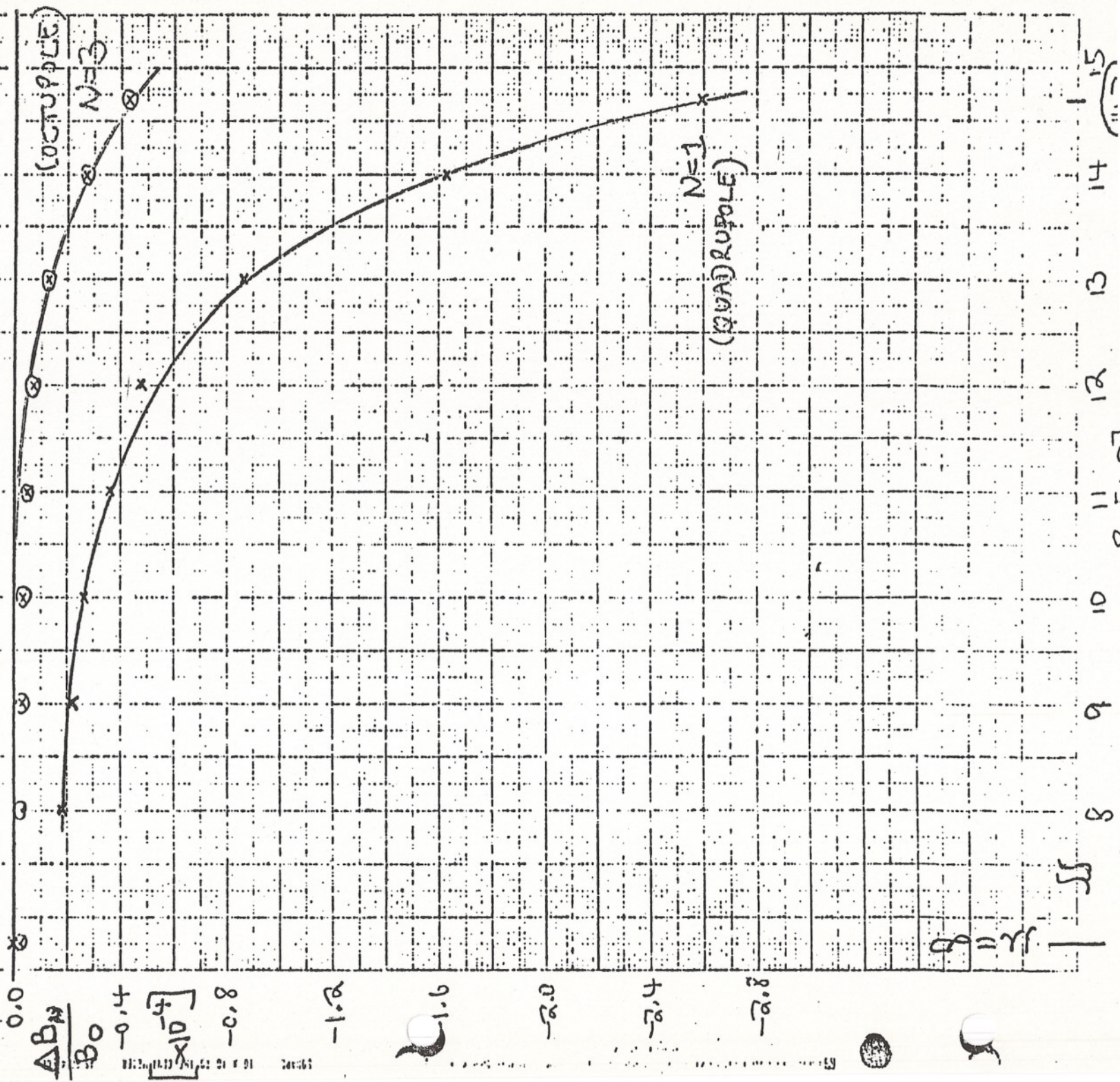
$$\frac{\Delta B}{B_0} = 1.9 \text{ PPM}$$

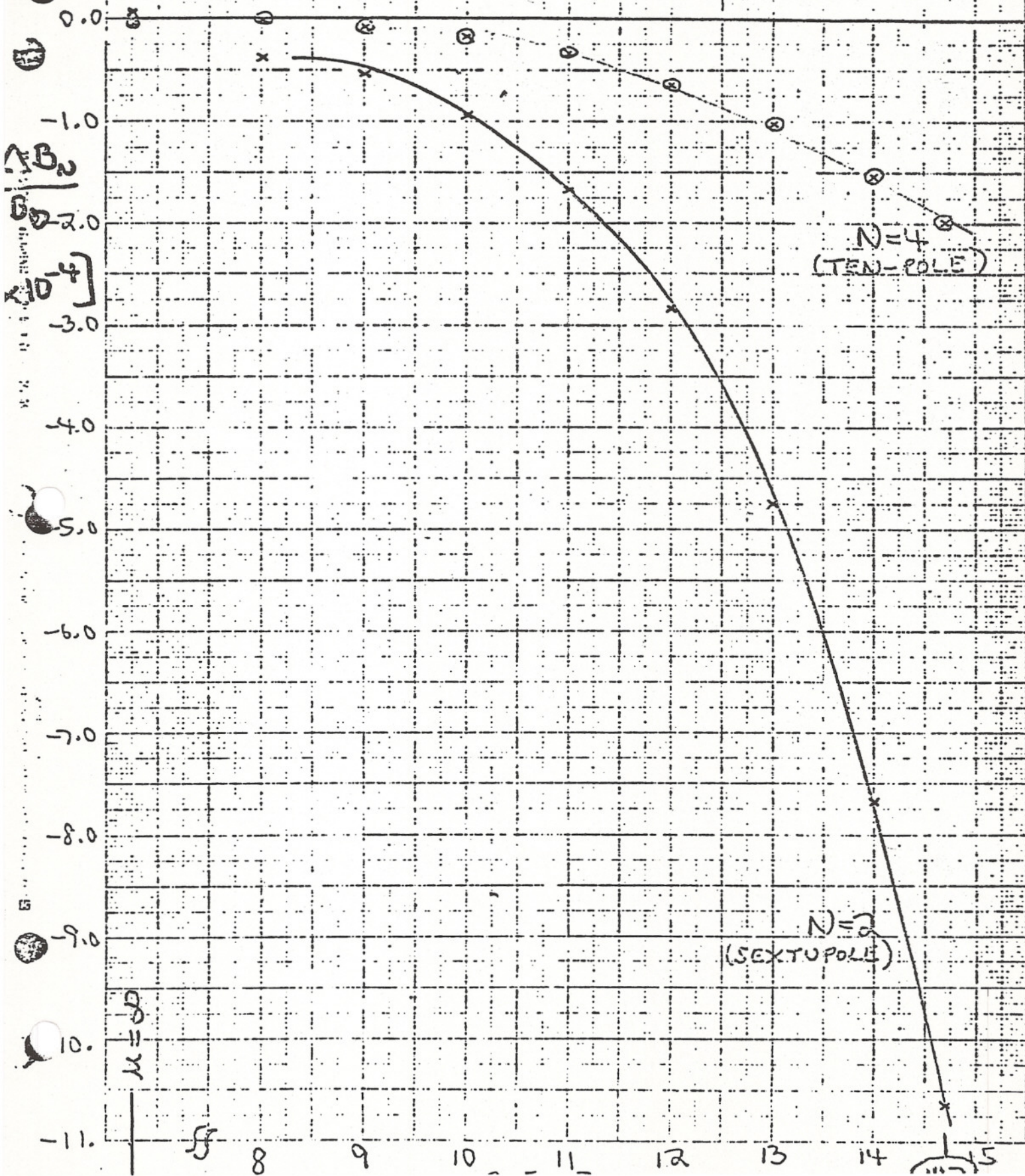
17 GAUSS = 1 PPM

- CASE (A) 2 BUMPS 3 CM x 0.4 CM
- (B) " 3 CM x 0.5 CM
- (C) " 3 CM x (0.5 ± .005) CM
- (D) " 3 CM x (0.5 ± .0125) CM

FIELDS EXPRESSED AT +5 CM FROM ϕ ON HMP (Y=0)

iii)





PERTURBATION STUDIES ON $g-2$ MAGNETS

G. T. Danby

J. W. Jackson

June 13, 1985

Perturbation Studies on G-2 Magnet

1. Parametric Study

For parametric study, the CERN magnet geometry was approximated as input to the POISSON Magnet Computation Code.

Figure 1 shows the basic cross section used.

Figure 2 shows the flux distribution in the air and in the iron.

The magnet was heavily impacted by saturation at $B_0 = 1.47T$. Since the magnet is only operated at a single field, bumps can be found for the basic pole face geometry, at that field, to produce the desired uniform field quality.

CERN has ground the pole faces to accomplish this level of field quality. Further grinding was done to correct for practical errors.

For our parametric purposes, saturation was changing the field shape too rapidly.

Simple single bumps at the outer edge of the plane poles were added to flatten the magnet field at low fields, $\mu = \infty$, (see Fig. 1).

Table 1 shows the computed multipoles expressed as ΔB in gauss at $x = +5$ cm on the HMP ($y=0$) for $\mu=\infty$. Column A is for 2(x2) identical bumps 3 cm wide x 0.4 cm high. Column B shows the effect of 2(x2) identical bumps 3 cm wide x 0.5 cm high.

Comparing columns A and B shows the value of the computations for perturbation calculations on the magnet. The 4-fold symmetric change from A to B should not effect the quadrupole ($N=1$) or octupole ($N=3$), only the allowed symmetry sextupole ($N=2$) and ten-pole ($N=4$) etc.

The calculations support this: the change in $N=1$ and $N=3$ are less than 1 PPM.

If one had chosen, a column B' could be linearly interpolated for even better flattening.

In column C, the average of the 4 bumps is identical to that in column B, so the symmetrical sextupole, etc., is exactly the same. However, the bumps at positive X farthest from flux return of the C-magnet) are 1% higher than in B, while the bumps at negative X are 1% lower. The quadrupole and octupole terms are reduced by this arbitrary change. The column D perturbation is a linear extrapolation of the change in ($N=1$) quadrupole produced by C. The extrapolation worked exactly. That is, column D computations give zero quadrupole, as predicted.

In practical application, precision measurements of actual magnets with NMR probes, for example, can be used, plus computed perturbations to find pole edge shims, etc.

2. Real Permeability

Figure 3 shows the effect of real permeability on the sextupole and the ten-pole term.

The geometry could be perturbed with pole face bumps etc. to make the terms zero at $B_0 = 1.47T$, and even to somewhat attenuate the very large slopes. However, the tolerances on steel properties, dimensions, etc., are inhibiting. Figure 4 shows the quadrupole and octupole. The same comments apply.

The goal is to perform the experiment with $\sim 10x$ greater accuracy than previously. From the above it was concluded that a greater ratio of pole width to pole gap is desirable, for $B_0 = 1.47T$, and generally lower B in the iron return as well as a broader interface between blocks 5 and 6 (pole material) in Fig. 1.

When the final magnet geometry is precisely defined, the perturbation analysis will be repeated for real permeability at B_0 , considering all orders and without reflection symmetry on the HMP.

3. 3D versus 2D Calculations

In preparation for the 1984 g-2 Summer Study, calculations were made on a $B_0 = 5T$ air core magnet, and on tolerances on coil locations.

The differences between theoretical solutions in cylindrical coordinates, centered at the center of the g-2 ring, and a 2D local expansion where $(x,y) = (0,0)$ is the center of the beam pipe, appears in low order terms.

We found it much easier to perturb in 2 dimensions, compute the 2D to 3D transformations, and then test the results with actual 3D computer calculations. The hardest part of the problem is high moments with a high power of (r,θ) . These are local in their origins, thus less 3 dimensional.

This approach will also be used on the actual $B = 1.5T$ iron poled magnet. The significant impact of the $\rho = 700$ cm radius of the ring is on practical questions. There are no theoretical difficulties relating to applying field perturbations to improve magnet uniformity.

4. Exercises on Geometrical Tolerances and Possible Fe Shimming

Figure 5 shows the effect of air between blocks 5 and 6 (see Fig. 1).

One possibility for the new magnets is to fabricate blocks 4 and 5 with conventional magnet tolerances and with conservative dimensions (lower yoke fields) and "no ends". Block 6 is the unconventional portion most highly sensitive to magnetic and mechanical tolerances.

Tolerances on dimension changes due to errors or possibly by adjustable shimming are explored.

$$b_n \equiv \frac{B_n}{B_0} \text{ at } x = +5, y = 0 \text{ cm.}$$

Figure 5 shows the effect of increasing the magnet half gap by 0.25 cm and 0.50 cm.

Figure 6 shows the multipoles produced by introducing "air" (or non-ferrous structural material) between block 6 and top plate 5.

For example, 0.25 cm of "air" means that 0.25 cm of Fe is removed from the top of block 6.

Note that the sextupole slope is opposite in sign and roughly equal in amplitude for the two perturbations in Figs. 5 and 6.

It is noted that all these perturbations are calculated for fixed ampere turns, chosen to give $B = 1.2T$ in the base magnet with a real permeability table used.

It was judged that the final magnet with its wider pole will roughly behave similarly at $B_0 \approx 1.47T$.

Table 2 gives the calculated field multipoles at $X = 5 \text{ cm}$, $y=0$ for the base magnet with $\text{gap}/2 = 7 \text{ cm}$, and also with $\text{gap}/2 = 7.25$ and 7.50 cm .

Note that this is done without bumps to flatten the base field. The purpose is to demonstrate differences due to gap changes. This is the same information shown in Fig. 5.

Table 3 gives the calculated differences due to "air" between blocks 5 and 6. This is the same information shown in Fig. 6.

In a further study, a standard gap of 0.25 cm was established at the top of pole block 6.

This region divided into 4 quarters which were either "air" or Fe in various combinations as shown in Fig. 7.

Table 4 lists the differences generated by various combinations of Fe shims in the 0.25 cm "air" gap.

Table 2, 3, 4 are very useful in established tolerances on construction parameters, and open up the possibility for additional shimming techniques.

Once the final magnet is established, the edges of the pole will be perturbed with Fe pole bumps to make it theoretically flat at $B_0 = 1.47T$.

Table 5 shows the difference effect for the present 3 cm wide x 0.5 cm high at $B_0 = 1.22T$. This is illustrative of a perturbation, even as far away as the edges of the pole. Note that $N=6$ (and higher) allowed terms must be considered at a level of $>10^{-2}$ of the sextupole ($N=2$).

More complex bumps will be used to reduce all moments theoretically.

Also shown in Table 5 is an (extrapolated) change in the bump of .05 mm, expressed in PPM.

This shows that careful construction tolerances should produce only low order terms "on paper."

The thickness of the vertical yoke member [block 4, Fig. 1] was varied for real permeability at $B = 1.22T$ and showed essentially only changes in dipole field. The changes were 6 gauss for 1 cm reduction and 13 gauss for a 2 cm reduction in the vertical yoke.

The dipole field, if uniformly changed by 1×10^{-4} parts, would move the average radius of the stored beam ρ_0 by 0.7 mm.

5. Current Shimming

Variations of the g-2 ring precision field with time, cycling, external world perturbations, etc., will in the end be easiest handled with pole-face windings.

These can generate all magnetic moments and can correct if necessary in closed loop operation, instructed by a very large network of precision measurement data.

However, pole-face windings, like magnetic or dimensional irregularities in the pole faces, are close enough to the beam that one would like to keep perturbation by currents small.

Experiments can establish the extent of "shimming" by slight changes of dimensions or additions or deletion of ferromagnetic material to minimize coil current requirements.

FIG. 1

--- CENTER OF g-2 KIN
→ $\rho = 700$ CM

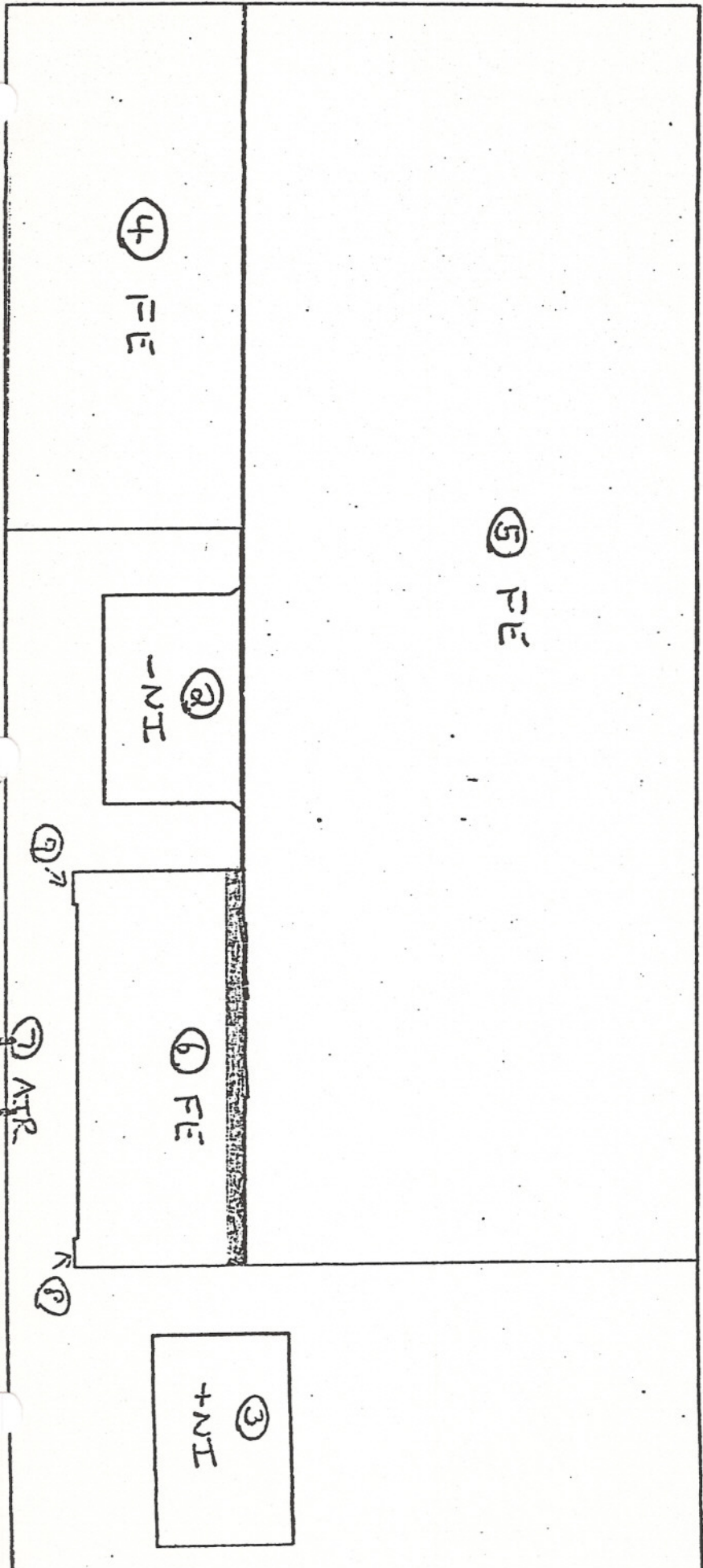
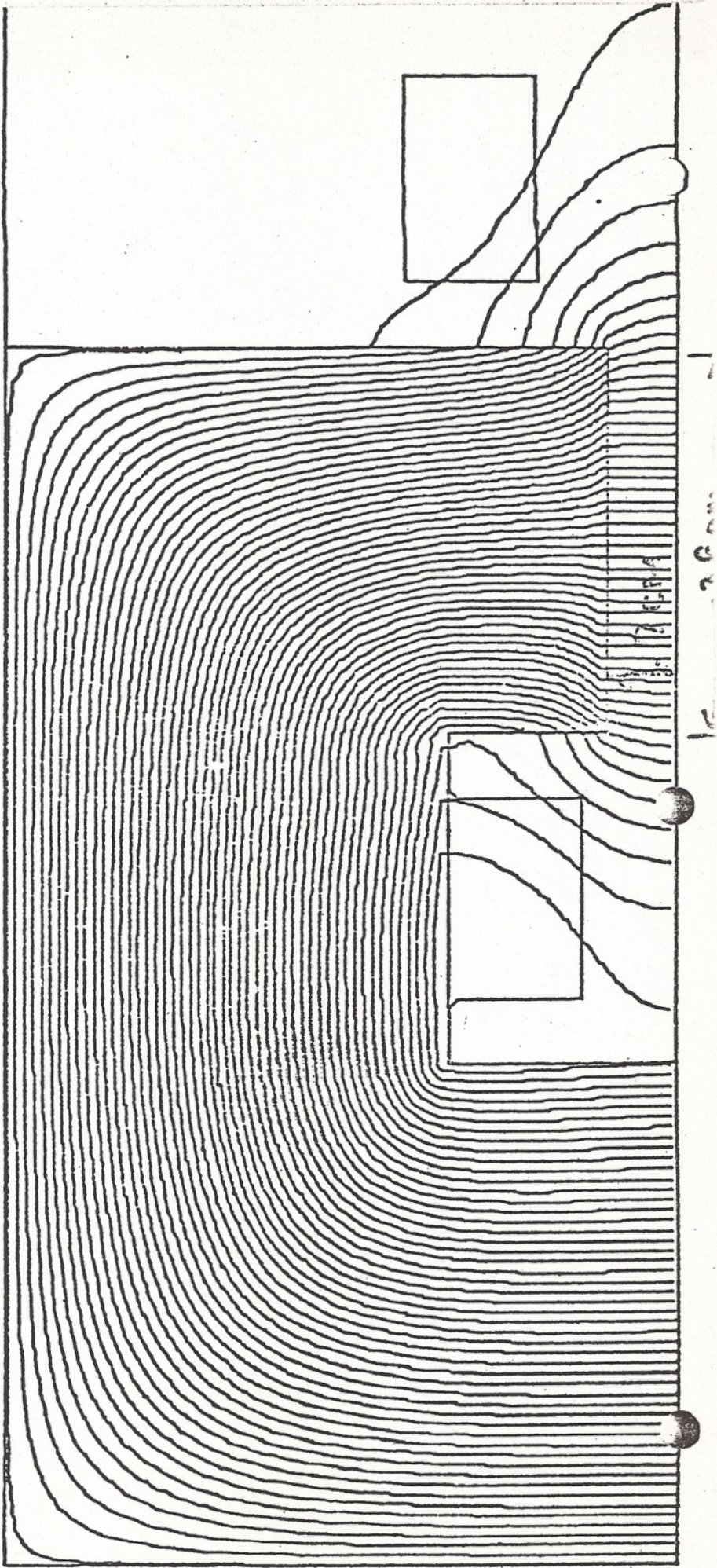


FIG. 2



FIELD BUMPS / TOLERANCES

$$\mu = \infty$$

TABLE 1

B_N	(A)	(B)	(C)	(D)
N = 0	17,053.	17,054.	17,054.	17,054. GAUSS
1	-.125	-.135	-.075	.000
2	-1.274	.027	.027	.026
3	-.143	-.153	-.103	-.040
4	-.543	-.004	-.005	-.005
5	.	.	.	-.000
6	.	.	.	-.013

$$\frac{\Delta B}{B_0} = 1.9 \text{ PPM}$$

0.17 GAUSS = 1 PPM

- CASE (A) 2 BUMPS 3 CM x 0.4 CM
- (B) " 3 CM x 0.5 CM
- (C) " 3 CM x (0.5 ± .005) CM
- (D) " 3 CM x (0.5 ± .0125) CM

FIELDS EXPRESSED AT +5 CM FROM Φ ON HMF (Y=0)

FIG. 3

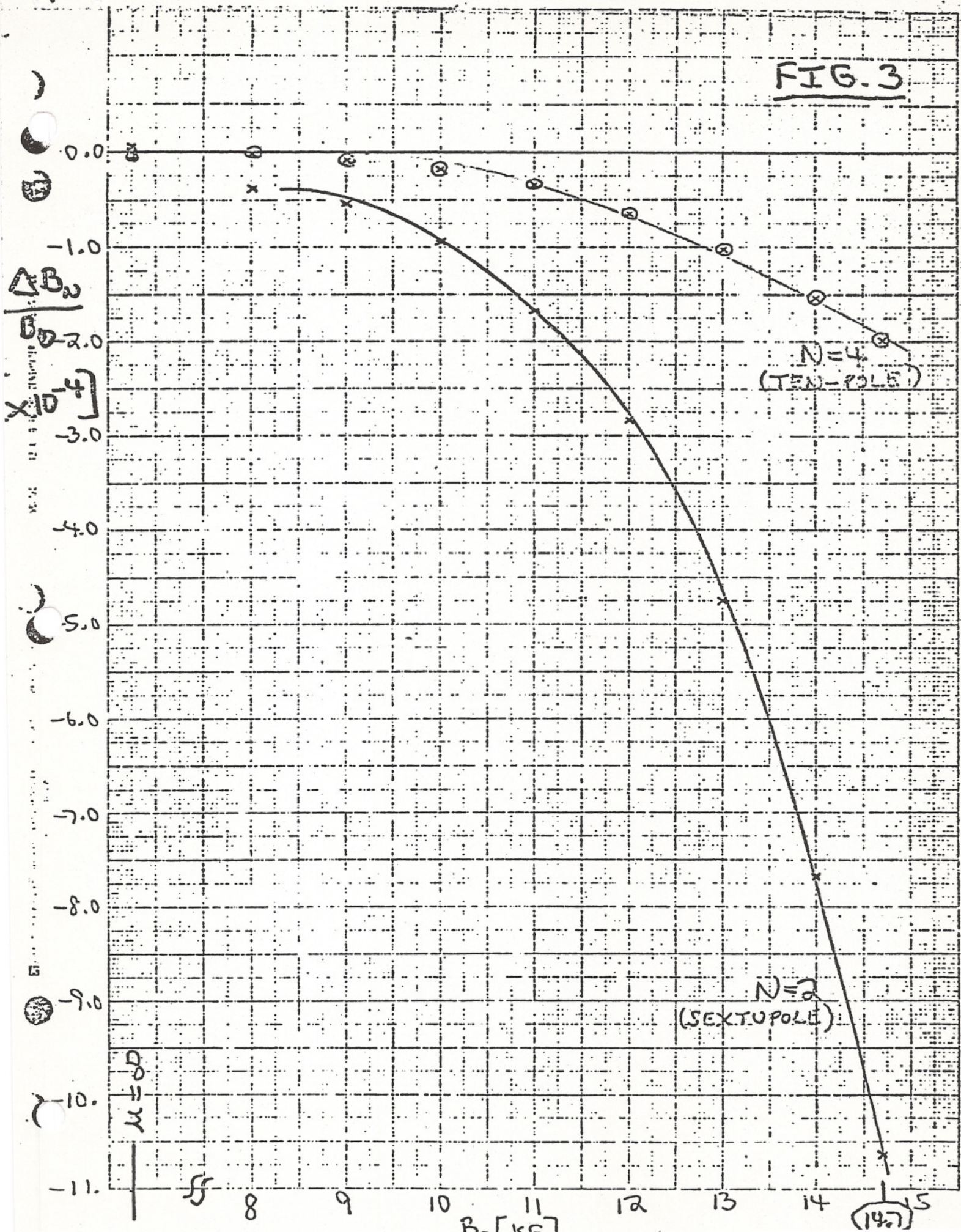


FIG. 4

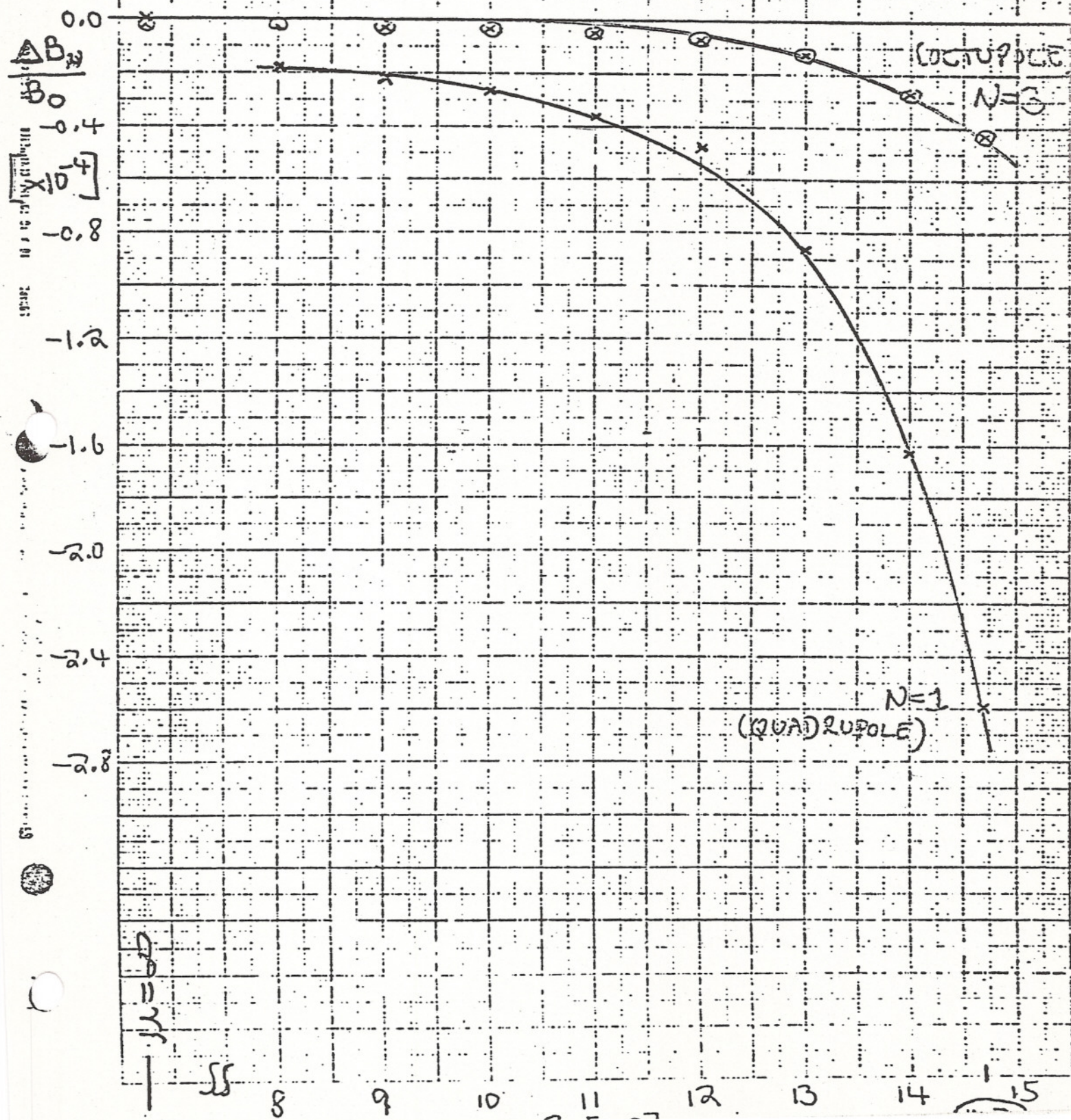
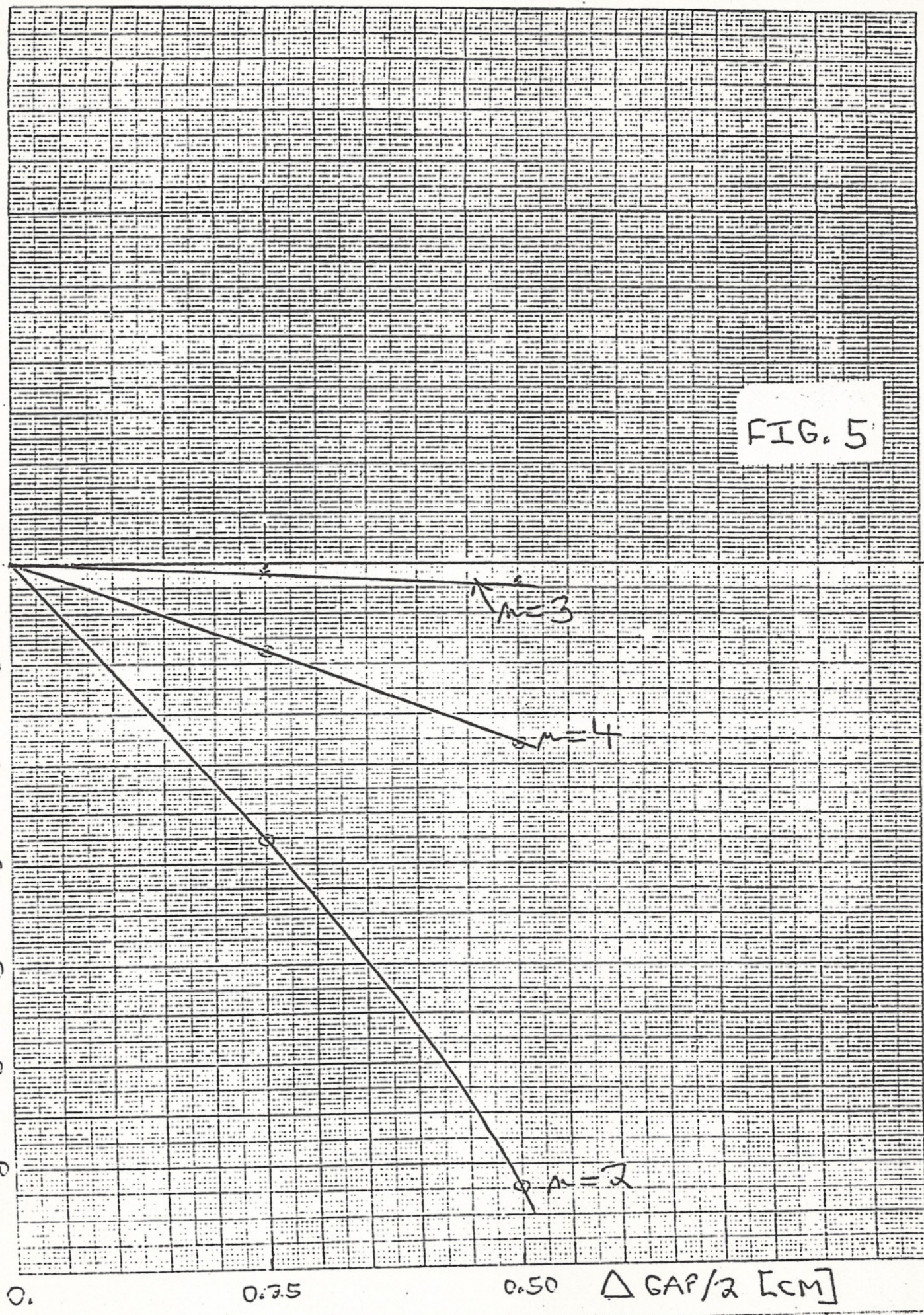


FIG. 5



0 0.5 1.0 ΔT_{AIR} [CM]

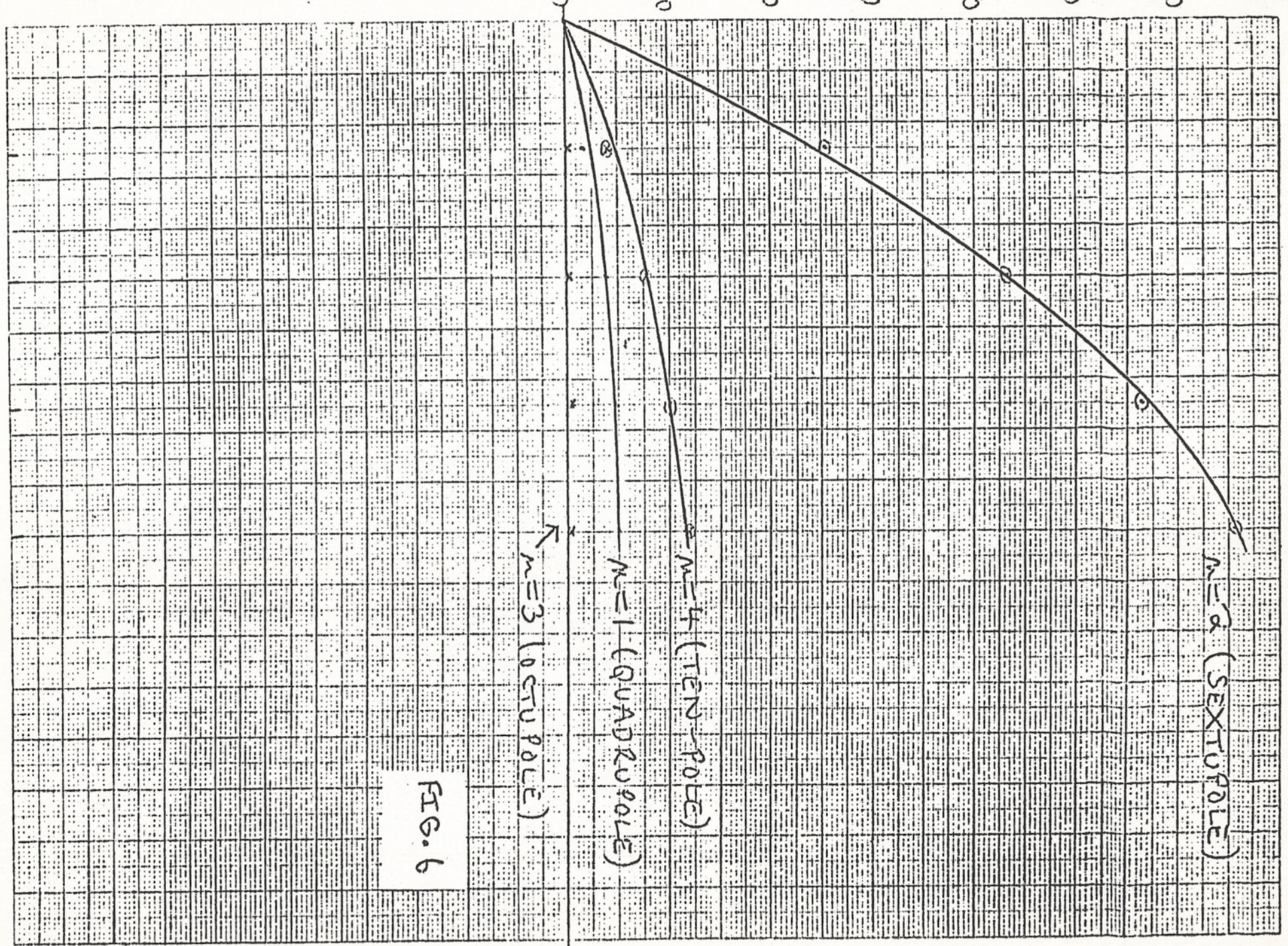


FIG. 6

$\delta - m$
[PPM]
130
100

$m=2$ (SEXTUPOLE)
 $m=4$ (TENU-POLE)
 $m=3$ (OCTUPOLE)

EFFECT OF CHANGES IN VERTICAL GAP

$\Delta \text{GAP}/2$ [CM] \rightarrow

b_m	0^*	$1/4$	$1/2$	
$m = 0$	0	-364.44	-716.09 GAUSS	
1	0	-1.0	-3.9 PPM	
2	0	-55.1	-124.5	↓
3	0	-2.1	-4.3	
4	0	-17.6	-36.2	
5	0	-0.5	-0.9	
6	0	-1.3	-2.4	

* = REFERENCE CASE

TABLE 2

EFFECT OF VARIOUS THICKNESSES OF "AIR"

t_{AIR} [CM] →

	0*	1/4	1/2	3/4	1	
$n = 0$	0	473.35	920.54	1335.6	1720.0	GAUS
1	0	3.6	7.3	9.6	10.1	PPM
2	0	50.8	87.1	112.8	131.3	↓
3	0	0.7	0.6	0.8	0.6	
4	0	7.9	15.4	20.1	23.5	
5	0	-0.9	-0.8	-0.9	-1.2	
6	0	0.4	1.3	1.8	2.2	

* = REFERENCE CASE

TABLE 3

SKETCH OF VARIOUS "AIR"/FE ARRANGEMENTS

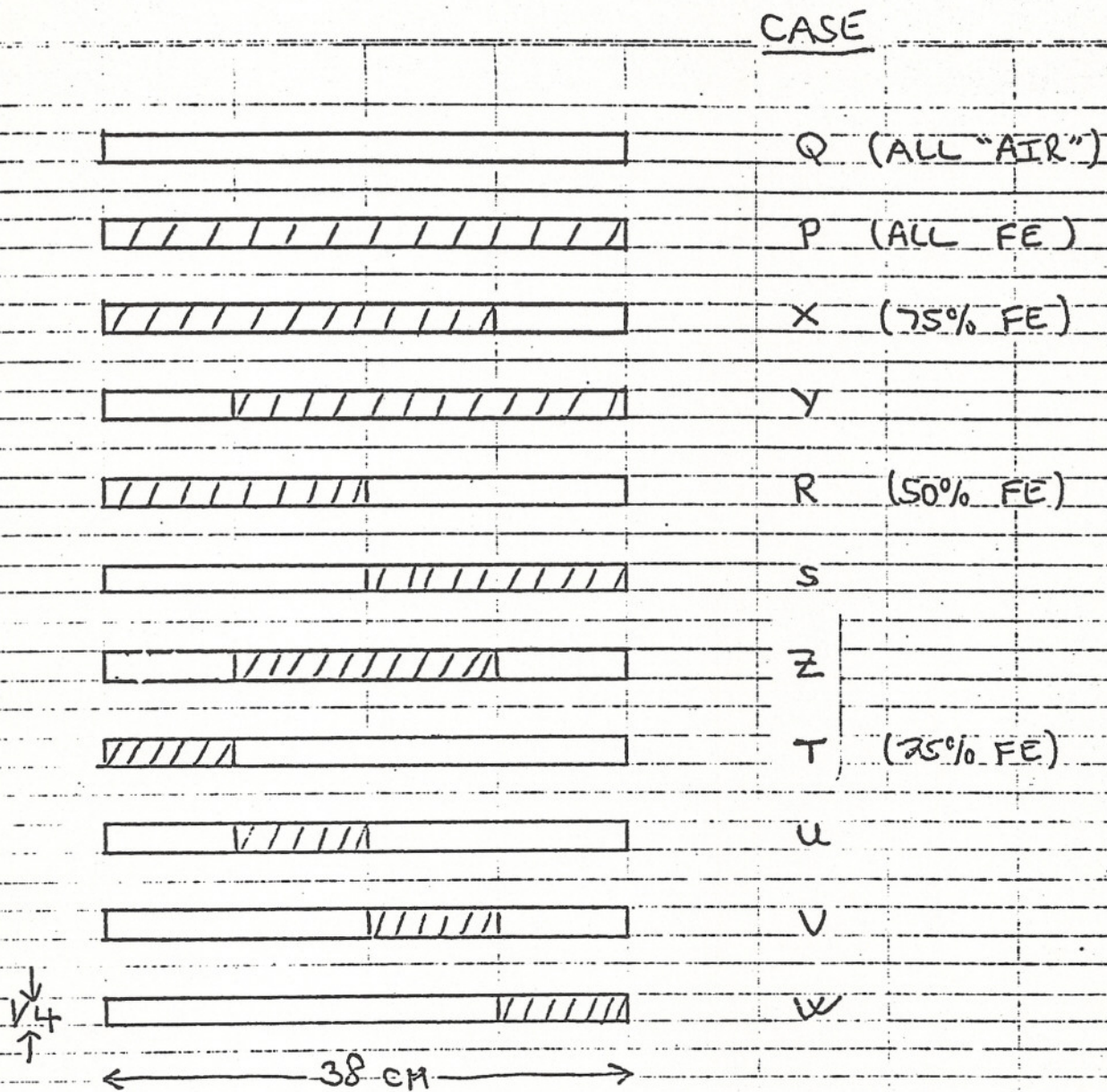


FIG. 7

EFFECT OF VARIOUS "AIR"/FE SHIM COMBINATIONS

TABLE 4

<u>l_m</u>	<u>P-Q</u>	<u>X-Q</u>	<u>Y-Q</u>		
$n = 0$	473.69	299.79	294.97	GAUSS	
1	-4.3	-162.1	100.3	PPM	
2	-50.3	-32.6	-29.1	↓	
3	0.1	3.9	-0.4		
4	-7.9	-2.4	-4.3		
5	0.3	0.5	-0.5		
6	-0.7	-0.7	-0.5		
	<u>R-Q</u>	<u>S-Q</u>	<u>Z-Q</u>		
$n = 0$	151.07	151.92		GAUSS	
1	-103.9	81.9		PPM	
2	-11.4	-11.0		↓	
3	1.1	-0.1			
4	-1.2	-2.1			
5	0.3	-0.5			
6	-0.4	-0.3			
	<u>T-Q</u>	<u>U-Q</u>	<u>V-Q</u>	<u>W-Q</u>	
$n = 0$	59.158	69.968	68.987	62.728	GAUSS
1	-41.7	-29.8	9.3	38.0	PPM
2	-4.4	-7.4	-7.1	-4.0	↓
3	0.3	-0.4	-0.7	-0.4	
4	-0.4	-0.6	-0.6	-0.7	
5	0.1	-0.4	-0.5	-0.4	
6	-0.2	-0.2	-0.1	-0.1	

EFFECT & TOLERANCE OF SYMMETRICAL FE POLE BUMP REAL PERMEABILITY

<u>l_m</u>	<u>EFFECT</u>	<u>.002"</u> <u>TOLERANCE</u>	
$n = 0$	-28.0	-0.28	GAUSS
1	-0.9	0.0	PPM
2	208.2	2.1	↓
3	1.8	0.0	
4	94.0	0.9	
5	0.8	0.0	
6	15.8	0.2	

TABLE 5

Magnet Field Correction and Shimming

G.T. Danby and J.W. Jackson

Introduction

A. How will the new G-2 experiment achieve an order of magnitude greater accuracy than the last CERN experiment on which it is based? The basic magnet design will incorporate several improvements.

1. The magnet is continuous in azimuth. This eliminates the 40 "ends" which were a dominant field error in the original experiment.
2. The magnet pole gap will be increased from 14 cm to 18 cm. The fundamental reason for the larger magnet is to allow space for very elaborate "in vivo" magnetic measurements and correction feedback as required.

The CERN experiment performed complete field measurements only between physics runs. During physics data taping, representative monitors were used to give field measurements sufficient for their required accuracy.

Strictly speaking, it is knowledge of the integrated magnetic field per revolution of the orbiting particles that is required to a few parts in 10^7 accuracy. The earlier experiment stopped at the point where $\Delta B/B_0$ errors were small compared to statistical errors.

NMR measuring probes can give the required precision. The greater the uniformity of the magnetic field, the smaller number of effectively simultaneous magnetic measurement data points are required. The precision of location of the position of a data point is eased.

The goals are to control the field to a few parts in 10^6 , and then to compute the last factor of ten. Both these goals will require the more elaborate measurement matrix planned during physics data taking. This is herein called "in vivo" measurement. This will also be used for feedback of magnet control.

3. An auxiliary benefit of the larger magnet gap is that the beam will be kept further from the pole surfaces. This will directly aid magnetic field uniformity.
4. The ratio of pole width to gap height will be made larger than in the original experiment. This will reduce somewhat the field enhancement in the poles due to the pole edge fringing flux, thus raising the permeability in the pole pieces.

In addition, wider poles place the pole edges further from the beam, thereby easing tolerances.

B. How is an improvement of two orders of magnitude in field uniformity to be achieved, as compared to conventional beam quality magnets with $\Delta B/B_0$ ($\sim 10^{-4}$)?

1. The idealized "paper" magnet is cylindrically symmetric designed with the aid of computer codes to give the required uniform field at $B_0 = 1.47T$. Figure 1 shows the cross section.
2. Bumps located at the edges of the plane parallel poles (designated by numbers 8 and 9 in Fig. 1) are designed with the aid of the computer so that they compensate for the finite pole width producing the required uniformity of field over the "good field" aperture occupied by the beam.

3. In detail, the geometry of bumps 8 and 9 are required to be slightly different. This compensates for the C-magnets asymmetry produced by having all the magnet flux return to the outside. This magnetic asymmetry is required to present an open mid-plane for muon counters.
4. Even the magnet idealized to have perfect cylindrical symmetry on the inside radius is subjected to field errors compared to computed prediction. For example, the geometry of the iron or of the coils may be different due to forces (the magnetization properties of the steel may be different from those assumed or the completed turns). The calculations themselves cannot be assumed to converge to a 1×10^{-6} absolute accuracy.

It is demonstrated, however, that perturbations can be computed for small differences and can be performed to define with confidence to the desired accuracy.

Measurements of the actual field errors in the x,y plane (see Fig. 1) will reveal the differences from the computed field. The computed perturbations will be added to cancel these errors. This is much easier and more accurate than totally empirical shimming experiments.

5. Finally, the real magnet will not be cylindrically symmetric. No practical computer codes exist to handle this part of the problem with the necessary precision.
6. The flux in the magnet aperture is directly proportional to the magnet reluctance. This is dominated by the magnet air gap. (Region 7 in Fig. 1.) The poles will be surface ground so that they are planar, parallel and equidistant to tolerance errors $\sim 10\times$ smaller than typical machining tolerances.

7. The reluctance of the iron will also contribute significantly to field errors, (see Fig. 2). Maximum uniformity produced in the pole pieces will be obtained by using Fe processed and corrected for homogenous magnetization. (Fig. 1, Block 6). The pole pieces are by far the most critical Fe members.
 - (i) The flux density is highest, resulting in lower permeability and greater sensitivity to variations in magnetization properties.
 - (ii) Being close to the beam, Fe variations not only can change the central field $B_0(z)$ but can generate higher derivatives (moments) in the field.
8. The massive flux return members are much more remote. These effect essentially only the dipole field. $B_0(z)$. Their cross sections can be empirically adjusted by adding or subtracting steel to give uniform Fe reluctance around the circle. After this is done residual $B_0(z)$ errors are gap determined. These variations of are short wavelength in the z direction (< 1 meter).
9. Localized field errors will be corrected locally to the necessary accuracy or by adding on ferromagnetic material, or by the use of the pole face coils.
10. These pole face correcting techniques might in fact be used to do the entire shimming job. However to obtain ultimate precision there is great advantage attained in correcting for remotely caused, long wavelength variations by the use of remote corrections. If both the cause of the error and the

corrections are remote from the pole face lower order, field variations with small azimuthal and transverse derivatives are produced. The better the field quality before local corrections are used, the better result is to be expected.

11. Finally, the circumference will be divided into 50 azimuthal zones which will have current control of dipole, quadrupole, sextupole, octupole and 10 pole field corrections. This zone is 0.88 m long. The average within each zone will be corrected. The variations in field due to small "pot holes" etc. will be analytically integrated over the 88 cm.
12. The correcting coils will correct both for reproducible short wavelength effects and for dynamical variation such as cyclic changes, environmentally induced, time dependent effects, etc.

Computed Field

The magnet cross section is shown in Fig. 1. This geometry is computed with the program POISSON. A representative low carbon steel permeability table is used. Computations are made in two dimensions (2D). The computations define the geometry of the bumps on the pole edges to effectively make the poles appear infinitely wide, as seen from the beam location, at $B = 1.47T$.

1. The 2D version of the program has a subroutine which fits the computed field very accurately to a multipole expansion description of the field. This is a very powerful, accurate way to calculate perturbations of the field. The tactic used in flattening the field is first to flatten the field in 2 dimensions. This pole profile cross section is then used for the 3D calculations. The transformation from a true 3D

cylindrical expansion of the magnetic potential and a 2D multipole approximation at any azimuth is straightforward. The difference involves low order terms in the field expansion. These deviations between 3D and 2D are removed by iteration, using 2D perturbations of equal amplitude and opposite sign (i.e. the deviation in 3D is corrected by a 2D iteration of the geometry until the calculated 3D field is uniform.

2. During the 1984 G-2 Summer Study an analysis of tolerances on a $B = 5T$ air core design was performed. The above 2D to 3D perturbation technique worked very straightforwardly, even with a 3 times smaller radius of curvature. For the present $B = 1.47T$ design the impact of $\rho = 700$ cm is quite small and straightforward to apply. This simply says that the impact on the field at a given point is dominated by nearby mechanical and magnetic imperfections (which is the hardest part of the shimming problem). The effect of the radius of curvature is systematic and non-local.
3. The accuracy of the "POISSON" Code for magnetic field calculation and analysis is illustrated in Appendix I.

The fields were generated for various small perturbations to the pole surface. These were fit to multipole expansions and used to extrapolate to uniform field with high precision ($\frac{\rho \Delta B}{B_0} \sim 1 \times 10^{-6}$).

4. The effect of real μ on the G-2 magnet is very large. Using a typical low carbon steel μ table, the dipole saturation calculated for the magnet geometry is shown in Fig. 2. Note that the central field is 10% less than for $\mu = \infty$ at $B = 1.47T$. This means the ampere turns (NI) required are more than 10% larger than for $\mu = \infty$.

5. The major significance is not the higher NI, but the impact on iron magnetization tolerances. The choice of $B_0 = 1.47T$ is arbitrary. It corresponds to the CERN field exactly.

From other computations, it is known that about one half of the 10% saturation induced increase in reluctance comes in the pole pieces themselves. They carry close to $B = 2T$, in order to provide the fringing flux. Figure 3 illustrates flux concentration in the poles.

6. Figure 4 shows the sextupole ($N=2$) and 10-pole ($N=4$) effects of saturation. Note that in this case the very large saturation effect is almost entirely due to the pole region, not due to the saturation in the remote flux return.
7. The pole edge bumps are modified to move the zero crossing on Fig. 4 to the operating field. However, tolerances on reluctance due to steel magnetization will result in variations at the operating field, particularly in sextupole.
8. Figure 5 shows the left-right asymmetry (quadrupole series) due to saturation. The same remarks apply as for the sextupole series shown in Fig. 4.

In summation, even assuming idealized cylindrical symmetry is maintained, the permeability as well as the geometry of the pole pieces strongly influence both the dipole field B_0 and the transverse field shape, or "multipole" content. As will be seen in the tolerance discussion, the more massive, remote flux return members essentially effect only the central field B_0 .

C. Dipole Tolerances and Initial Shimming

Strictly speaking, the tolerances on the absolute dipole field are not too tight. A change in the average field of 1×10^{-4} would result in

0.7 mm shift in the radius of curvature. This is small compared to the momentum acceptance. Similarly, a cylindrically symmetric tilt of the magnet midplane producing a uniform horizontal field B would be compensated by the electrostatic quadrupoles.

In practical terms, this is of little benefit to shimming the real magnet, which is not cylindrically symmetric.

Variations in the magnitude and direction (twist) of the field at the central orbit as a function of z will result in field derivatives in the transverse plane (x,y). Since $\text{div } B=0$ applies over any elemental volume, the spatial derivative should be small in all directions from a field reference point.

1. The variation in central field at the nominal orbit center, B_0 , around the azimuth of the ring will consist of long wave length components and short wave length, or local variations.
2. Long wave length is defined as greater than the pole width.
3. Long wave length tolerances can be explored with the POISSON calculations.

Table 2 shows the effects of very large changes in the thickness of the return flux iron. Column **II** shows the effect of a 4% reduction in width of the midplane flux return piece (Block 4 in Fig. 1).

This very large change in cross section causes a 0.1% drop (1000 PPM) in the dipole field. All other field moments are unchanged to < 1 PPM.

Column III shows a 4.65% reduction in the thickness of the top and bottom pole pieces (Block 5 in Fig. 1). Note that with a 0.426% change in the dipole field, the only significant multipole is the sextupole with 5.6 PPM.

4. The effect of steel magnetization tolerances will be small compared to these above perturbations, even with routine magnet construction materials.
5. The first shimming operation will be to reduce the long wavelength $B_0(z)$ variations to a level \leq the design mechanical tolerances of the pole pieces, by adjusting the reluctance of the return yokes.
6. This can be performed either by adding steel to the periphery, or by inserting steel in tuning holes drilled in the returns.
7. Measurements at a low field as well as at operating field with separate geometric reluctance variations from steel variations to the extent that magnetic forces are cylindrically symmetric in their resultant strain on the structure.
8. After the returns are tuned to give cylindrically symmetric reluctance, the field problems are concentrated on the pole regions and short wave lengths.
9. The best uniformity pole piece materials that are economically practical will be used.
10. The surface grinding of the pole faces of the 18 cm height gap, will provide maximum practical parallelity and planarity of the pole surfaces. This will make geometrical errors $\sim 10\times$ smaller than for conventional ($\sim 10^{-4}$) magnet construction.

11. The magnet gap will be determined by the surface ground bridge structures between the poles, also with gap errors $\sim 10\times$ smaller than conventional.

Table 5 shows in Col. II the effect of 25 μm gap change (large for ground surfaces).

12. Since the gap controls 90% of the reluctance and thus of the field $B_0(z)$, these special measures should give a magnet already at the few parts in 10^5 level of uniformity. Table 6 shows the effect of 25 μm of air between the pole pieces and the Fe return. Again, only the dipole term is significantly effected.

D. Multipole Shimming

Temporarily setting aside the question of magnetic potholes or other local irregularities in the steel, quadrupole, sextupole, etc. field tolerances are controllable to small levels, even before considering the use of current correction.

1. A smooth gap variation of 25 μm across the width of the poles results in a quadrupole of 12 PPM at $x=5$ cm, or a gradient of $2.3 \times 10^{-6} \text{cm}^{-1}$.
2. In Table 3 the effect of bump geometry errors is considered for real permeability.

Just as in the $\mu=\infty$ cases in Appendix A, conventional good construction tolerances suffice.

Column II shows that if all $(2x)2$ bumps are raised in height $25 \mu\text{m}$, the multipole content changes by $< 1 \text{ PPM}$. Thus $25 \mu\text{m}$ RMS errors will have no significant effect.

3. Iron uniformity dominates static field shimming considerations. Table 4 illustrates a type of possible quadrupole control.

A block of steel 2.54 cm thick was added to the width of top and bottom, block 5 in Fig. 1 directly above and below the pole pieces, towards center of the rings.

Column II shows a 10.4 PPM quadrupole change, with no other significant multipole change.

4. Modifications to the height of the edge bumps can be made to correct for changes in the pole steel magnetization properties for long wave lengths.
5. Transverse field flattening and azimuthal flattening can be applied iteratively.

E. Local Field Errors and Correction

As the magnet is progressively flattened, short wave length azimuthal and transverse descriptions of errors become progressively indistinguishable.

Finally, three dimensional expansions around a locations, $z=z_n$, $x=0$, $y=0$ will have to be used with appropriate local ferromagnetic grinding, adding of shims, and/or current shimming to correct to an acceptable level in an empirical manner.

1. Strictly speaking, it is knowledge of the field over the particle orbits which is required.
2. If the pole steel is uniform, the "potholes" within each of the defined 50 zones round the circumference should be sufficiently small in their field variation that a practical matrix of measurements will average the fluctuations analytically for possible current corrections.
3. The goal is to minimize or avoid completely spot grinding or shimming of pole surfaces near the beam. Local corrections can generate higher moment "lumpy" errors which were not present in the field before correction.

F. Localized Static Shimming

Setting aside questions of hysteretic or time varying environmental changes to be discussed in the next section, static shimming to a very high degree of accuracy is practical.

1. The hardest question, to define, short wavelength local variations in the poles, is fortunately subject to experimental testing on a small scale. This will finally define a realistic network of data points for averaging and corrections.
2. If experiments so indicated, more localized Fe shimming to control the reluctance at the base of the pole pieces could be incorporated into the pole design.
3. In Appendix 2 an analytic example of diverting flux transversely is given. Such a technique could be used either transversely or longitudinally for short wavelength tuning.
4. Other short wavelength passive techniques could be employed on the pole pieces, such as very small tensioning rods for very fine tuning.

G. Dynamical Considerations

1. With a solid core magnet, charge times of several hours are desirable to prevent eddy currents redistributing flux during charging of the magnet. This might result in a very small but significant effect on magnetization after operating field is obtained.
2. Thermal effects, i.e. hysteretic heating, is comparatively a smaller effect: typically millidegrees both due to enthalpy charge.
3. Magnetostriction will lead to dimensional changes which are small compared to mechanical tolerances and should be cylindrically symmetric.
4. The Curie Temperature of iron is 770°C. This results at ambient temperature in a change of saturation magnetization of 1.0×10^{-4} parts per degree C.

Again, the effect on the magnetic field should be small and cylindrically symmetric.

5. The coefficient of thermal expansion is 12.3 PPM per degree C. The enthalpy and thermal flywheel is enormous. Insulation and good thermal contact between pieces should suffice if room temperature is well controlled.
6. It is especially important to prevent temperature differences between pieces and thus twisting forces.

H. Current Control and Ripple

Magnet electrical parameters are 30 turns per coil x 3.9 kA x 2 coils, or $NI=234$ kAT. The inductance is 0.75h. The stored energy is 11 megajoules.

1. One advantage of superconducting coils is that a low voltage, highly filtered power supply of small cost and small power consumption can be used.
2. Consider a one hour time constant.

$$V = L\dot{I} = 0.75h \times \frac{3900}{3600} \text{ amps/sec} = 0.81 \text{ volts}$$

Thus, a servo controlled power supply of very low voltage will suffice.

3. Consider the magnet response to ripple.

$$\omega L (60 \sim) = 283 \Omega$$

$$(360 \sim) = 1,696 \Omega$$

$$(729 \sim) = 3,393 \Omega$$

For 100% voltage modulation (totally absurd) and 1 volt output

$$I_{60}/I_0 = 9 \times 10^{-7}, \quad I_{360}/I_0 = 1.5 \times 10^{-7}, \text{ etc.}$$

4. The power supply filter will suppress these very small ripple currents to negligible levels.

In addition, eddy currents in the solid iron core magnet will suppress field ripple.

5. Servoed current control using the NMR monitored field can give 10^{-6} absolute field regulation.

6. The usual "power dips" at BNL which play havoc with electronic protection equipment, etc., should appear as a ripple transient. However, in the event magnet current were to drop significantly, the magnetization cycle would have to be restored.

The probability of such a major dip during a run will have to be compared with other alternatives to operating the magnets.

7. One basic question will be the relative probabilities of cryogenic failure versus electrical utility failure.

Liquid helium and nitrogen volume requirements per day are small enough that extended operation is practical, even if the dedicated liquifier was down.

It is practical to consider the entire experiment being performed on a single magnet cycle.

8. It is feasible to consider persistent switch operation. In that case, the 3 separate cryostats housing the four main coils would be interconnected with superconducting leads designed to minimize joint resistance.

A single persistent switch across the four series operated coils would guarantee equal currents in all main conductors.

9. However, even with all series resistance as low as 10^{-10} ohms, for example, the decay time constant would be 10^5 days.
10. Persistent mode operation may require auxiliary coils adjacent to the main coils which servo the field to compensate for the decay.

Periodically as the auxiliary coil approached its maximum current, the main coil would be recharged.

If transients are avoided, this can be performed with constant total ampere turns and the field undisturbed.

11. Bifilar, twisted current leads to each of the four main coils will make no significant contribution to the field in the useful aperture. If desired, these leads could be quadrifilar.

In Table X (note, not calculated yet), the effect of 1 mm displacement of the main coils is demonstrated.

Small auxiliary coils in the cryostat can compensate over the good field aperture for displacements of the main windings.

I. Pole Face Windings

1. The use of pole face windings to provide refined correction of the field is well known. The CERN ISR employed fully distributed windings to give accurate field control of its stored beams.
2. We assume that the circumference will be divided into 50 equal zones, each with independent sets of normal and skew multipole corrections.
3. These will be very weak, typically one ampere-turn capability for $\frac{\Delta B}{B} \sim 1 \times 10^{-5}$.
4. Much higher capability is practical. However, it is desirable to keep the space occupied to a minimum and also to generate very little heat.

5. If cyclical effects can be kept very small by careful cycle control, for example, by exciting several percent above B_0 , coming down to B_0 and establishing of a very small minor loop, static shimming can be carried very far towards the design goals.

As discussed earlier, it may be possible to carry out the experiment on a single cycle.

6. The above, plus environmental effects will finally establish the requirements for local, short wave length, pole face corrections like spot ferromagnetic grinding, the less required, the better.

J. Experimental Effects

1. External magnetic fields sources and magnet reluctance perturbations will be minimized by shielding the experiment with a ferro-magnetic structure. This should be cylindrically symmetric and adequate to reduce any residual earth's field to a vertical component. Horizontal fields entering the magnet opening on the HMP which are not cylindrically symmetric are undesirable.
2. The temperature of the magnet Fe blocks should be held very constant. The very large enthalpy will control this automatically, provided the separate blocks of the structure are thermally coupled to keep differences very small.

K. Survey and Positional Control Vibration

This is the most difficult environmental control problem.

1. The slab under the magnet and the fill material under the slab must be very uniform.

2. The slab should "age" for several months with a load approximately the same as the magnet to get beyond settling.
3. The magnet is not a "terrain-following" design. The blocks are bolted and keyed together to create a "rigid structure" to high precision.
4. The space will have to be laid out to maximize the ease and accuracy of survey, before, during, and after assembly of the magnet. Survey during operation will be permissible, as required.
5. The eight separate blocks making up the bottom return yoke will be set up on pre-surveyed, many-point support jacks.
6. These blocks must be absolutely aligned: concentric and in a horizontal plane as accurately as can be obtained using many 50 μm readings.
7. The HMP blocks then are attached, locking the substructure into a single mechanical ring. The alignment is constantly monitored and touched up.
8. The inside cryostat is then inserted in the magnet.
9. The top yoke blocks are then assembled. The ground bridges providing reference shop tolerances on the pole piece gaps are inserted and the Fe structure "locked up".
10. The outside two cryostats and other auxiliaries are added.
11. During the above, the alignment must be precisely controlled in order not to overstress supports, yield materials, etc.

12. Vibrations of the ground should not lead to undermining the support, provided water erosion is not a factor in undermining the subfill. Care must be taken to avoid erosion.
13. The structure, if assembled and maintained to its structural tolerances and good but practical surveying tolerances, should behave as a single ring to required accuracy.

The field errors then should be dominated by properties of the poles and the reluctance of the flux return, as discussed in earlier sections.

L. Modelling Program

1. It appears clear that a next generation G-2 experiment with 10x greater accuracy has been credibly established. This uses refinements to the magnet and much more elaborate monitoring, "in-vivo" field calculations, and responsive current feed back control.
2. A modelling program is not required to justify proceeding.
3. However, refined quantification of the most difficult problems does not have to await final construction. Much of this could be carried out in parallel with construction.
4. This will inevitably reveal that several of the multipole problems attacked in the Proposal are easier than feared to solve.

The result will be a less elaborate and expensive experiment, with effort focused on the most difficult problems.

Appendix 1

Parametric Demonstration of Pole Edge Bumps

In Fig A1, a simple rectangular bump was added at each pole edge and the field calculated. This was first performed for low fields ($\mu = \infty$) to demonstrate the precision of the perturbations and the multipole fits.

At $B = 1.47T$, considerable saturation and field shape changes occur. The magnet geometry was perturbed to flatten the field only at operating $B = 1.47T$. This is done also by perturbation of the bumps.

For purposes of illustration of field perturbations, the $\mu = \infty$ case is clearer. The predictability of the multipole fits is not obscured by rapidly varying permeability.

1. Table A1 lists in Col. I the multipole terms: $N=0$ (dipole), $N=1$ (quadrupole), $N=2$ (sextupole), etc.
2. Column II shows the field content for an arbitrary choice of $2(x2)$ bumps on each pole edge, 3 cm wide x 0.4 cm high. The field components are expressed at $x = 6.43$ cm on the horizontal midplane (HMP).
3. Column III shows the results for increasing the height of the $2(x2)$ bumps by 0.13 cm. Note that the left-right symmetric terms $N=2, 4$, etc. have been significantly changed.
4. At the level $\Delta B/B \sim 1 \times 10^{-6}$, the dominant residual error in Col. III is the asymmetry of the C-magnet design left to right: quadrupole ($N=1$), octupole ($N=3$).

5. To attack this asymmetry, an arbitrary charge of ± 0.0064 cm in the bump heights was imposed to raise the field furthest from the flux return side. This is shown in Col. IV.
6. Assuming linear extrapolation of the quadrupole to zero, an asymmetry of ± 0.01446 was obtained. This was calculated, Col. V, and indeed gave zero.

The $N=3, 5$, etc., terms are also very small.

7. In going from Col. III to Col. V, the average of the $(2x)2$ bumps is unchanged. Note that $N=2, 4$, etc., are unchanged, reflecting this average.
8. In summary, even the simplest bump structure resulted in a "paper" magnet of $\Delta B/B \sim 1 \times 10^{-6}$ over the entire good field aperture required by the beam.
9. Slightly more elaborate bump structure could have made even more accurate field shape.
10. In Table A2 the tolerances on dimensional control of the bump structure is explored.

Column II shows the effect of all $(2x)2$ bumps being 25 μ meters too high. Note that all field terms are changed by $< 1 \times 10^{-6} B_0$.

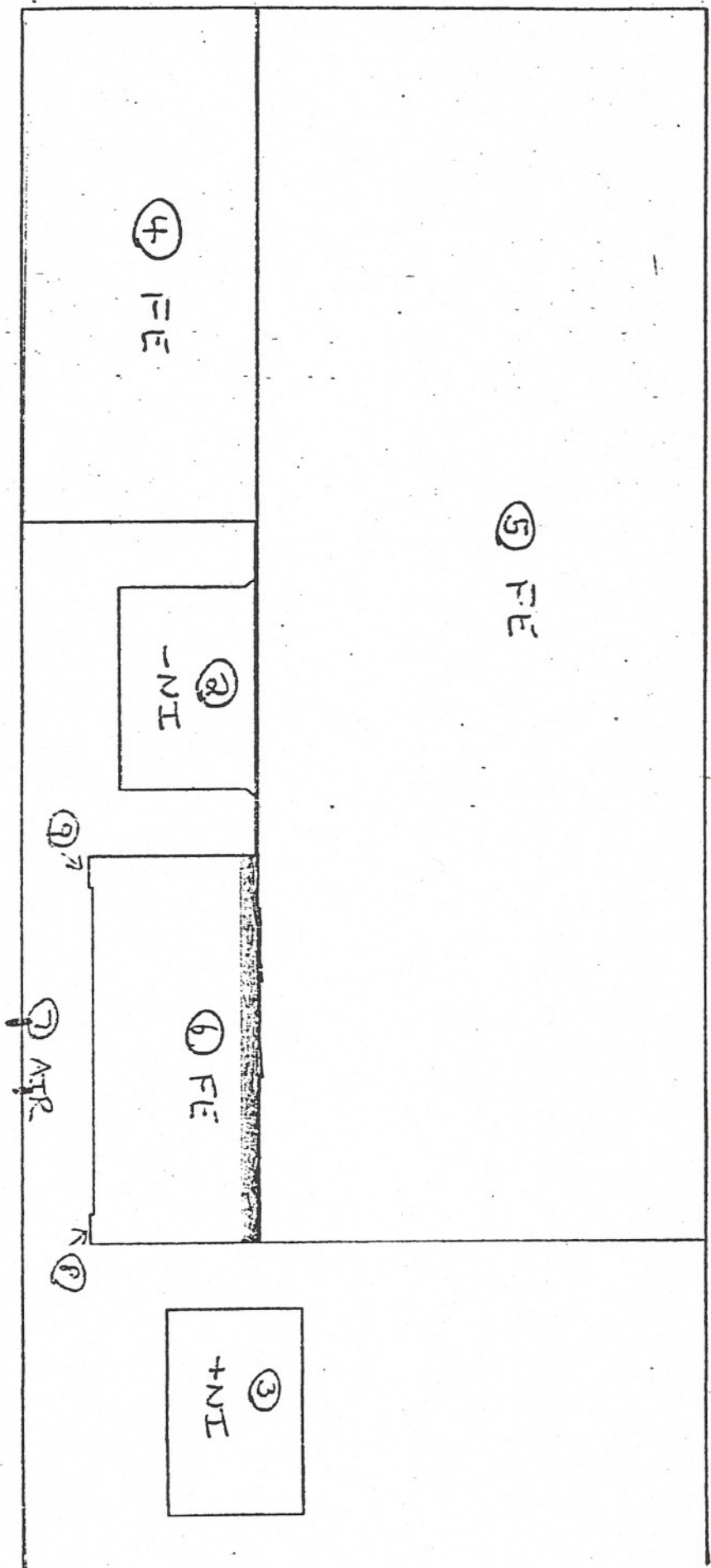
Column III shows a "worst case" quadrupole error; i.e. both bumps closest to the flux return are -25μ m in height, and both furthest bumps are $+ 25 \mu$ m in height. The left-right asymmetry is slightly larger than $1 \times 10^{-6} B_0$.

RMS errors in bump height of $25 \mu\text{m}$ will have smaller effects than the above, and will generate both the normal multipoles listed in Table A1 and A2, and also skew multipoles (where $B_y=0$ on the HMP).

11. $B = 1.47\text{T}$ with realistic real μ pole pieces requires modification to the shape of the bumps. Keeping the bumps as near the pole edges as possible suppresses generation of higher moments by the bump themselves, qualitatively behaving like the $\mu - \infty$ illustration.

FIG. 1

--- CENTER OF g-2 RING
→ $\rho = 700$ CM



g-2

$\mu = 1006$

FIG. 2

$\frac{B/I}{(B/I)_0}$

46 1320

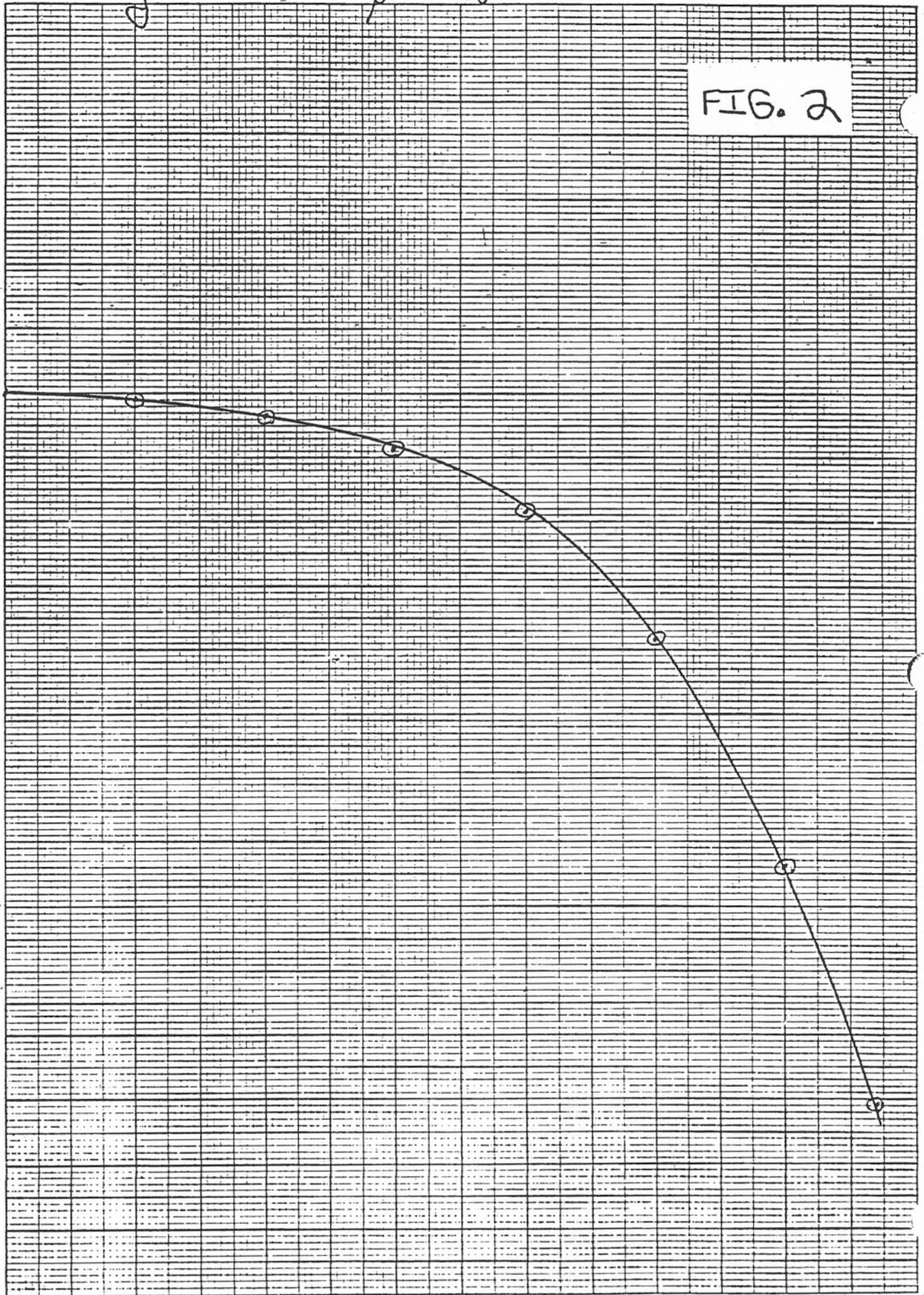
KE 10 X 10 TO 1/2 INCH 7 X 10 INCHES
KEUFFEL & ESSER CO. MADE IN U.S.A.

1.000
.98
.96
.94
.92
.90
.88

9 10 11 12 13 14 15

B_0 (RG)

7/1/85



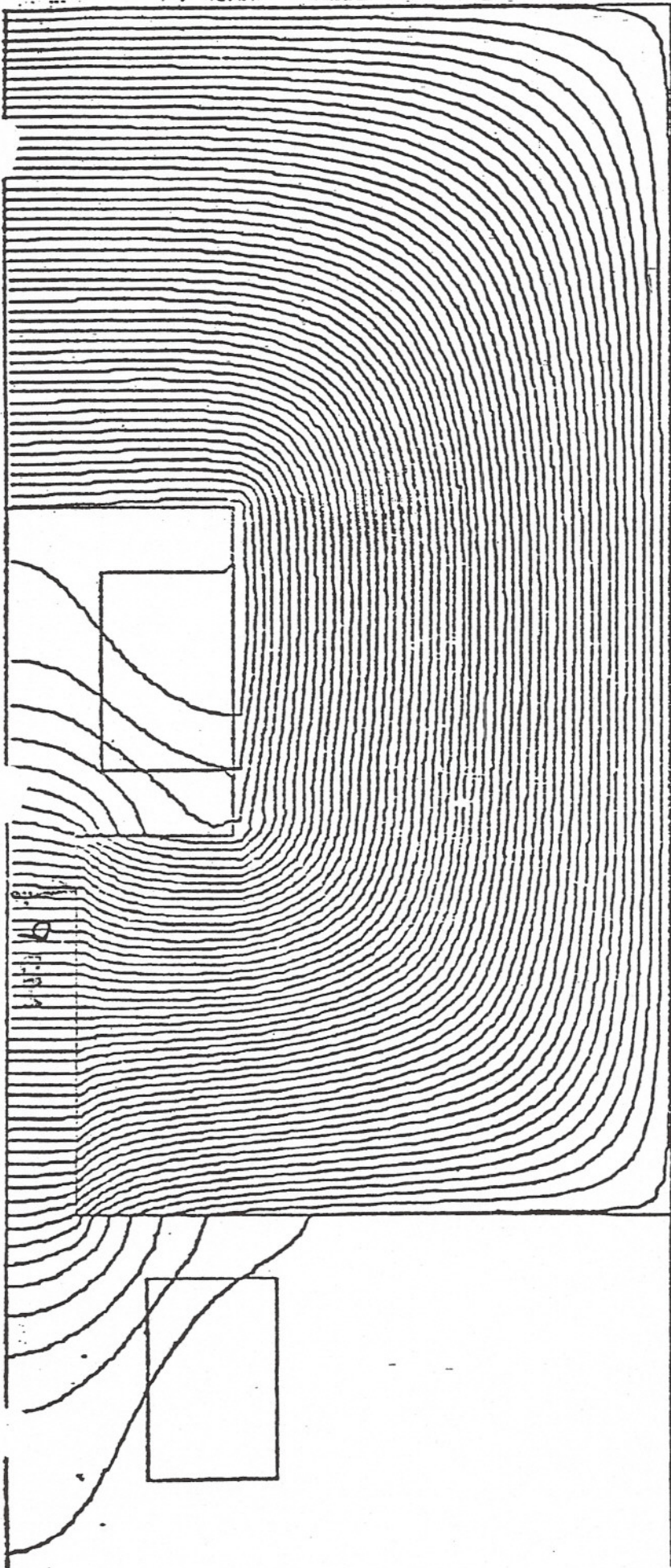


FIG. 3

FIG. 4

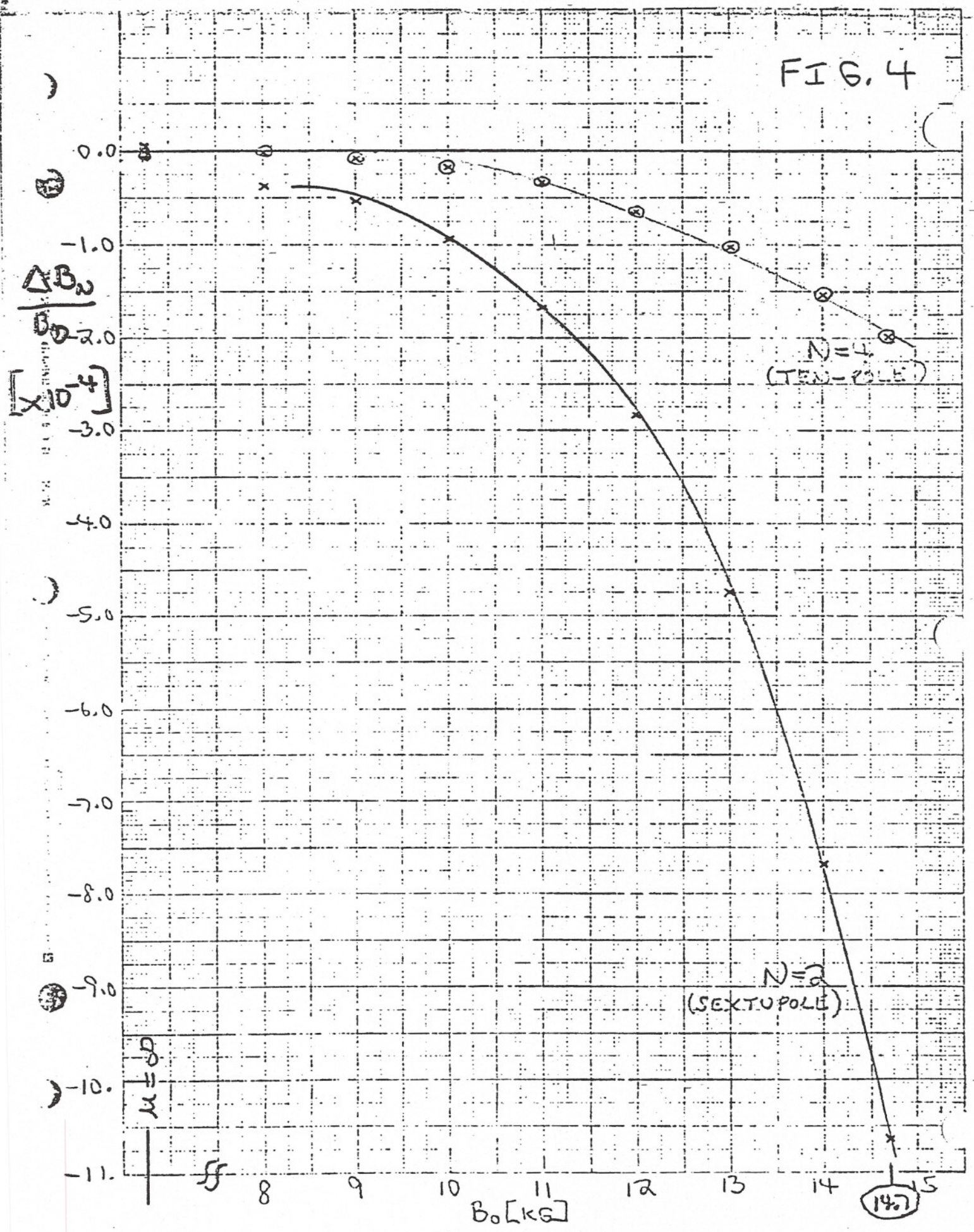
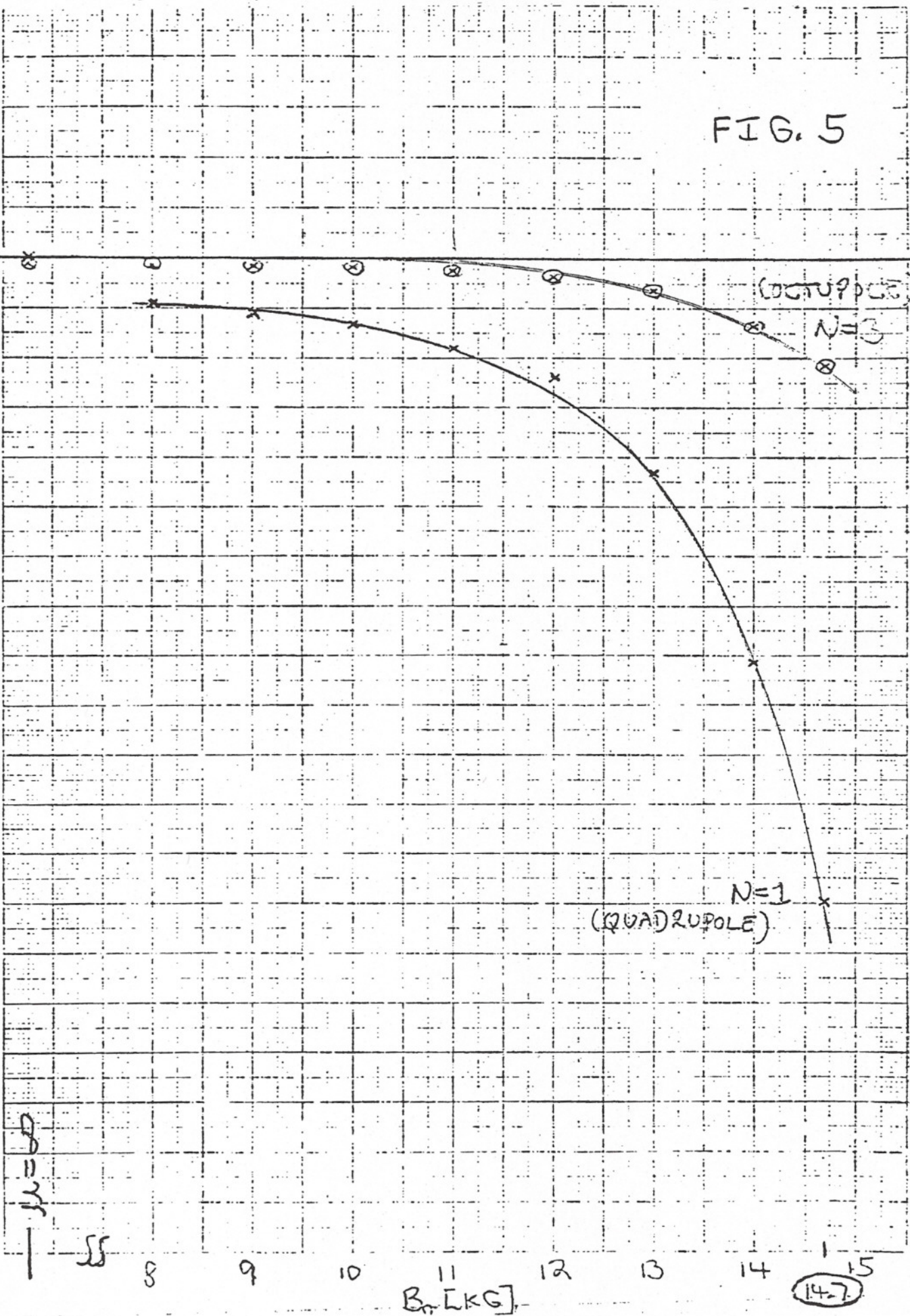


FIG. 5

$\frac{\Delta B_z}{B_0}$
 $\times 10^{-4}$



I

II

III

	<u>b_m</u>		
$n =$	0	-0.1%	+0.426%
	1	~ 0 PPM	+1.3 PPM
	2	~ 0 ↓	+5.6 ↓
	3		-0.
	4		+0.9

TABLE 2

TABLE 3

	I	II
	<u>b_n</u>	
$n = 0$	0	8.85 PPM
1	1	0 ↓
2	2	0.81
3	3	0
4	4	0.35
5	5	0
6	6	0.077

TABLE 4

	I	II
	<u>b_n</u>	
$n = 0$	0	0.12%
1	1	10.4 PPM
2	2	-0.3 ↓
3	3	0.6
4	4	0.1

TABLE 5

	I	II
	<u>b_m</u>	
$n =$	0	0.012%
	1	0 PPM
	2	0.22 ↓
	3	0
	4	0.07
	5	0
	6	0

TABLE 6

	I	II
	<u>b_m</u>	
$n =$	0	0.03%
	1	0.03 PPM
	2	0.39 ↓
	3	0
	4	0.06
	5	0
	6	0

FIG. A1

| CENTER OF g-2 RING
→ $\rho = 700 \text{ CM}$

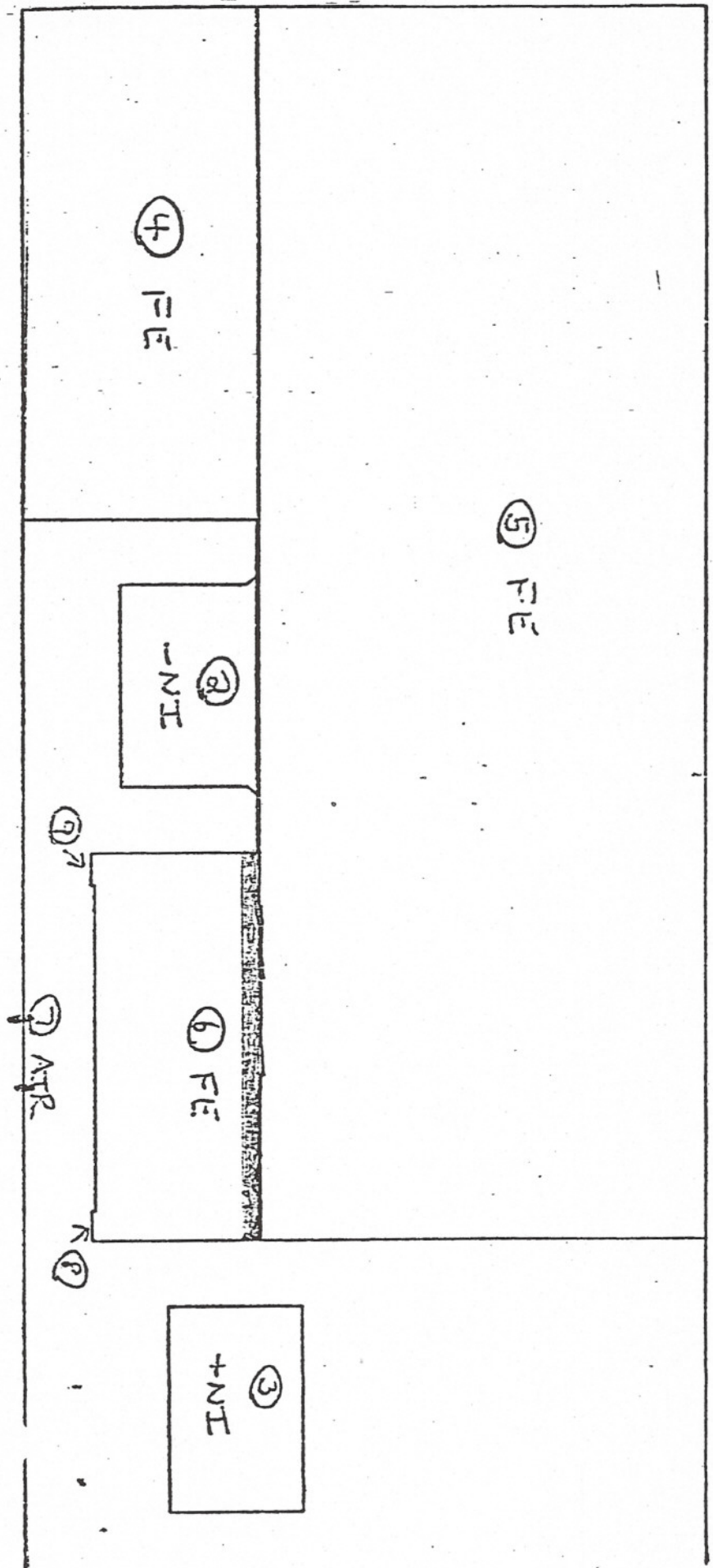


TABLE A1

	I	II	III	IV	I
ν_m					
$n=0$					
1		-7.3 PPM	-7.9 PPM	-4.4 PPM	0.0
2		-74.7 ↓	1.6 ↓	1.6 ↓	1.5
3		-8.4	-9.0	-6.0	-2.3
4		-31.8	-0.2	-0.3	-0.3
					\pm
					$\frac{\Delta B}{B_0} = -1.1 \text{ PPM}$

TABLE A2

	I	II	III
ν_m			
$n=0$		0.46 PPM	0 PPM
1		0 ↓	1.40 ↓
2		0.58	0
3		0	1.17
4		0.24	0

HEADLINE MASS. AW Distribution 1964

HEADLINE MASS. AW Distribution 1964

BROOKHAVEN NATIONAL LABORATORY

MEMORANDUM

DATE: November 1, 1985

TO: Robert B. Palmer

FROM: John Tarrh, Gordon Danby, J. Jackson

SUBJECT: Position requirements for G-2 Coils

One question that arose during the discussion of the G-2 proposal was the requirements on coil position to obtain the desired field homogeneity. While detailed analysis on this question has not yet been performed, we estimate that, on the basis of preliminary calculations, a 1 mil coil displacement will yield less than a 1 part in 10^6 change in the magnetic field (see table). This requirement will be substantially loosened when the effects of other considerations are included. This is true for a number of reasons. First, the field homogeneity is most strongly dominated by the shape of the iron pole, given the low field level of 1.47T and the substantially increased volume of iron that is proposed (relative to the CERN experiment) to minimize the effects of saturation.

The homogeneity of the assembled magnet including pole shimming is 1 part in 10^5 . Based on field measurements, correction coils will then be used to obtain 1 part in 10^6 . The magnet is designed to be operated continuously, and at only one field value. The use of superconducting coils will minimize the magnetic cycling while maximizing the magnet stability from not only a magnetic and electrical viewpoint, but from a thermal viewpoint as well. In addition, the location of the coils can be adjusted while the magnet is energized. The ability to make magnetic measurements and adjust the magnetic configuration (by adding shims to the pole and/or the return frame, by using correction coils, and by adjusting the location of the main coils) means that the requirements on coil position are significantly reduced.

In comparison to other magnet systems, note the attached figure (pg. 48 of the proposal) which shows the small coil cross section proposed, located far from the good field region. In the Tevatron, SSC, etc., a 1 mil motion of the coils will yield on the order of 1,000 ppm, but the stability of operation of the Tevatron indicates the absence of coil motion to a high accuracy compared to 1 mil. The coils proposed have considerably lower currents and coil fields, by comparison, and will therefore have forces that are only a few percent of those

in an accelerator magnet. We believe that the key issue for this magnet is stability, and that the proposed concept is an ideal approach from this perspective.

In addition to the NMR trolley measurements, we will have continuous field monitoring at many locations on the outside of the vacuum chamber. This, coupled with two and three dimensional analyses, will provide detailed knowledge of the field configuration, which is required.

In summary, a simple air core perturbation analysis indicated that a 1 mil coil displacement will yield approximately a 1 ppm field change. The gradient effects will be roughly a factor of 50 times less due to the coil locations and size relative to the good field region. Images in the iron act to substantially reduce these errors, as indicated by the tabulated computer results (attached).

/mif

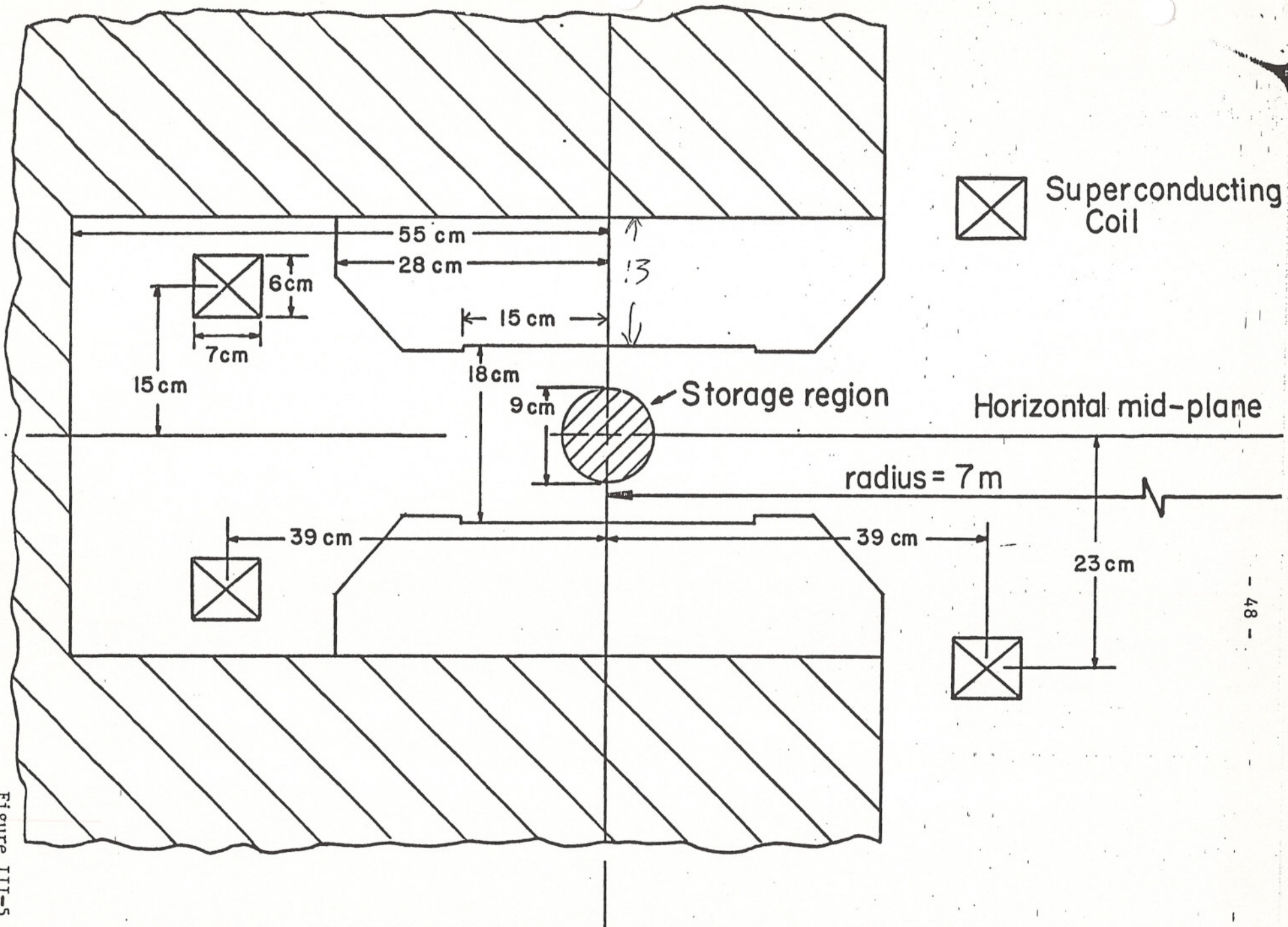


Figure III-5

PRELIMINARY POLE PROFILE - COMPUTER SIMULATED

G-2

EFFECT OF COIL MOTION

<u>M</u>	<u>TERM</u>	↑ INNER COIL	→ INNER COIL	← OUTER COIL
0	DIPOLE	-0.602	+0.189	+0.050
1	QUADRUPOLE	+0.020	+0.013	-0.019
2	SEXTUPOLE	-0.004	-0.005	-0.006
3	OCTUPOLE	+0.001	+0.003	-0.002
4	DECAPOLE	-0.001	-0.001	-0.001

NOTE: EFFECT EXPRESSED AS PPM PER MIL (0.001") OF MOTION OF 1 COIL AT $\rho = +6$ CM ON HORIZONTAL MIDPLANE OF MAGNET.

EFFECT COMPUTED FOR COIL MOTIONS OF 1 CM AND LINEARLY SCALED TO 1 MIL.

JWJ 11/1/85
J.W. JACKSON

G-2

3/21/86

G. DANBY

J. JACKSON

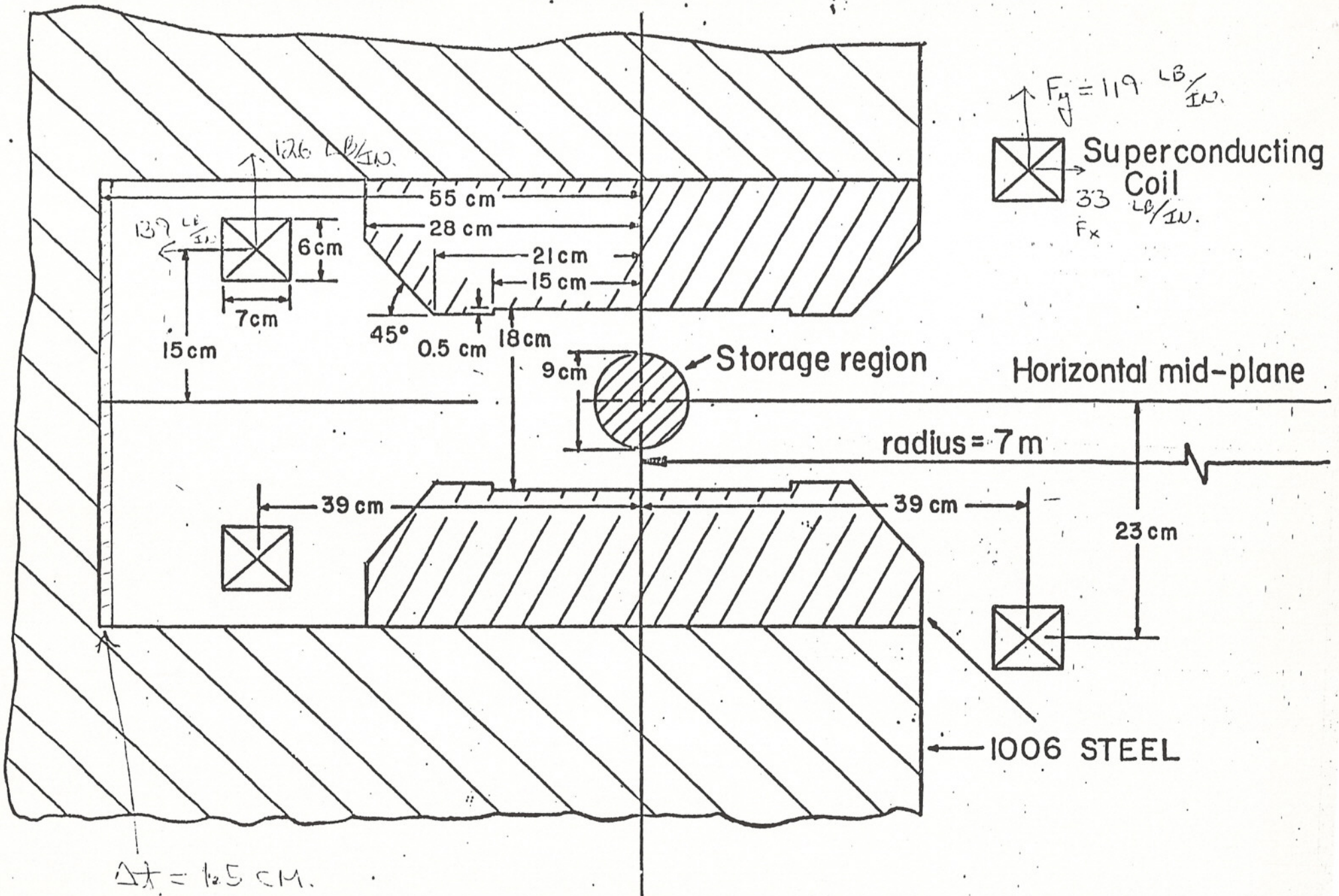
The following table shows the effect of increasing the width of the vertical FE return by 1.5 cm (to 66.5 cm). Fig. 1 indicates this modification.

Table I

<u>b_m</u>	<u>$\Delta t = +1.5 \text{ cm}$</u>
$n = 0$	+769 PPM
1	-3.70 ↓
2	+2.37
3	-2.21
4	+1.05

Figure 1 also indicates the forces on the coils for the "standard" coil location. These forces are sensitive to coil location and will be summarized as a function of location for the next meeting.

PRELIMINARY MAGNET POLE PROFILE



ETC - 1

GTD/JWS 3/21/86

BROOKHAVEN NATIONAL LABORATORY
MEMORANDUM

DATE: April 11, 1986
TO: Muon G-2 Group
FROM: G.T. Danby and J.W. Jackson
SUBJECT: Magnet Design

Some further computations were performed using Brookhaven's CDC7600 and the POISSON code installed on that machine.

Table I shows the computed field harmonics as a function of convergence criteria. These computations were performed for two types of magnet steel, 1006 (Table II) and decarburized iron (Table III), in order to obtain some feel for the permeability tolerance.

The R/L parameter tests the convergence of the potential solution of air, interface and iron points with $R/L = 5 \times 10^{-7}$ being the standard (default) value in POISSON.

The field harmonics are expressed in PPM's at $X, Y = 5, 0$ cm. The center of the storage region is defined as 0,0 for the magnet geometry included in the AGS g-2 proposal (Fig. 1).

The quantity, δ , is defined as the difference between the field at 5,0 and the field as obtained from summing the harmonic values expressed at 5,0. This quantity is a measure of the internal consistency and fitting accuracy of the POISSON code.

In order to test the consistency of the computation between the CDC7600 (60-bit word length) and the VAX 785 (32-bit word length), the "standard" magnet geometry (Fig. 1) was set up and run on each machine with identical ampere-turns and permeability table. Since the VAX version of POISSON contains a "bug" which prevents obtaining a harmonic analysis for a C-magnet type geometry, the difference in the HMP field deviations was plotted as a function of distance along the HMP (Fig. 2). This plot shows a random jitter of $\sim \pm 2$ PPM, peak-to-peak.

$$\frac{R}{L} = 5 \times 10^{-7}$$

$$\mu = 1006$$

DECAKBr
 $\mu = \text{IRON}$

$n=1$	PPM	-143.7	-139.6
2	↓	-5.4	-5.8
3		-7.3	-10.4
4		+8.7	+7.9
5		-0.3	-0.0
6		-1.8	-1.8
B_0	GAUSS	14,286.616	14,369.398
δ	PPM	+3.9	+4.3

$$\frac{R}{L} = 1 \times 10^{-7}$$

$n=1$	PPM	-146.0
2	↓	-5.2
3		-8.1
4		+8.75
5		-0.8
6		-1.8
B_0	GAUSS	14,286.780
δ	PPM	+1.0

TABLE I

$$\frac{R}{L} = 0.5 \times 10^{-7}$$

$n=1$	PPM	-146.2	-142.3
2	↓	-5.1	-5.5
3		-8.2	-11.3
4		+8.8	+8.0
5		-0.3	-0.5
6		-1.8	-1.8
B_0	GAUSS	14,286.800	14,371.793
δ	PPM	+0.6	+0.6

MATERIAL NO. 2, STACK=1.000

N	B-SQUARED	GAMMA	R	H	MU	D GAM/O B-SQ
1	1.000000E+06	.000556	1000.0	.56	1798.6	-1.7000E-11
2	4.000000E+06	.000505	2000.0	1.01	1980.2	-5.4000E-12
3	9.000000E+06	.000478	3000.0	1.43	2092.1	-2.0000E-12
4	1.600000E+07	.000464	4000.0	1.86	2155.2	-5.5556E-13
5	2.500000E+07	.000459	5000.0	2.30	2178.6	0.
6	3.600000E+07	.000459	6000.0	2.75	2178.6	3.0769E-13
7	4.900000E+07	.000463	7000.0	3.24	2159.8	5.3333E-13
8	6.400000E+07	.000471	8000.0	3.77	2123.1	5.8824E-13
9	8.100000E+07	.000481	9000.0	4.33	2079.0	7.8947E-13
10	1.000000E+08	.000496	10000.0	4.96	2016.1	1.0952E-12
11	1.210000E+08	.000519	11000.0	5.71	1926.8	1.6087E-12
12	1.440000E+08	.000556	12000.0	6.67	1798.6	2.6122E-12
13	1.690000E+08	.000588	12500.0	7.35	1700.7	3.5294E-12
14	1.960000E+08	.000633	13000.0	8.23	1579.8	6.1132E-12
15	2.250000E+08	.000714	13500.0	9.64	1400.6	8.6549E-12
16	2.560000E+08	.000833	14000.0	11.66	1200.5	1.3123E-11
17	2.890000E+08	.001020	14500.0	14.79	980.4	1.5593E-11
18	3.240000E+08	.001250	15000.0	18.75	800.0	1.7377E-11
19	3.610000E+08	.001515	15500.0	23.48	660.1	2.1397E-11
20	4.000000E+08	.001852	16000.0	29.63	540.0	3.2554E-11
21	4.410000E+08	.002381	16500.0	39.29	420.0	3.8746E-11
22	4.840000E+08	.003030	17000.0	51.51	330.0	5.6232E-11
23	5.290000E+08	.004000	17500.0	70.00	250.0	8.7662E-11
24	5.760000E+08	.005556	18000.0	100.01	180.0	8.6959E-11
25	6.250000E+08	.007143	18500.0	132.15	140.0	1.0389E-10
26	6.760000E+08	.009091	19000.0	172.73	110.0	1.9426E-10
27	7.290000E+08	.011667	20000.0	333.34	60.0	3.8138E-10
28	7.840000E+08	.014390	20500.0	500.00	41.0	2.0149E-10
29	8.410000E+08	.018571	21000.0	599.99	35.0	1.8762E-10
30	9.000000E+08	.024558	21500.0	700.00	30.7	3.8395E-10
31	9.610000E+08	.032909	22000.0	900.00	24.4	5.5838E-10
32	1.024000E+09	.045333	22500.0	1199.99	18.8	5.2237E-10
33	1.090000E+09	.065217	23000.0	1499.99	15.3	8.1098E-10
34	1.160000E+09	.103333	24000.0	2479.99	9.7	6.8205E-10
35	1.230000E+09	.171538	26000.0	4459.99	5.8	4.9016E-10
36	1.300000E+09	.281333	30000.0	8439.99	3.6	

RECONSTRUCTION OF THE TABLE FOR MAT. NO. 2 WITH EQUAL INCREMENTS OF B-SQUARED

MAXIMUM B-SQUARED = 9.000000E+08, WITH TRUNCATION FOR HIGHER VALUES

B-SQUARED INCREMENT = 1.125000E+06

TABLE II

MATERIAL NO. 2, STACK=1.000

N	B-SQUARED	GAMMA-	B	H	MU	D GAM/D B-SQ
1	0.	.000250	0.0	0.00	4000.0	0.
2	8.000000E+07	.000250	8944.3	2.24	4000.0	9.0625E-13
3	1.440000E+08	.000308	12000.0	3.70	3246.8	2.7308E-12
4	1.960000E+08	.000450	14000.0	6.30	2222.2	7.4828E-12
5	2.250000E+08	.000667	15000.0	10.01	1499.3	1.7574E-11
6	2.402500E+08	.000935	15500.0	14.49	1069.5	3.0159E-11
7	2.560000E+08	.001410	16000.0	22.56	709.2	4.7385E-11
8	2.722500E+08	.002180	16500.0	35.97	456.7	6.3284E-11
9	2.890000E+08	.003240	17000.0	55.08	308.6	6.3768E-11
10	3.062500E+08	.004340	17500.0	75.95	230.4	7.4930E-11
11	3.240000E+08	.005670	18000.0	102.06	176.4	8.3288E-11
12	3.422500E+08	.007190	18500.0	133.02	139.1	9.6533E-11
13	3.610000E+08	.009000	19000.0	171.00	111.1	1.0909E-10
14	3.802500E+08	.011100	19500.0	216.45	90.1	1.1139E-10
15	4.000000E+08	.013300	20000.0	266.00	75.2	1.5309E-10
16	4.202500E+08	.016400	20500.0	336.20	61.0	1.8313E-10
17	4.410000E+08	.020200	21000.0	424.20	49.5	2.2723E-10
18	4.515620E+08	.022600	21250.0	480.25	44.2	2.8069E-10
19	4.622500E+08	.025600	21500.0	550.40	39.1	4.3470E-10
20	4.730620E+08	.030300	21750.0	659.02	33.0	6.7654E-10
21	4.840000E+08	.037700	22000.0	829.40	26.5	8.0247E-10
22	5.062500E+08	.055555	22500.0	1249.99	18.0	8.2715E-10
23	5.196840E+08	.066667	22796.6	1519.78	15.0	8.2206E-10
24	5.321600E+08	.076923	23068.6	1774.51	13.0	8.0315E-10
25	5.495740E+08	.090909	23443.0	2131.18	11.0	7.7063E-10
26	5.757890E+08	.111111	23995.6	2666.18	9.0	5.9372E-10
27	6.292590E+08	.142857	25085.0	3583.57	7.0	8.6601E-10
28	6.567530E+08	.166667	25627.2	4271.21	6.0	5.9041E-10
29	7.132100E+08	.200000	26706.0	5341.20	5.0	5.0539E-10
30	8.121430E+08	.250000	28498.1	7124.53	4.0	3.8477E-10
31	1.028720E+09	.333333	32073.7	10691.21	3.0	2.7573E-10
32	1.270500E+09	.400000	35644.1	14257.63	2.5	1.7862E-10
33	1.830334E+09	.500000	42782.4	21391.20	2.0	1.1418E-10
34	2.316900E+09	.555555	48134.2	26741.19	1.8	7.4035E-11
35	3.254900E+09	.625000	57051.7	35657.33	1.6	4.8176E-11
36	4.119800E+09	.666667	64185.7	42790.47	1.5	3.1995E-11
37	5.608100E+09	.714285	74887.2	53490.84	1.4	

RECONSTRUCTION OF THE TABLE FOR MAT. NO. 2 WITH EQUAL INCREMENTS OF B-SQUARED

MAXIMUM B-SQUARED = 5.608100E+09, WITH TRUNCATION FOR HIGHER VALUES

B-SQUARED INCREMENT = 7.010125E+06

(18) = 12 DECARBURIZED IRON 3/8969

TABLE III

PRELIMINARY MAGNET POLE PROFILE

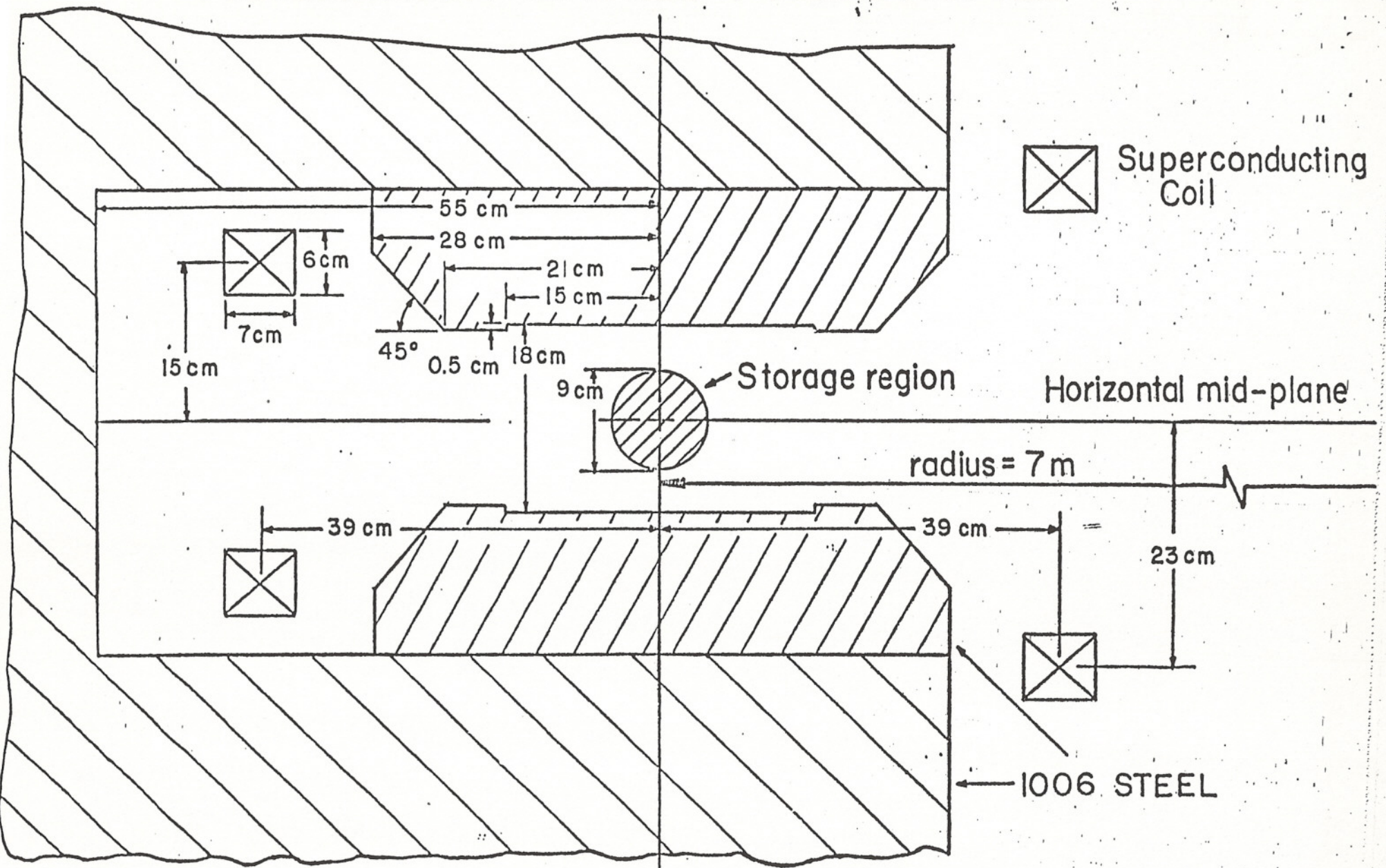


Figure 1.

Figure 2.

$\Delta B_y [VAX = CDC]$

[USS]

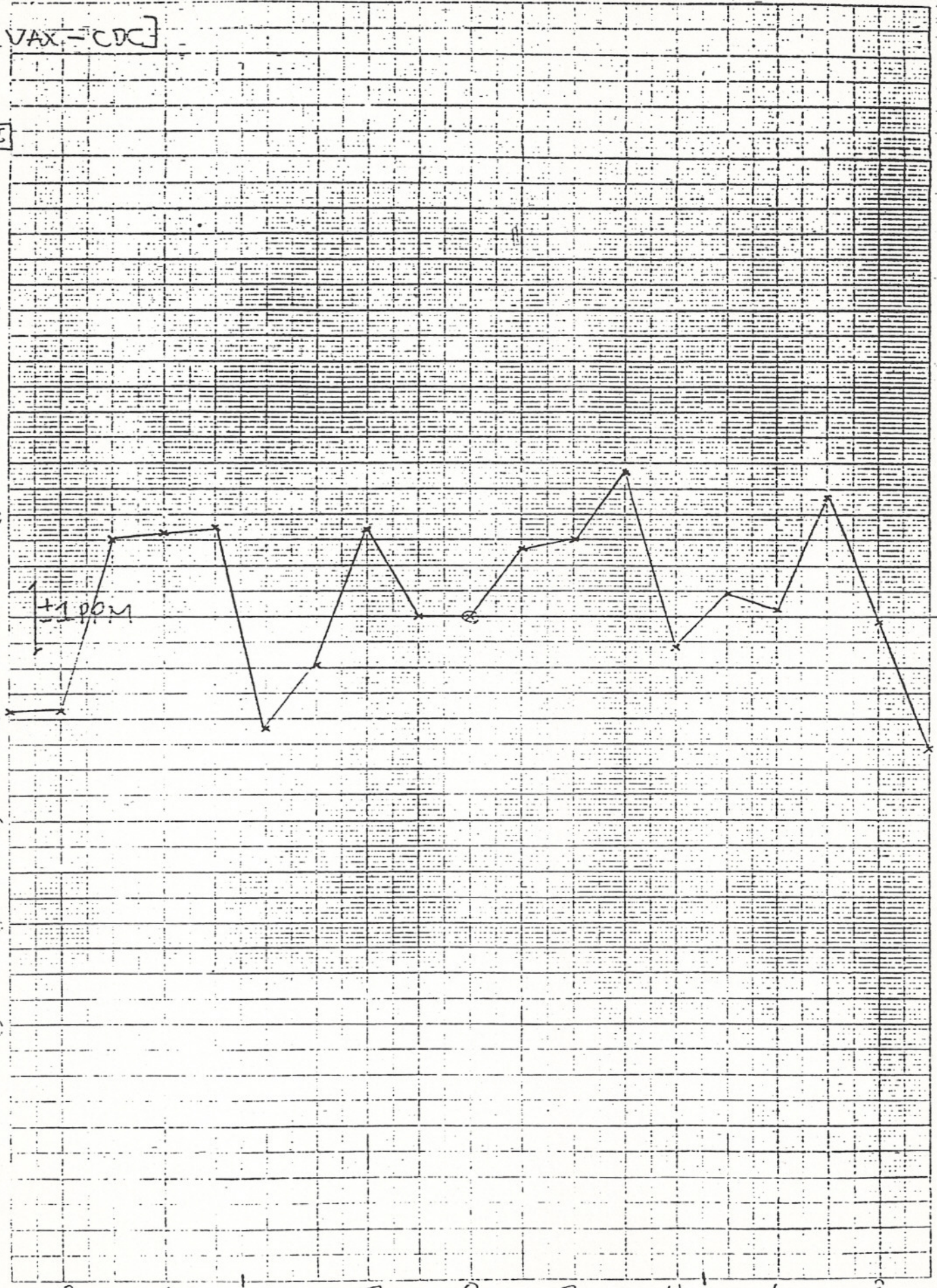
461510

10 X 10 TO THE CENTIMETER 16 X 25 CM.
KEUFFEL & ESSER CO. MADE IN U.S.A.

.160
.120
.080
.040
0
-0.040
-0.080
-0.120
-0.160

-8 -6 -4 -2 0 2 4 6 8

$X_{HIP} [CM]$



4/22/86

Ralph,

Please find attached some computation that Gordon promised you at the last g-2 magnet meeting.

Fig. 1 shows the standard set-up of the magnet geometry. In order to allow access to the pole base for shimming and to find a "force-free" location for the ^{inner} coil I have moved the inner coil to various heights and computed the force on the coil. These results are summarized in Table I with the "standard" value for the vertical center line of the inner coil being $23 \text{ cm}^{(10)}$ (Fig. 1) and the coil being

moved to 26, 28 + 30 cm. I also plotted (Fig. 2)
the Force in the horizontal direction on the inner coil
as a function of γ in order to indicate where
 $F_x = 0$.

John John

PRELIMINARY MAGNET POLE PROFILE

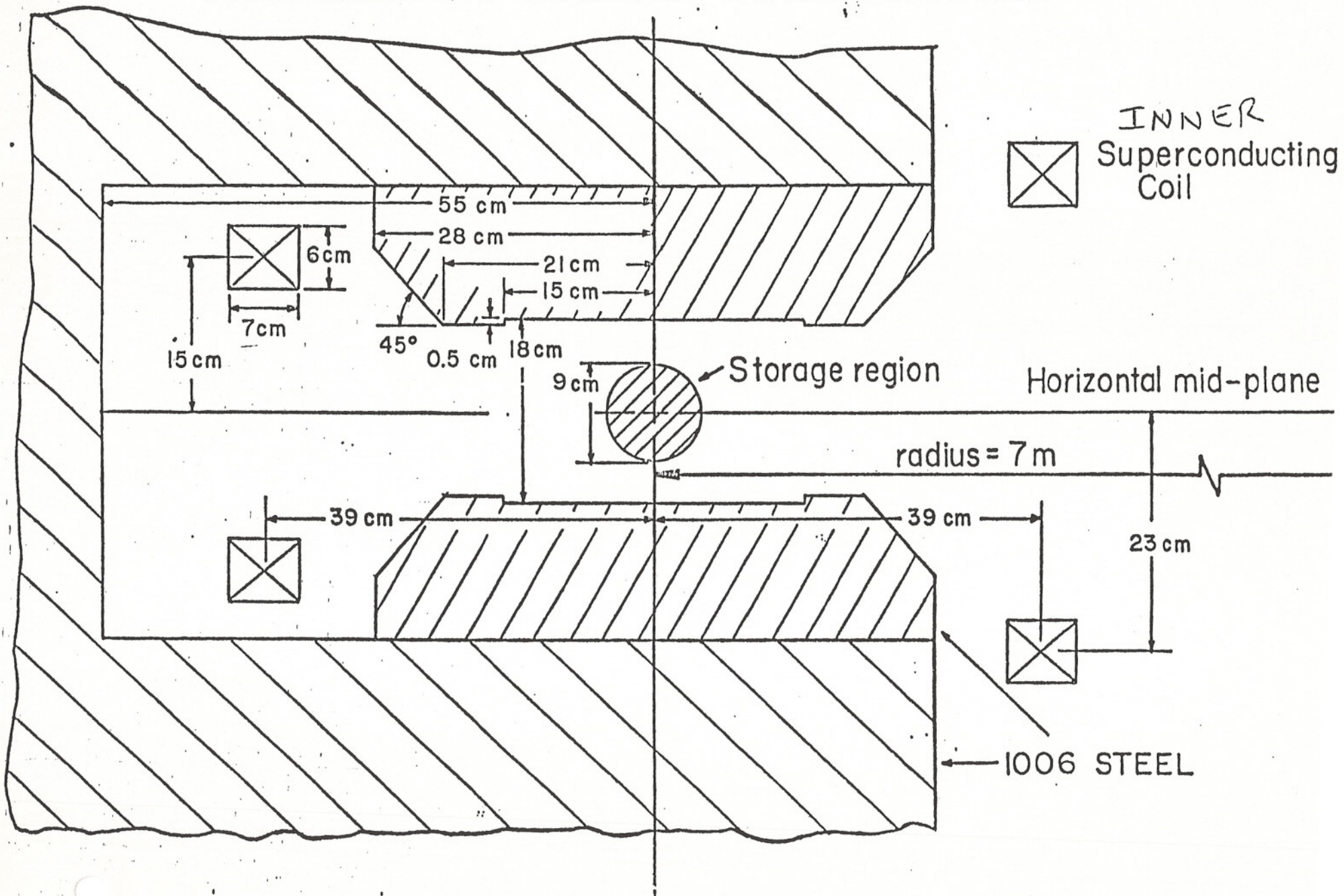


FIG. 1

G-2

INNER
COIL

Y/E
[CM]

B_0
[RG]

INNER
COIL

F_x F_y
[LB/IN]

OUTER
COIL

F_x F_y

23

14,368

+33 +119

-140 +127

26

14,349

+15 +114

-140 +127

28

14,338

+6.2 +110

-140 +127

30

14,325

~~-1.4~~
+105

-140 +127

TABLE I

GTD/JWW

4/86

FIG. 2

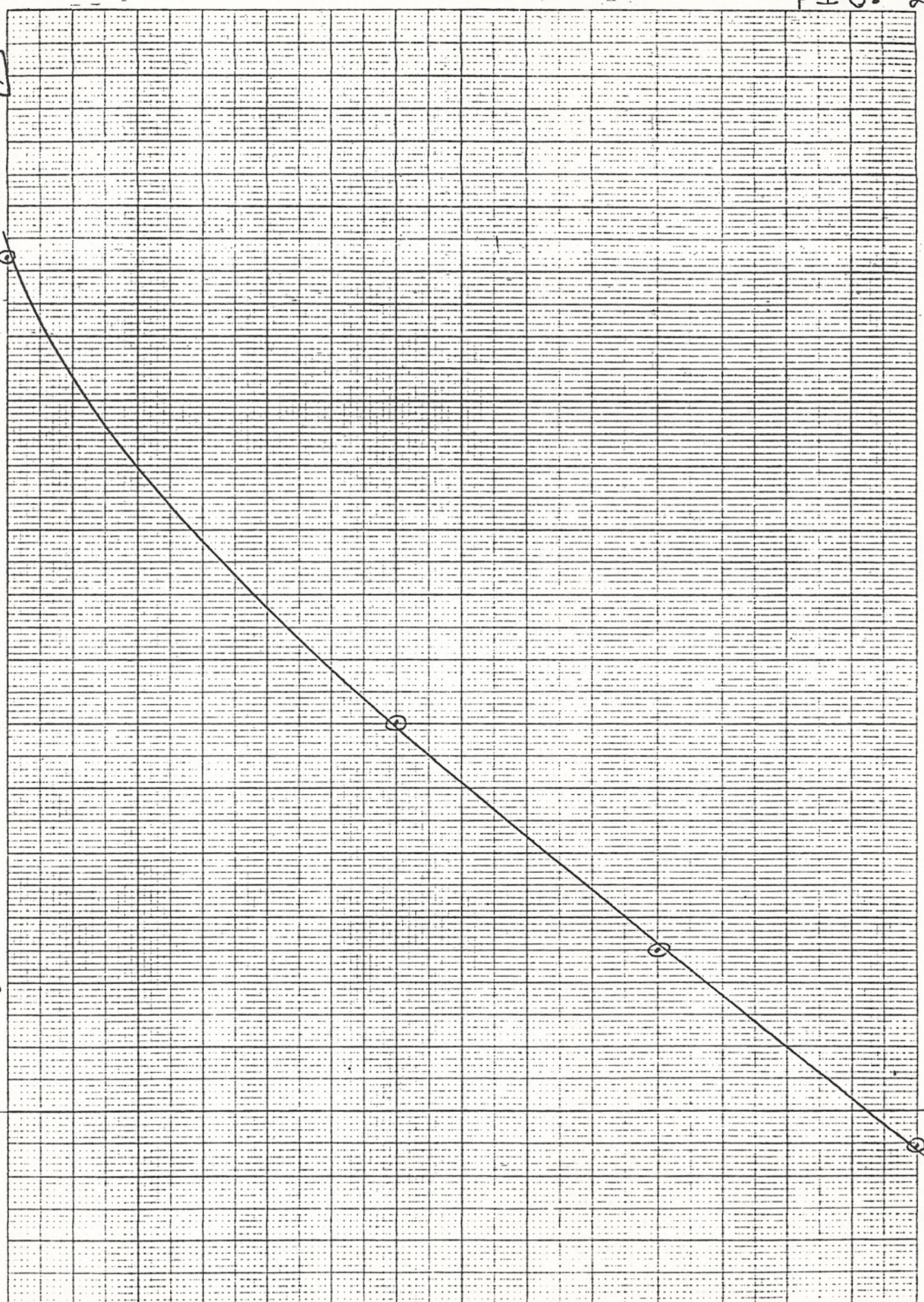
F_x
[LB./IN.]

46 1320

10 X 10 TO 1/2 INCH 7 X 10 INCHES
KEUFFEL & ESSER CO. MADE IN U.S.A.

35
30
25
20
15
10
+5
0
-5

23 24 25 26 27 28 29 30



BROOKHAVEN NATIONAL LABORATORY

MEMORANDUM

DATE: May 19, 1986
TO: Muon G-2 group
FROM: G.T. Danby/J.W. Jackson
SUBJECT: Magnet Design

The purpose of this memorandum is to provide the magnet design subgroup with certain computations which had limited distribution last month and also to provide additional comments on magnet shimming.

Figure 1 shows the standard set-up of the magnet geometry. In order to allow access to the pole base for shimming and to find a "force-free" location for the inner coil we have moved the inner coil to various heights and computed the force on the coil. These results are summarized in Table I with the "standard" value for the vertical center line of the inner coil being 23 cm (Fig. 1) and the coil being moved to 26, 28 and 30 cm. We also plotted (Fig. 2) the force in the horizontal direction on the inner coil as a function of Y_t in order to indicate where $F_x = 0$.

Comments

- 1) Column 2 in Table I shows very little change in B_0 for large vertical inner coil displacements with constant ampere-turns.
- 2) Most importantly, the "force-free" inner coil location provides easy access to the large air gap between the pole and yoke for precision ferromagnetic shimming.
- 3) This method of shimming was explored for the CERN magnet design in the 1985 Summer Study, but was not included in the AGS proposal.
- 4) For this year's Summer Study we expect to repeat the shimming exercise on the present magnet design.
- 5) The results should be quite similar to 3). The earlier study showed that this shimming method provided an attractive way for adjusting with short wavelengths the dipole field as well as the allowed and error multipoles.

PRELIMINARY MAGNET POLE PROFILE

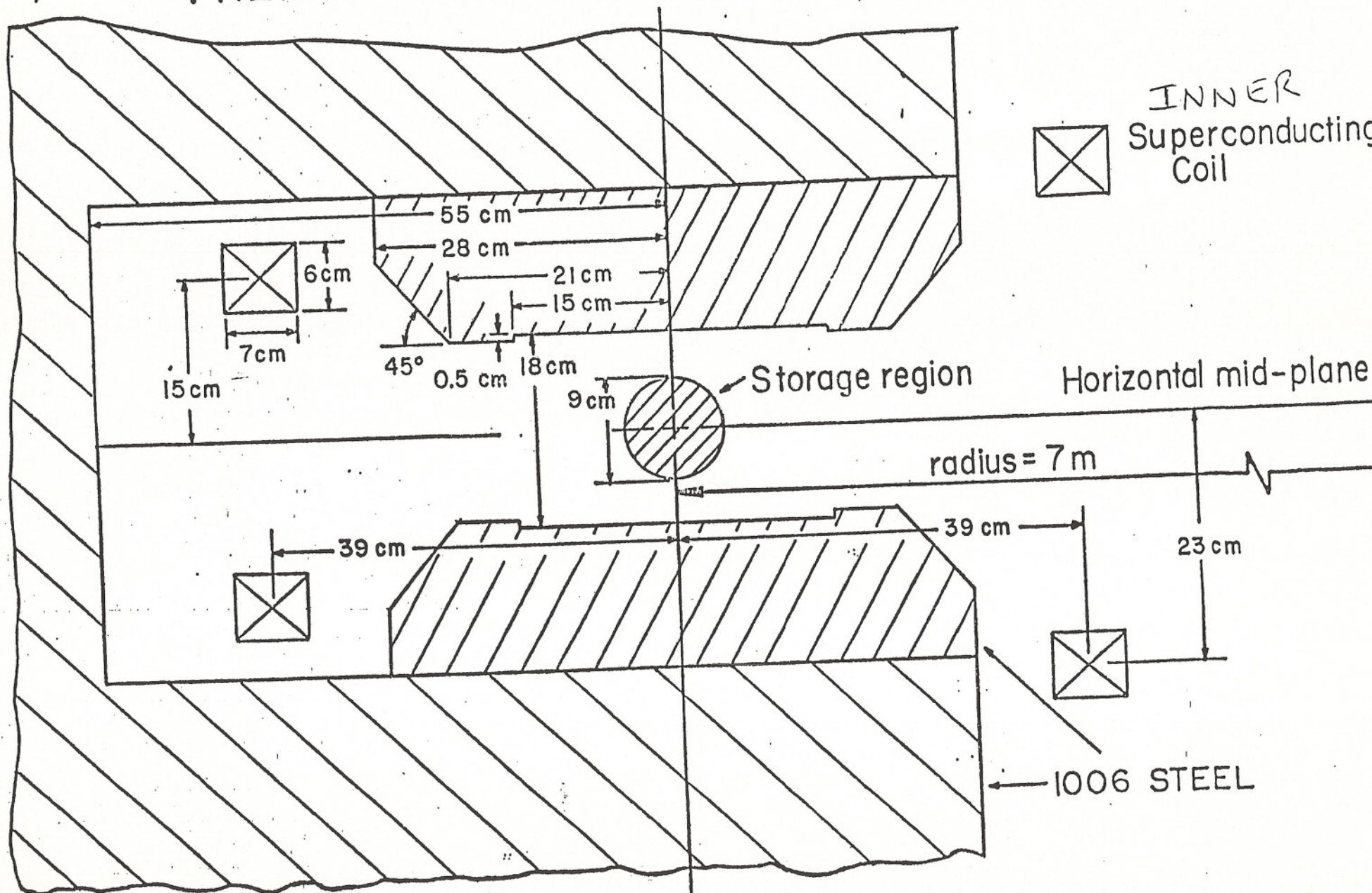


FIG. 1

G-2

INNER
COIL

γ/ϵ
[CM]

B_0
[RG]

INNER
COIL

F_x F_y
[LB/IN]

OUTER
COIL

F_x F_y

23

14.368

+33 +119

-140 +127

26

14.349

+15 +114

-140 +127

28

14.338

+6.2 +110

-140 +127

30

14.325

~~-1.4~~
~~-440~~ +105

-140 +127

TABLE I

GTD/JWJ

4/86

FIG. 2

F_x
[LB./IN.]

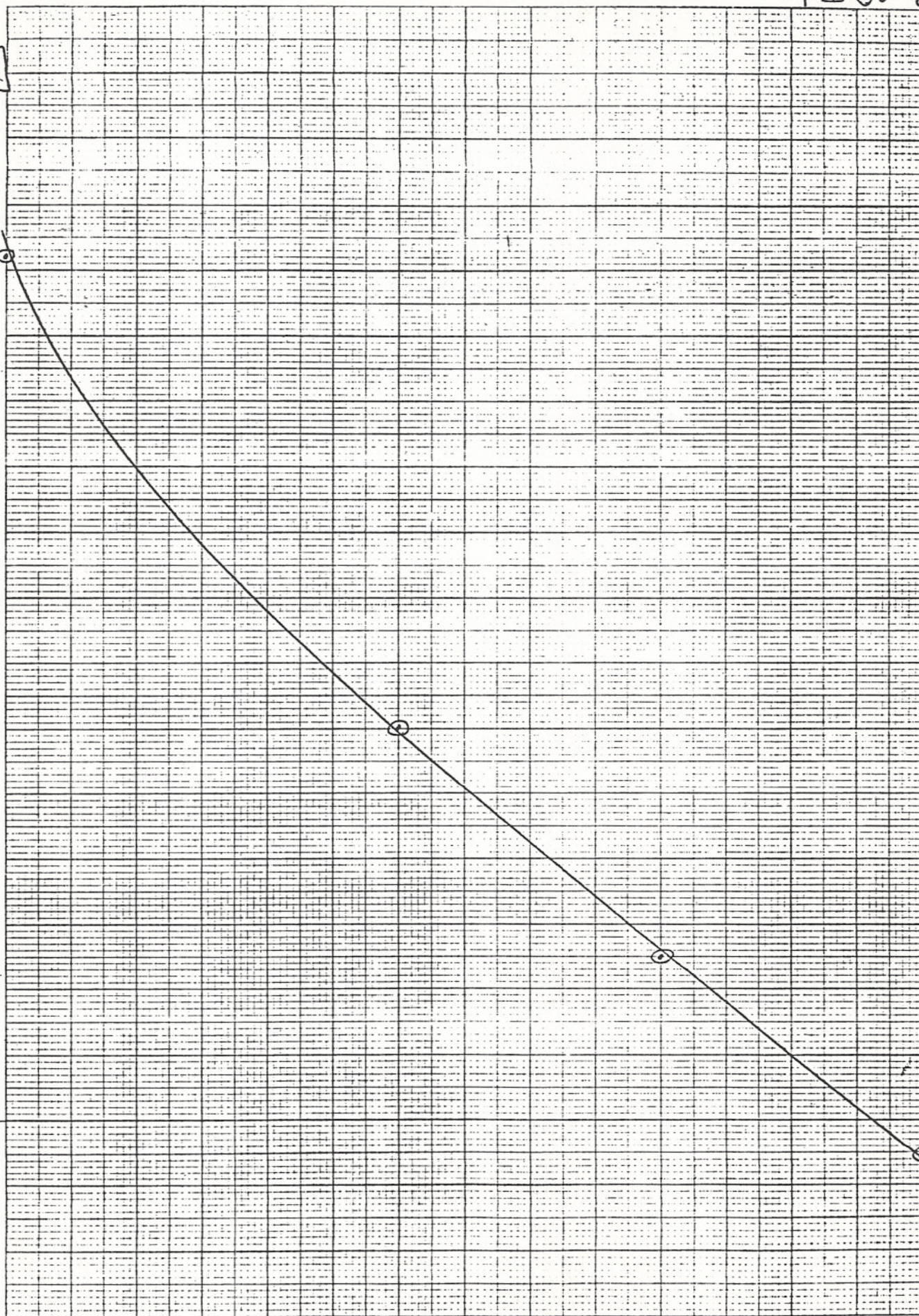
46 1320

K&E
10 X 10 TO 1/2 INCH 7 X 10 INCHES
KEUFFEL & ESSER CO. MADE IN U.S.A.

35
30
25
20
15
10
+5
0
-5

23 24 25 26 27 28 29 30

Y_0 (CM)



June 13, 1986

Muon g-2 Group

G.T. Danby/J.W. Jackson

Magnet Design

July 86 Meeting
Presentation B

①

We would like to report on [1] recent (1986) magnetic design work that has contributed to the parameters and tolerance of the preliminary engineering drawings.

In addition [2], comments will be given on earlier work prior to the Proposal and [3] on plans for new activities prior to the proposal revisions later this summer.

1. 1986-Magnetic Design Work

- a. The POISSON calculations were compared for different convergence criteria for two different but realistic permeability tables (1006 and decarburized Fe/sheet steel) and also for the agreement between the multipoles and the actual computed field.
- b. The version of the POISSON code on the BNL CDC7600 and the VAX code were compared. They agreed on the calculated field, but disagreed on the multipole description of the field. This problem was due to a "bug" in the VAX version as related to calculating C magnets (zero not at the center of the universe of the problem).
- c. This problem with the VAX at Yale was rectified by Y. Kuang.
- d. During 1985 we explored locating an air gap at the base of the poles. This can be shimmed to control the field. This technique would be much easier to use if the inside coils were located further from the horizontal midplane.

The magnetic field produced for constant current and the efficiency of the magnetic circuit were observed by calculating the magnet for various coil locations. In fact, the efficiency of the magnet is only very slightly effected, so the weight of Fe required does not change as the coil is moved above the pole.

- e. An additional advantage is that near the desired new location, the inside coil becomes "force-free" in the horizontal plane. At the original location, the force created a negative hoop stress.

f. The efficiency of the magnet, as defined by minimizing the Fe volume, requires minimizing the integrated flux across the HMP

$$B_0 W = \int_{\text{inside}}^{\text{outside}} B dr$$

In fact, by this criteria, the present preliminary design with the chamfered pole is somewhat more efficient than the CERN design.

2. Work Prior to Proposal

- a. The magnet in the Proposal weighed 1000 tons. It was costed by MIT at 0.50 \$/lb or 1M\$ in total for the magnet iron components. Two late modifications were made to the design in the Proposal by the authors.
- b. The design used the 2D computed cross section, but applied directly to a closed ring structure. Since the Fe return is at a larger radius, this results in a larger overestimate in required Fe. Corrected for this 3D effect, the Fe weight is 794 tonnes.
- c. A preliminary design of a detailed pole profile was computed to demonstrate the necessary field uniformity. This was included in the Proposal.
- d. With this pole profile, it was observed that the magnet was slightly more efficient than the CERN magnet. The field in the yoke is at present 15 kG, as compared to the 16 kG in the CERN magnet.
- e. The CERN magnet weighed 450 tonnes. It is noteworthy that the Proposal magnet weight of 794 $\left[\times \left(\frac{14}{18} \right)^2 \times \frac{15}{16} \right] = 450$ tonnes. Thus, scaling the Proposal magnet from 18 cm gap to 14 cm gap and reducing the yoke thickness by $\frac{15}{16}$ results in the same weight as the CERN magnet.

3. New Activities

- a. During the summer of 1985, the question of an air gap between the poles and yoke return was explored by the authors in two reports. This approach was not included in the Proposal because it was too preliminary and the design in the Proposal was more directly based on CERN.
- b. For the late July meeting, it is intended to study shimming of a thick air gap at the pole base for field control.
- c. An auxiliary benefit of decoupling the poles from the yoke return is that we can operate the yoke at somewhat higher fields and save some additional weight.

From Proposal

(3)

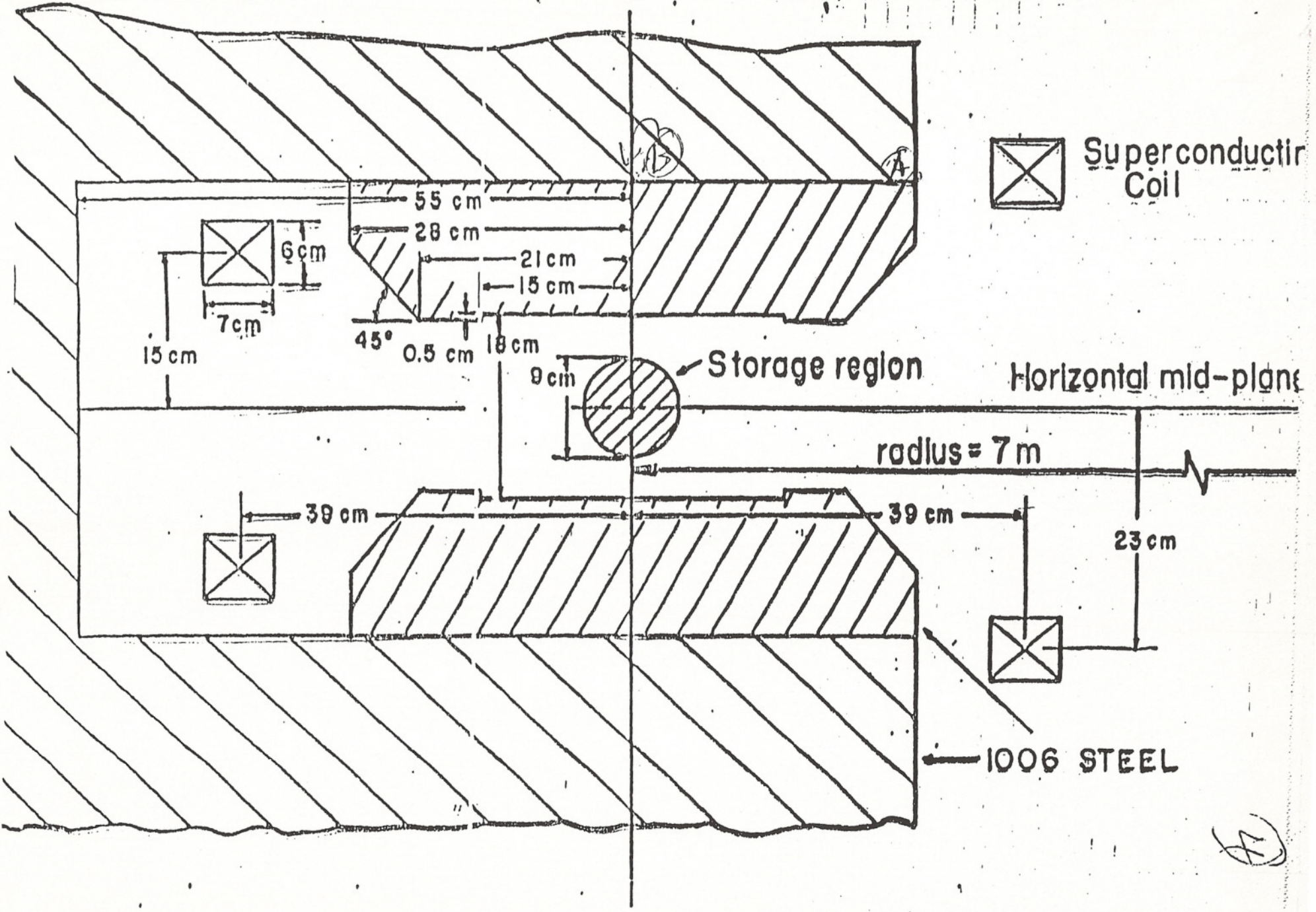
Table 1

Design Characteristics
Storage Ring Magnet for g-2 Experiment

Central field	1.47 T
Beam centerline radius	7.0 m
Gap	18.0 cm
Pole Width	56.6 cm
Operating current	3,700 A
Ampere turns	221,000 A
Inductance	0.81 H
Overall dimensions:	
Yoke inside radius	6.72 m
Yoke outside radius	8.13 m
Yoke height	170.0 cm
Weights (kilograms):	
Conductor cable	370
Conductor stabilizer	2,660
Helium vessels (coil container)	4,970
Vacuum vessels (including thermal shields, supports, etc.)	16,060
Steel	792,540
TOTAL WEIGHT (kg)	816,500

Note. This is correct weight assuming
Fe cross-section modified so that continuous
(3D) ring has the same cross-sectional area as
computer design gives in 2D. This is $2\pi \times 7$ m
times 2D area. Since the Fe flux return is a large
radius, its cross-section diminishes.

PRELIMINARY MAGNET POLE PROFILE



Proposed \downarrow Minimum possible vertical distance \downarrow

INNER COIL $\left\{ \begin{array}{l} \Phi = 23 \text{ cm} \\ \text{SURFACE} = 20 \end{array} \right.$

15 cm
12

CERN
14cm gap

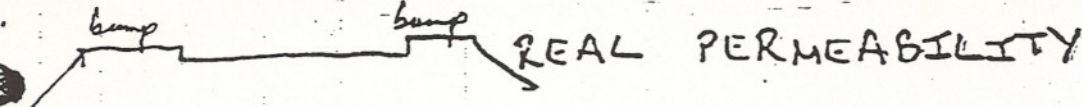
(5)

[UNITS]

B_0	[DG]	14.29566	14.349	14.573
FIELD AT (A)	[DG]	17.42	16.96	19.80
see Φ (4) for location		(1.22)	(1.18)	(1.36)
FIELD AT (B)	[DG]	17.24	16.83	19.73
		(1.21)	(1.17)	(1.35)
"AMP FAC"		1.026	1.022	1.122
BYOKE	[DG]	15.1	14.8	16.0
$\langle W \rangle$	[CM]	68.64	66.90	54.91
$\langle w \rangle / g$		3.81	3.72	3.92
$\langle w \rangle = \frac{\int B dl}{B_0}$				
$g = \text{gap}$				

EFFECT & TOLERANCE OF SYMMETRICAL FE POLE BUMPS

6



l_m	EFFECT	TOLERANCE
$n = 0$	-28.0	-0.28 GAUSS
1	-0.9	0.0 PPM
2	208.2	2.1
3	1.8	0.0
4	94.0	0.9
5	0.8	0.0
6	15.8	0.2

TABLE 5

Coil Position Tolerances

<u>M</u>	<u>TERM</u>	↑ INNER COIL	→ INNER COIL	← OUTER COIL (2)
0.	DIPOLE	- 0.602	+ 0.189	+ 0.050
1	QUADRUPOLE	+ 0.020	+ 0.013	- 0.019
2	SEXTUPOLE	- 0.004	- 0.005	- 0.006
3	OCTUPOLE	+ 0.001	+ 0.003	- 0.002
4	DECAPOLE	- 0.001	- 0.001	- 0.001

NOTE: EFFECT EXPRESSED AS PPM PER MIL (0.001")
 MOTION OF 1 COIL AT $\rho = +6$ CM ON
 HORIZONTAL MIDPLANE OF MAGNET.

EFFECT COMPUTED FOR COIL MOTIONS OF
 1 CM AND LINEARLY SCALED TO 1 MIL.

JWJ 11/1/85
 J.W. JACKSON

G-2

WITH 1 CM AIR GAP @ POLE BASE

1 cm air gap under pole

(8)

R=6 CM "BASE" [BASE]
[PPM] ($\mu=0$)

-4 CM
TOP

-8 CM
TOP

-10 CM
TOP

-12 CM
TOP

Fe removed from top
and bottom yoke pieces.

n=1	-12.4	-237.5
2	+115.1	-11.1
3	-11.1	-14.1
4	+26.4	+17.2
5	-1.2	-1.8
6	-4.7	-5.3

	-242.2	-242.3	-243
	-10.1	-10.1	-10.0
	-16.3	-16.4	-17.0
	+17.4	+17.4	+17.4
	-3.1	-3.1	-3.3
	-5.2	-5.2	-5.2

B_0 (HG) 14.7 14.7

14.7

14.7 14.7

NI/2 118.74 [121.60]
(kA)

[123.05]

[124.02] [125.1]

"AMPLIFAC" 1.0 1.024

1.036

1.044 1.050

R=4.5 CM

[PPM]

4.5 cm

1	-178.1	-181.7 PPM	-181.7	-182.0
2	-6.2	-5.7	-5.7	-5.7
3	-6.0	-6.9	-6.9	-7.2
4	+5.4	+5.5	+5.5	+5.5
5	-0.4	-0.7	-0.7	-0.8
6	-0.9	-0.9	-0.9	-0.9

Note field shape change is dipole only.
aberrations not effected by large steel
reduction.

old results (no air gap)

(9)

G. DANBY
J. JACKSON

The following table shows the effect of increasing the width of the vertical FE return by 5 cm (to 66.5 cm). Fig 1 indicates this modification.

Table I

b_m	$\Delta T = +1.5 \text{ cm}$	
$m = 0$	+769	PPM $< 1 \times 10^{-5}$
1	-3.70	↓
2	+2.37	
3	-2.21	
4	+1.05	

Figure 1 also indicates the forces on the coils for the "standard" coil location. These forces are sensitive to coil location and will be summarized in a function of location for the next meeting.

R = 4.5 cm

(10)

[PPM]

"BASE"

± 0.1 cm

± 0.5 cm

SLOPE

SLOPE

M

1 (quadupole)	-186.1	-144.5	-4.1
2	-23.1	-23.0	-19.1
3	-6.8	-7.5	-9.2
4	+0.2	+0.2	+0.1
5	-0.8	-0.8	-0.9
6	-1.2	-1.2	-1.2

NOTES:

2 cm AIR SPACE UNDER POLE

STANDARD POLE BUMP (PROPOSAL)

$B_0 = 14.7$ KG

This illustrates shimming air gap
to reduce quadupole.

OPTIMIZATION OF SYMMETRIC TERMS

(Slight change from old pole profile)

(11)

[PPM]

4.5 cm

4.0

3.0

5.0

n	4.5 cm		4.0		3.0		5.0	
	HMP	VMP	HMP	VMP	HMP	VMP	HMP	VMP
2	0.0	-0.0	0.0		0.0		0.0	
4	+1.5	+1.5	+0.9	+	+0.3	+	+2.3	+
6	-1.1	+1.1	-0.5	+	-0.1	+	-2.1	+
8	-0.2	-0.2	-0.1	-	-0.0	-	-0.5	-
	+0.2	+2.4	+0.3	+1.3	+0.2	+0.4	-0.3	+3.9

©

See p 12 for graph

12

7/88

K&E 10 X 10 TO THE CENTIAR PER
MUMFEL ASSOCIATED MANUFACTURING

5.0

4.5

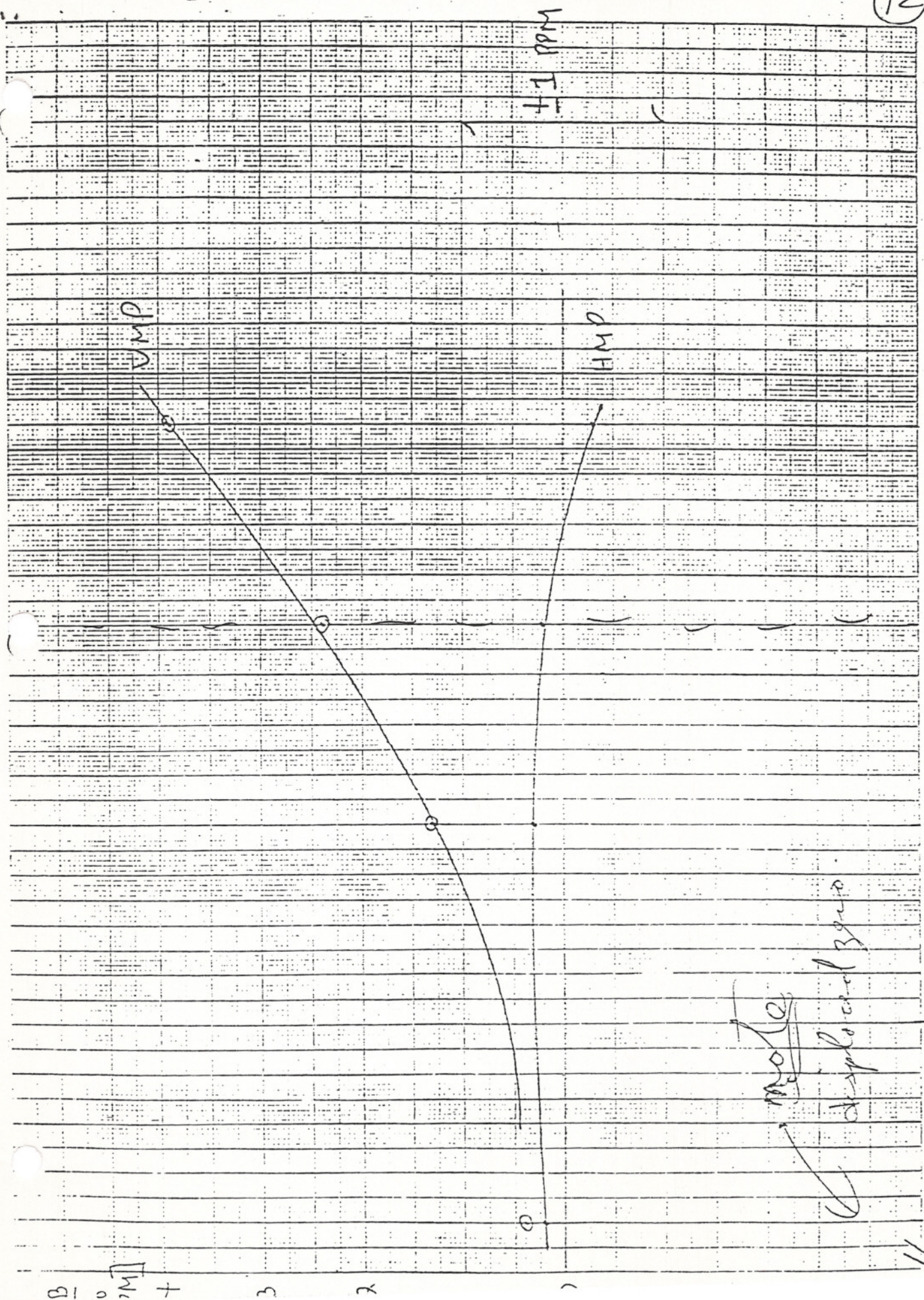
4.0

3.5

3

ΔR [cm]

461510



41 ppm

VMP

HMP

note
displaced zero

BI [m]

3

2

1

||

M A T E R I A L F O R G-2 M E E T I N G

September 7-8, 1986

G.T. Danby and J.W. Jackson

Material for G-2 Meeting

September 7-8, 1986

G.T. Danby and J.W. Jackson

A. Summary: Review of magnet development prior to the 1985 G-2 Proposal.

1. The purpose of the magnet effort was to base the design in the Proposal closely on the very successful third generation CERN experiment, for enhanced credibility.
2. The conceptual engineering design was primarily performed by Marston et al. (MIT). This design for the iron yoke was essentially the CERN magnet cross-section, sealed up from 14 cm to 18 cm gap to allow space for more detailed field monitoring and correction.

Superconducting excitation coils replaced the Cu coils used in the CERN design.

Since Fe was judged to be cheap, the cross-section was more conservative (larger), with 10% to 15% lower field in the return yoke than in the CERN magnet. The engineering design drawings appear in the Proposal.

3. The computer-aided precision magnetic field design of the pole shapes and of field shimming was carried out by Danby and Jackson (BNL). This included:
 - (i) demonstration of very high precision (PPM) field shaping capability for perturbations.
 - (ii) tolerances on pole-pieces, yoke pieces, and coil locations were calculated.
 - (iii) shimming methods to provide fine control of field shapes to very high tolerances, i.e., small compared to construction errors even with the very best machining.

Some of this precision field design effort appeared in the Proposal and some did not.

4. In the Proposal was:

- (i) a preliminary pole shaped to demonstrate theoretically a very uniform field.
- (ii) the necessary 2D to 3D transformation of the return yoke was recognized and calculated. This will be explained in Appendix I. This impacts on the total magnet weight and provides the equivalent 3D yoke reluctance to that computed (2D).

The reduced 3D weight was included in the Proposal, as was a sketch of the 3D cross-section. However, the engineering drawings showed the 2D cross-section.

5. Not in the Proposal was a computer-aided precision shimming design study of a large air gap located between each pole piece and the return yoke. This has two great potential benefits to exploit.

- (a) The air gap makes the field in the aperture much less sensitive to the properties of the yoke flux return.
- (b) The studies demonstrated that shimming at various locations in this air gap behind the pole piece was a powerful technique for very sensitive field shaping.

6. This air gap study was not included in the Proposal because, in spite of its attractiveness, it deviated from the CERN experiment and was judged to need more development.

B. Progress during 1987 related directly to the Proposal update.

- 1. The efforts of an enlarged Group at BNL (Shutt et al.), Yale, and Boston University have concentrated on solicitation of industrial quotes to establish a cost basis for the magnet return yoke.
- 2. The engineering cross-section contained in the Proposal was used, with the computer designed pole pieces assumed. (This is a small change in terms of cost.)

During the preparations for the solicitation of industrial suppliers, additional study of assembly, support, and tolerance consideration was carried out and small modifications made.

3. During the course of 1987, the theoretical design of poles with a large shimable air gap interfacing with the yoke return has been accepted as the main stream approach presently favored.

Experimental studies of this concept will be carried out in existing magnets during the next year.

Subject to this verification this approach will be assumed to be correct, and its consequences for second generation pole profile design and for large yoke weight reduction will be exploited for the next stage of iteration.

C. Comments on meeting with Kobe Steel

1. They responded to the Solicitation which has a cross-section substantially the same as that in the Proposal, and assumes 30° sections of arc.
2. Removing of corners or other simple shaping of geometries is practical for either casting or forgings. Cost reductions will be linear with weight reductions.
3. The 2D to 3D transformation will itself result in a 12% weight reduction.
4. Raising the field level in the return yoke by ~ 10% (still less than in the CERN design) will bring the reduction in weight to 25%.
5. Kobe said that a 25% weight reduction would result in 25% cost reduction.

Furthermore, reducing the number of arc sections would result in considerable savings.

6. The BNL weight limits would now permit 40° arc sections, resulting in 3/4 as many pieces.

7. For comparison, note that the CERN magnet (450 tonnes) scaled up in cross-section directly from 14 cm to 18 cm gap would weigh 84% as much as the original solicited magnet.
8. As a result, a magnet solidly based on the CERN experience, weighing 75% of the weight in the Solicitation and with 75% as many pieces as were costed, should have cost savings of > 30% compared to the Solicitation price responses.

This ignores any further gains from slicing off corners.
9. This puts the magnet Fe as a very reasonable cost with basically an established "CERN" design.
10. If further work on the air gap pole design is confirmed in the next year, newer designs can result in large additional savings prior to actual construction.

Appendix I

The 2-to-3 Dimensional Transformation

[2D to 3D]

1. The CERN magnet yoke was essentially a polygon, composed of 40 straight magnet sections.
2. The present design assumes a continuous ring assembly to avoid the field errors associated with magnet ends.
3. The magnet yoke cross-section was designed in two dimensions: the total weight of a polygon design would be the weight per meter of length times a length of $2\pi \times 7$ meters.
4. In the continuous ring design, the bulk of the Fe flux return yoke is at a considerably larger radius and the cross-section should be scaled down accordingly.. An angular section which is one meter long at the aperture center line radius of 7 m should have the same weight as the 1 m long 2D section.
5. This transformation was not performed on the engineering drawings in the Proposal.
6. Consider first the horizontal mid-plane block to establish the smaller 3D outside radius Γ_3 .

2D area = 3D area (for same reluctance)

$$(\Gamma_2 - \Gamma_{in}) \times 2\pi \times 7 \text{ m} = (\Gamma_3^2 - \Gamma_{in}^2)\pi$$

7. Finally, a $1/\Gamma$ thickness adjustment should be applied to the top and bottom yoke pieces.
8. It should be emphasized that the 2D to 3D core transformation not only saves weight and cost, but it is necessary to make the magnet equivalent to the computer calculations. Otherwise there is excess yoke cross-section.

NOTES OF g-2 MEETING

February 5, 1987

G.T. Danby and J.W. Jackson

1. Asked to speak on the status of the magnet.
2. Magnet Fe has received the bulk of the attention to date
 - (a) dominates the precision of the field
 - (b) dominates cost.
3. After the g-2 Group decided to concentrate on a 15 kG design similar to the CERN ~1 PPM magnet system, the decision was made to increase the gap from 14 cm to 16 cm.
4. The extra space was allotted for additional field monitoring and correction coils, etc. to try for a factor of > 10 improvement in the field uniformity and knowledge of the field.
5. The credibility of a Proposal for such a superprecise experiment was greatly enhanced by basing it on the very successful CERN design.
6. Vernon and Gordon went to MIT to talk about the experiment. P. Marston suggested the credibility achieved was not diminished by going to superconducting excitation coils [Super Ferric].

This was accepted and the Group proceeded with a larger cross section C magnet design than CERN, also operating at $B_p = 14.7 \text{ kG} \cdot \text{m}$ radius.
7. Marston et al. at MIT carried out the bulk of the preliminary steel and coil design and cost estimates which appear in the 1985 Proposal.
8. We (Danby and Jackson) specifically contributed a precision pole design and a reduction in weight (in the tables--not the drawings) by the appropriate 2D to 3D transformation.
9. Of course the entire Group involved contributed to the evolution of the design and to the material in the Proposal.
10. The Proposal was well received, and attention shifted to the credibility of the costs, especially the dominant cost factor, the magnet steel which was costed at 50¢/lb.
11. An enlarged BNL Group (Shutt et al.) took on the task principally of preparing for solicitations on the steel so that the 1986 Proposal Review would have established steel costs.
12. More recently the coil design is receiving considerable attention, but that is Ralph Shutt's story.

TABLE II. ERRORS IN AGS EXPERIMENT

COUNTING RATES AND STATISTICAL ERRORS

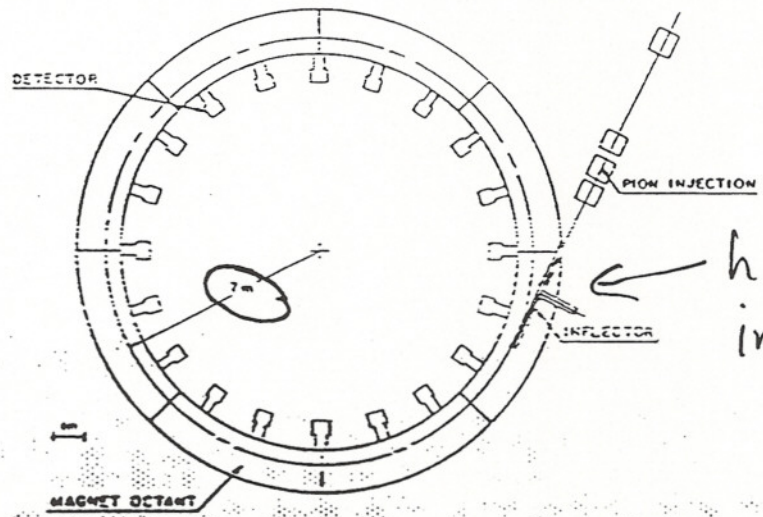
STORAGE APERTURE DIAMETER	90 mm
PROTONS PER RF BUNCH WITH BOOSTER	4.7×10^{12}
BUNCHES EJECTED PER RING-FILL	2
PROTONS PER FILL	8.4×10^{12}
PION μ/μ	$\pm 0.6\%$
PIONS AT INFLECTOR EXIT PER FILL (1.28×10^7 PER 10^{12} PROTONS)	1.07×10^4
PIONS STORED PER FILL (AT 134 PPM CAPTURE EFFICIENCY)	14×10^4
ELECTRONS COUNTED ABOVE 1.6 KEV PER FILL (20% OF THE DECAYS)	2.8×10^4
FILLS PER AGS CYCLE (1.4 s)	3
FRACTION OF AGS PROTONS USED	50%
FILLS PER HOUR	7714
ELECTRON COUNTS PER HOUR	77×10^6
RUNNING TIME FOR 0.3 PPM (1 STD. DEV.)	1722 HOURS

high performance
(post booster)
AGS

SYSTEMATIC ERRORS

SOURCE	COMMENTS	ERROR (ppm)
MAGNETIC FIELD	INCLUDES ABSOLUTE CALIBRATION OF NMR PROBES AND AVERAGING OVER SPACE, TIME, AND PION DISTRIBUTION.	0.07
ELECTRIC FIELD CORRECTION	0.7 PPM CORRECTION	0.03
PITCH CORRECTION	0.2 PPM CORRECTION	0.02
PARTICLE LOSSES		0.5
TIMING ERRORS		0.01
	TOTAL	0.09

very accurate!



holes for injector etc.

Fig. 1: AGS MUON $\sigma=2$ Experiment. Spin motion - In a magnetic field B,

$$\omega_s = \frac{eB}{mc\gamma} + \frac{e}{mc} aB;$$

$$\omega_a = \omega_s - \omega_c$$

In a magnetic field B and electric field E

$$\omega_a = \frac{e}{mc} \left[aB + \left(a - \frac{1}{\gamma^2 - 1} \right) \left| \beta \times \vec{E} \right| \right]$$

$\gamma_{magic} = 29.3, \omega_a = \frac{e}{mc} aB$

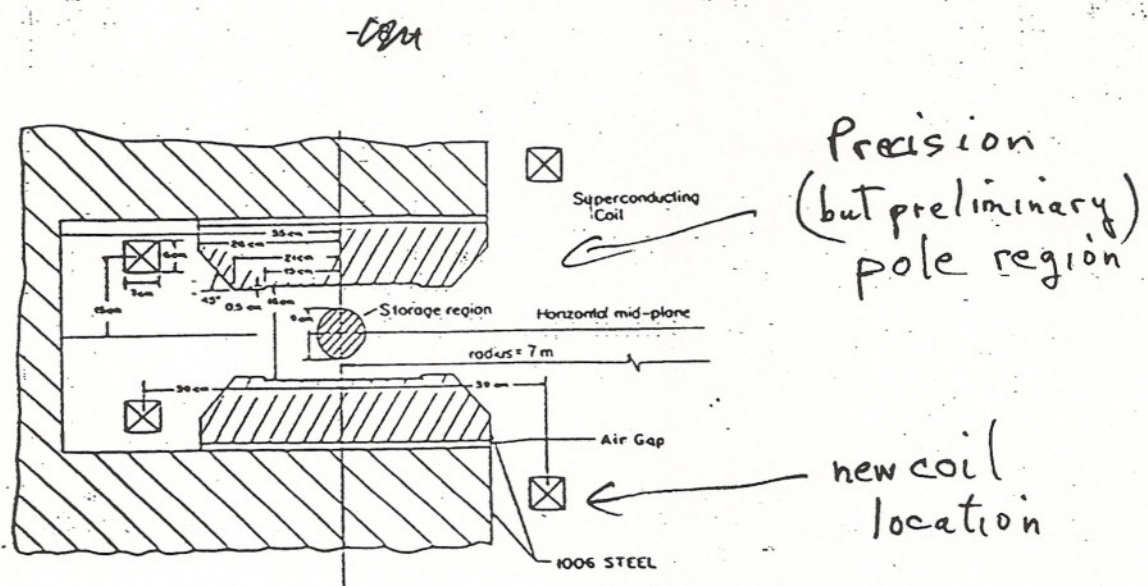


Fig. 3: Preliminary profile of magnet pole face-computer simulated.

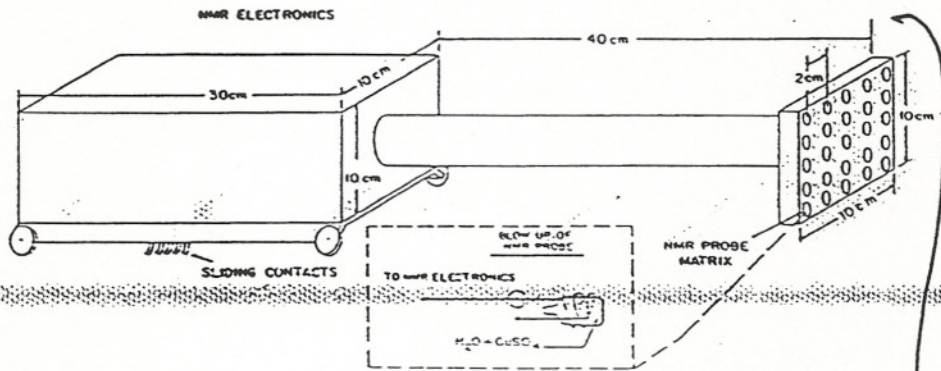
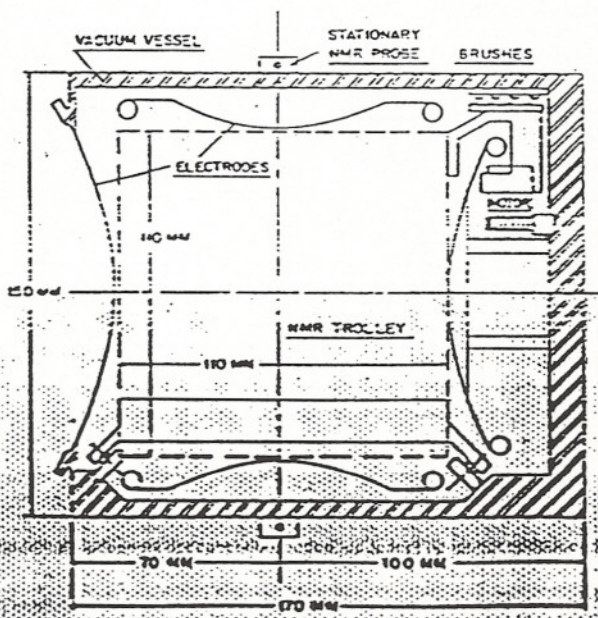
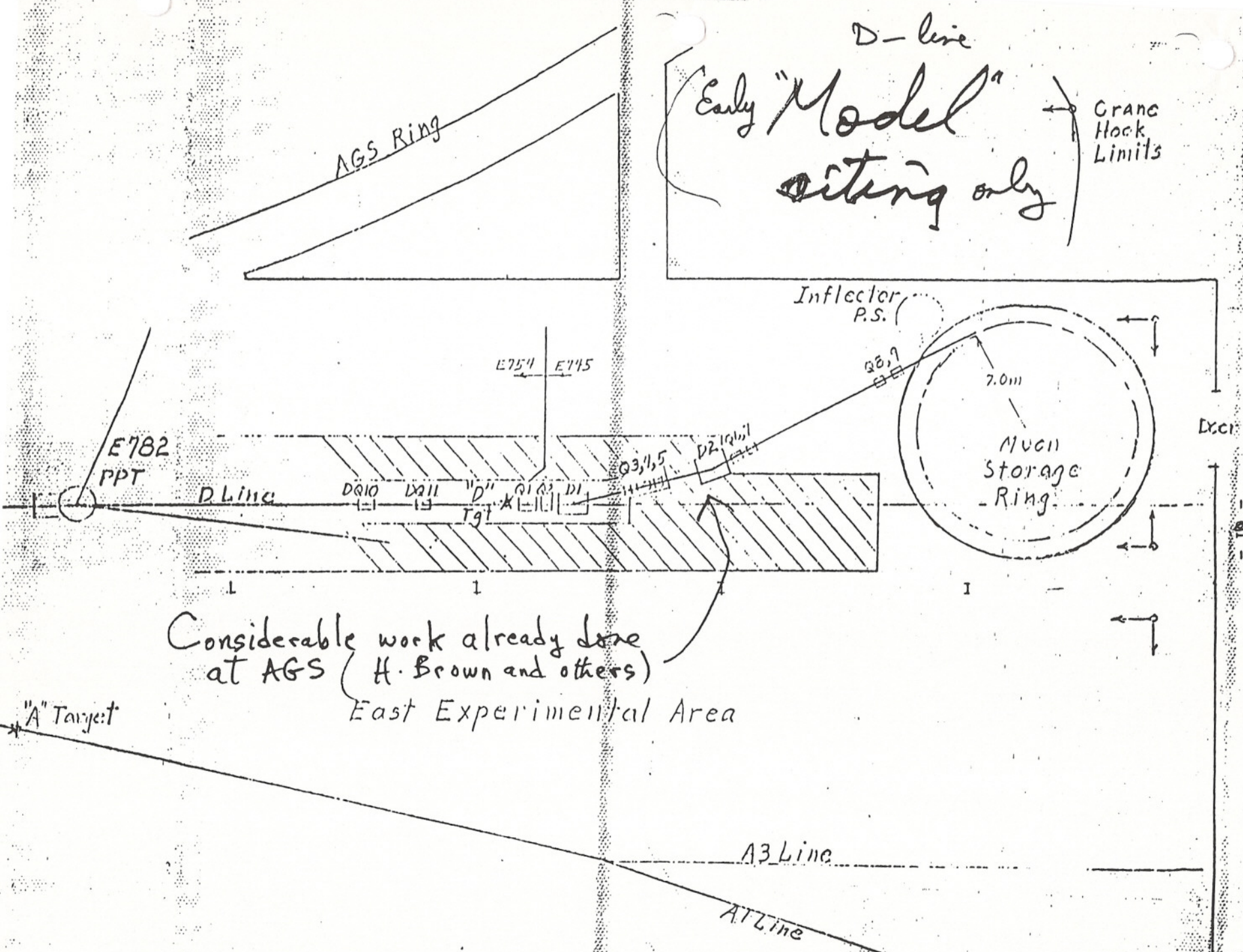


Fig. 4: NMR trolley with probe matrix.



must fit in.

Fig. 5: Configuration of the quadrupole electrodes showing the arrangement for movement of the NMR trolley.

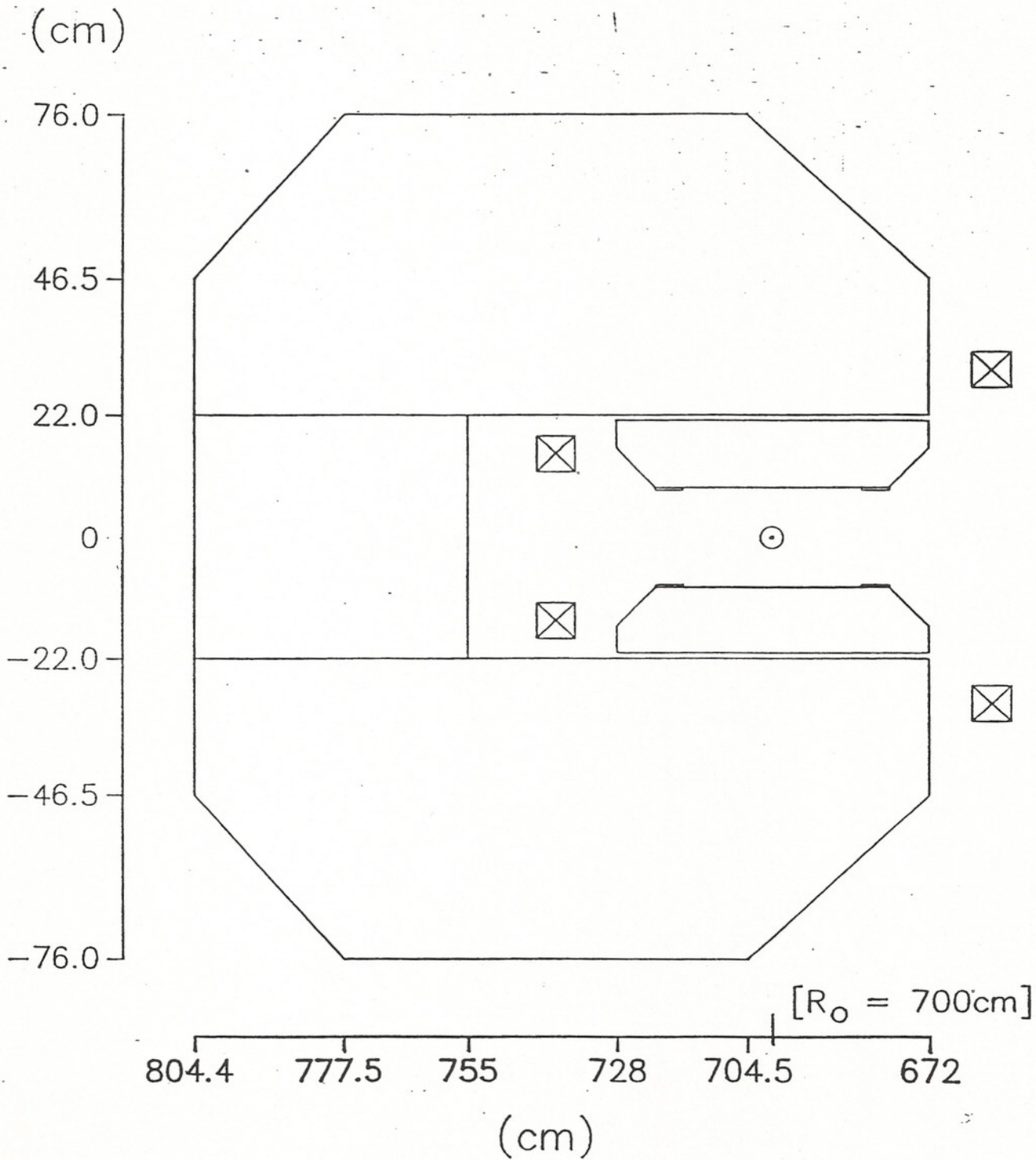


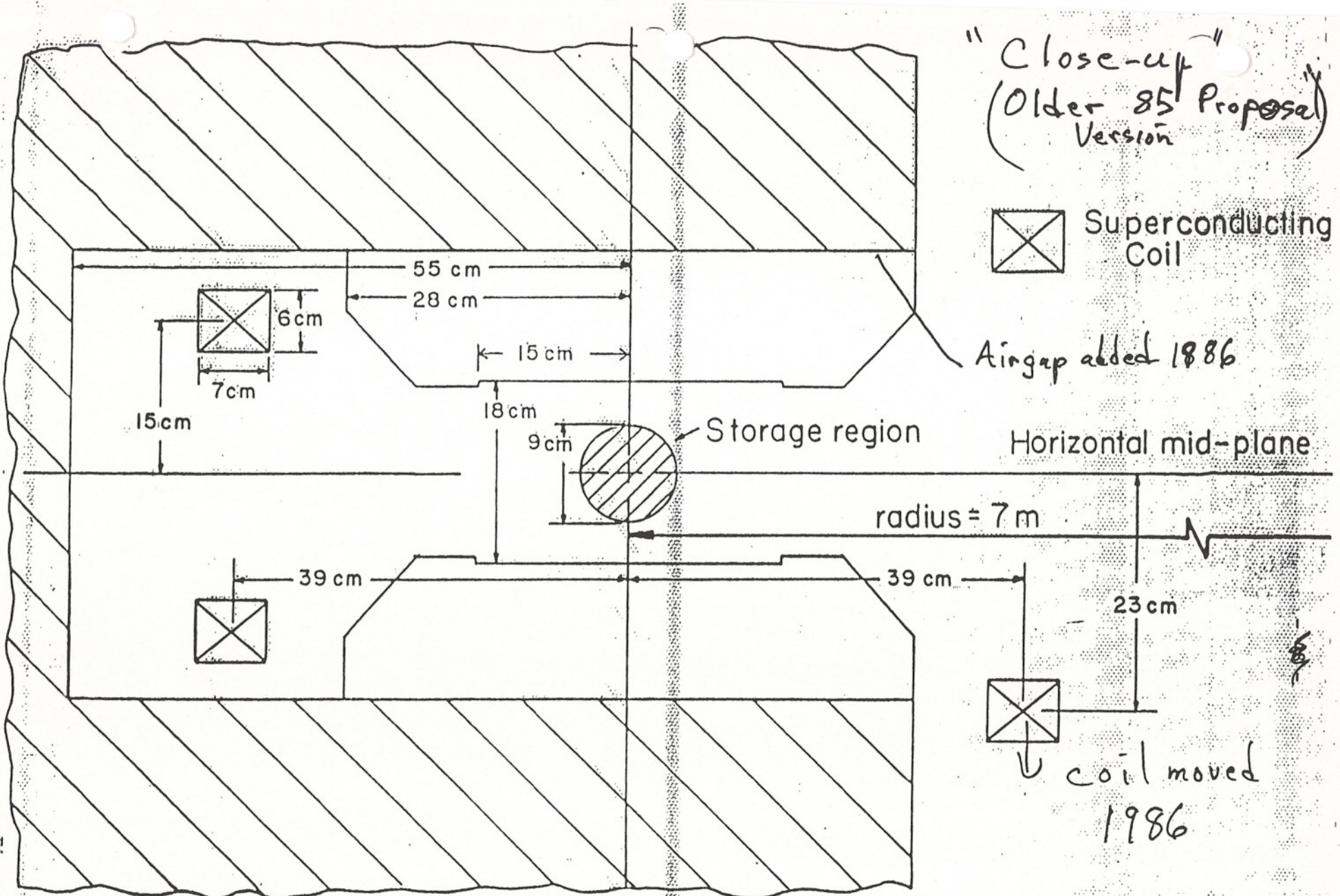
Considerable work already done
 at AGS (H. Brown and others)
 East Experimental Area

Experimental layout of pion beam transport system and muon storage ring in the East Experimental Area.

[2-87]

CROSS-SECTION G-2





"Close-up"
(Older 85 Proposal)
Version

☒ Superconducting
Coil

Airing added 1986

Storage region

Horizontal mid-plane

radius = 7 m

23 cm

coil moved
1986

PRELIMINARY POLE PROFILE - COMPUTER SIMULATED

Figure III-5

7.

8.
First page of earlier report on
type of computer input.

June 13, 1986

Muon g-2 Group

G.T. Danby/J.W. Jackson

Magnet Design

We would like to report on [1] recent (1986) magnetic design work that has contributed to the parameters and tolerance of the preliminary engineering drawings.

In addition [2], comments will be given on earlier work prior to the Proposal and [3] on plans for new activities prior to the proposal revisions later this summer.

1. 1986 Magnetic Design Work

- ①
"computer"
accuracy →
studies
- a. The POISSON calculations were compared for different convergence criteria for two different but realistic permeability tables (1006 and decarburized Fe/sheet steel) and also for the agreement between the multipoles and the actual computed field.
- b. The version of the POISSON code on the BNL CDC7600 and the VAX code were compared. They agreed on the calculated field, but disagreed on the multipole description of the field. This problem was due to a "bug" in the VAX version as related to calculating C magnets (zero not at the center of the universe of the problem).
- c. This problem with the VAX at Yale was rectified by Y. Kuang.
- ② →
air gap
- d. During 1985 we explored locating an air gap at the base of the poles. This can be shimmed to control the field. This technique would be much easier to use if the inside coils were located further from the horizontal midplane.

The magnetic field produced for constant current and the efficiency of the magnetic circuit were observed by calculating the magnet for various coil locations. In fact, the efficiency of the magnet is only very slightly effected, so the weight of Fe required does not change as the coil is moved above the pole.

- ③ →
forces
- e. An additional advantage is that near the desired new location, the inside coil becomes "force-free" in the horizontal plane. At the original location, the force created a negative hoop stress.

PERTURBATION OF POLE BUMPS

[This is update results [2-87] at $B = 14.76G$]

MULTIPOLE #	BASE	(A) ADD .02 CM TO BOTH BUMPS (x2)	(B) ADD .02 TO INNER BUMPS	(C) ADD .02 TO OUTER BUMPS
	<u>PPM</u>			
1 (quad)	-222.9	-223.6	-204.9	-241.3
2 (sex)	-38.8	-8.7	-23.9	-23.7
3	-6.1	-6.0	+1.8	-13.8
4	-0.2	+5.6	+2.7	+2.7
5	-0.6	-0.6	+0.2	-1.4
6	-1.3	-0.9	-1.1	-1.1

	I <u>(A)-BASE</u>	II <u>(B)-BASE</u>	III <u>(C)-BASE</u>
1 quad	-0.7	+18.0	-18.4
2 sex	+30.1	+14.9	+15.1
3 oct.	+0.1	+7.9	-7.7
4 10-pole	+5.8	+2.9	+2.9
5 12-pole	0.0	+0.8	-0.8
6	+0.4	+0.2	+0.2

NOTE: MULTIPOLES EXPRESSED IN PPM AT $X=4.5, Y=0$ CM

- (a) Column I shows π -fold symmetric bump gives even powers only
- (b) Cols II and III each give $\frac{1}{2}$ of symmetric and equal + opposite antisymmetric terms with real permeability.
- (c) Note that 1mil (25 μ m) rms bump errors would give 2 PPM sextupole and \sim nothing else (symmetric) and 2 PPM quadrupole " " " (antisymmetric).
- (d) skew moments (not computed yet) will be comparable.

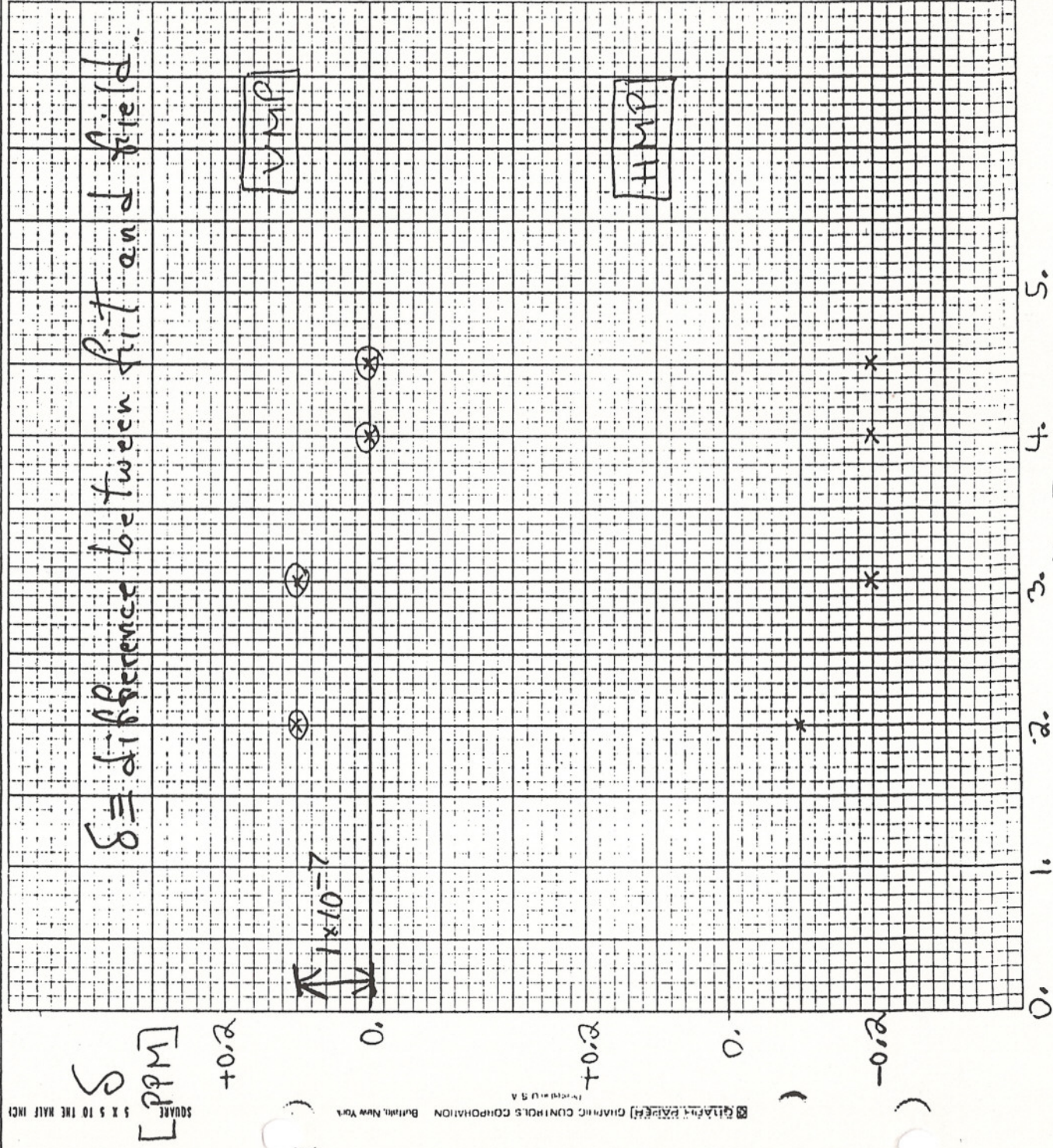
LITHOGRAPHED IN U.S.A. ADDRESS: WILEY PUBLISHING COMPANY INC. READING, MASS. A-W Distributors

Computer calculates field at 14.766 and 1006 μ -table
 Multipoles are fitted to resultant field

FIELD DIFFERENCE δ

(COMPUTED - HARMONIC ANALYSIS RECONSTRUCTION)

[Multipoles are great aid to field analysis & correction]
 [2D to 3D transformation straight-forward]



Example of perturbing 1cm air gap at pole base. = 11.

MULTIPOLE #	I POLE SLOPE	II POLE SLOPE	III EFFECT of gap "wedge"
	1 ± 0.0 cm	1 ± 0.40 cm	
1 (quad)	-204.6	+3.4	+208.0
2 (sex)	-38.9	-32.8	+6.1
3	+1.7	-1.1	-2.8
4	-0.2	-0.5	-0.3
5	+0.2	+0.2	0.0
6	-1.3	-1.3	0.0
7	-0.0	-0.0	0.0
8	-0.2	-0.2	0.0

NOTE: MULTIPOLES EXPRESSED IN PPM AT $X=4.5, Y=0$ cm
 $B_0 = 14.7$ kG

(a) Same effect can be accomplished (e.g. I \rightarrow II) by air gap shimming.

(b) Note that II shows a more advanced pole design [2-87] than before

(1) slight touchup will make antisymmetric terms ≤ 1 PPM

(2) Symmetric profile needs to be modified to adjust 33 PPM sextupole; other terms 1 PPM.

(c) III shows that gradient tuning in air gap region gives almost pure quadrupole correction.

COIL POSITION TOLERANCE

12.

<u>m</u>	<u>TERM</u>	OUTER	OUTER
		COIL	COIL
		<u>UP 1 MM.</u>	<u>INWARD 1 MM.</u>
0	DIPOLE	-24.1	+7.57
1	QUADRUPOLE	+0.60	+0.38
2	SEXTUPOLE	-0.09	-0.12
3	OCTUPOLE	+0.02	+0.04
4	DECAPOLE	-0.01	-0.02

NOTES:

1. EFFECT EXPRESSED AS PPM PER MM. (0.040") OF MOTION OF 1 COIL AT $\rho = +4.5$ CM.
2. MULTIPOLES EXPRESSED AT $(\rho, y) = (4.5, 0.0)$ CM.
3. OUTER COILS ARE LOCATED INSIDE C-SHAPED FI YOKE AT $R = 739$ CM, $Y = \pm 15$ CM.
4. INNER COIL NOT TABULATED, BUT COIL POSITION SENSITIVITY LESS.
5. ALL MULTIPOLE TERMS < 1 PPM, EXCEPT FOR DIPOLE TERM.

BTD/JWJ

10/86

PROBLEMS ADDRESSED

1. Thickness and tolerances on yoke pieces. (W and W/O air gap.)
2. Yoke shimming and pole shimming ("wavelength").
3. Studied air gap before 1985 Proposal. Not included until 1986 version. (Untested)
4. Shimming in the air gap is ~ 2 orders of magnitude less sensitive than pole face shims. ($\Delta_{\text{gap}} = 1 \text{ mil} \sim 140 \text{ PPM.}$)
5. Longer "wavelength" shimming, implies smooth pole surfaces.
6. Forces and positional tolerances on coils.
7. Moving inner coil to "force free" radial/condition to prevent collapsing forces on the coil hoop.
8. Reduced Fe weight to ~ 2/3 original
 - (a) air gap permits higher B yoke
 - (b) "3D" not discussed today
 - (c) "corners" can be cut and save raw steel in forgings
 - (d) weight reduction permits 45° sectors which are within AGS crane limits

PROBLEMS TO BE ADDRESSED (incomplete list)

1. Yoke pieces have conventional tolerances and requirements (most of cost) but dimensions etc. are subject to feedback.

Caution: Interaction with other components is quite incomplete.
2. Pole pieces are special:
 - (a) grinding and/or polishing is possible if necessary
 - (b) testable and interchangeable (removable)
3. CERN did extensive grinding in situ on pole surface
 - (a) time consuming
 - (b) makes "potholes" if perturbations are near beam aperture.
4. Hope to minimize Item 3, if possible. Experiments are required.

5. Modeling Program (1987)

- (a) > 1/2 scale pole profiles in existing AGS beam magnet (with coils spread)
- (b) will model pole surfaces, air gap, and air gap shimming
- (c) need transistor regulation if NMR used.

GENERAL PROBLEMS

1. Interaction

- (a) injector
- (b) coil support
- (c) coil ends
- (d) vacuum system, etc.
- (e) correction coils

2. Environment

- (a) siting at AGS
- (b) Stable mechanical and thermal base with temperature control
- (c) vibration "free"
- (d) housing - flux and thermal screening
- (e) redundant very reliable cryogenic system to minimize magnet cycles (magnetization)
- (f) stable magnet support, with survey and adjustment of supports.

Experimental Program: for Pole Development Only

DANBY / JACKSON 2/87

1. Purpose.

- (i) Test pole materials for magnetic and mechanical properties: i.e. better magnetic steels, inclusions ("potholes") and other mechanical properties of pole surfaces
- (ii) Pole support: i.e. methods of support of poles (pole surfaces).
- (iii) Pole surfaces: polishing & grinding for uniformity?
- (iv) Pole shimming: bumps, etc.
- (v) Air Gap: adjustment and shimming.
- (vi) Test of measurement techniques.

Note. This is not a G-2 magnet model.

2. Initial Program.

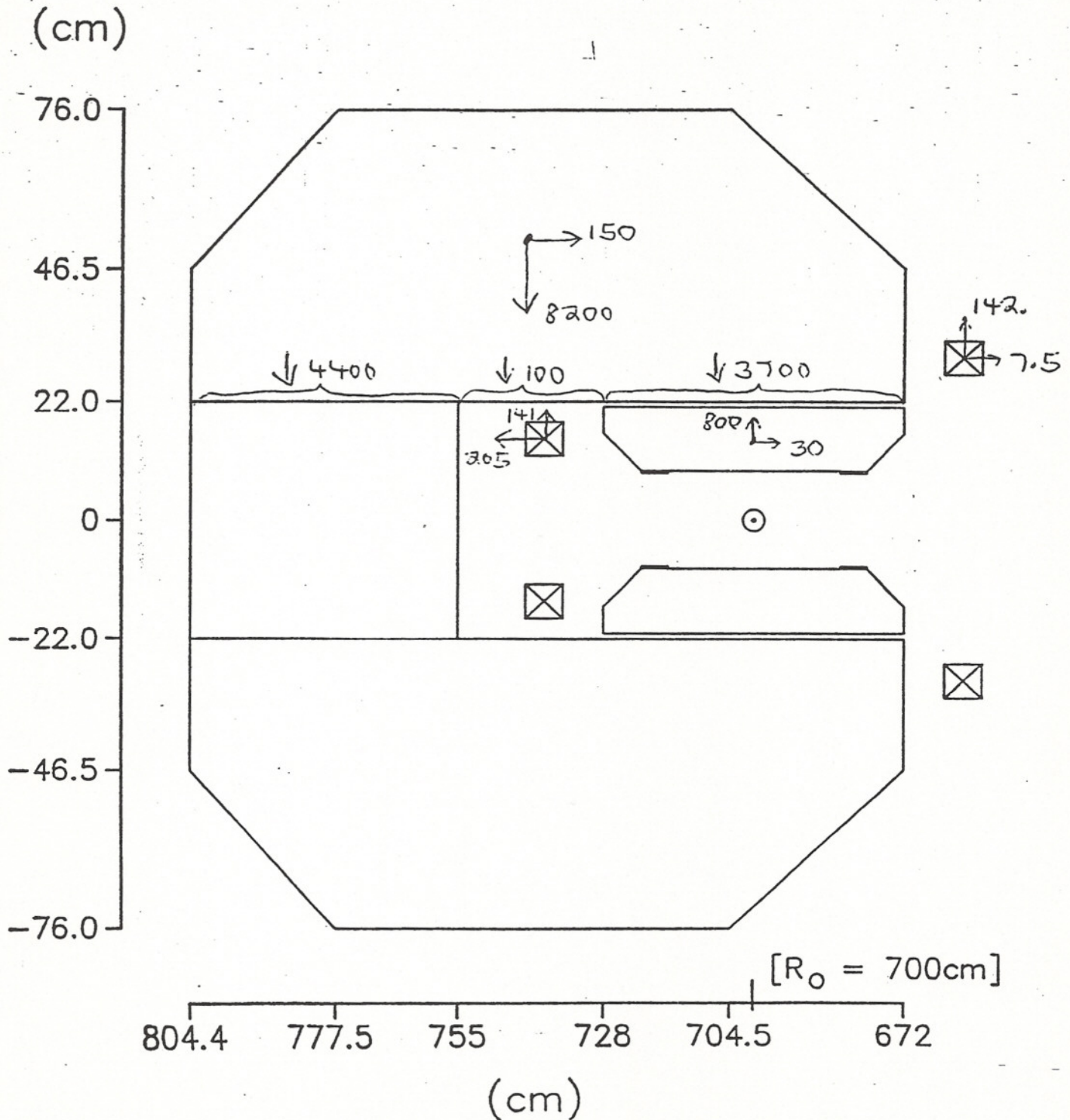
- (i) Standard AGS 18D36 magnet will have gap increased by $\sim 1/2$ ". This is routine procedure, (by adding flux return blocks on HMP).
- (ii) The magnet is available. The modifications and the location of operation for studies is under discussion
- (iii) A space of $\sim 1/2$ " vertically by 36" long will be used to insert a $\sim 0.56X$ scale model of the G-2 polar region. (See Figure)
- (iv) Note that considerable access space exists on either sides of the poles and air gaps.
- (v) Up to ~ 5 " gap ($0.706X$ scale) possible.

FORCES (PRELIMINARY)

2/10/87

@ $B_0 = 14.7 \text{ \AA G}$

CROSS-SECTION G-2



FORCES IN LB./LINEAR INCH AT $R = 7.0$ METERS.

AT RADIUS R , FORCE IS $\text{LB./INCH} \times \left[\frac{R}{7.00} \right]^{-1}$ (POLAR)

Example of perturbing 1 cm air gap at pole base. 11.

MULTIPOLE #	I POLE SLOPE	II POLE SLOPE	III EFFECT of gap "wedge"
	± 0.0 cm	± 0.40 cm	
1 (quad)	-204.6	+3.4	+208.0
2 (sex)	-38.9	-32.8	+6.1
3	+1.7	-1.1	-2.8
4	-0.2	-0.5	-0.3
5	+0.2	+0.2	0.0
6	-1.3	-1.3	0.0
7	-0.0	-0.0	0.0
8	-0.2	-0.2	0.0

NOTE: MULTIPLES EXPRESSED IN PPM AT $X=4.5, Y=0$ CM
 $B_0 = 14.7$ kG

(a) Same effect can be accomplished (cf. I \rightarrow II) by air gap shimming.

(b) Note that II shows a more advanced pole design [2-87] than before

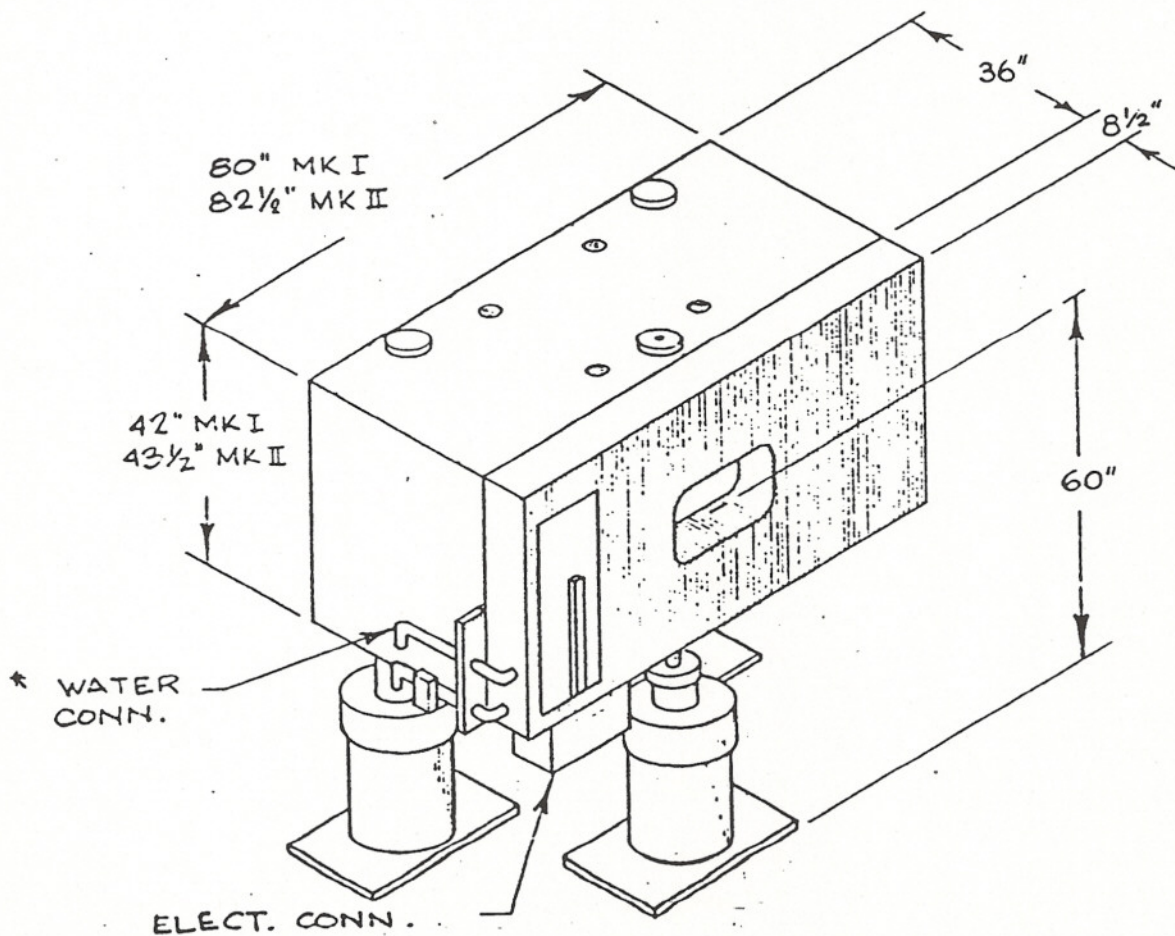
(1) slight touchup will make antisymmetric terms ≤ 1 PPM

(2) Symmetric profile needs to be modified to adjust 33 PPM sextupole; other terms 1 PPM.

(c) III shows that gradient tuning in air gap region gives almost pure quadrupole correction.

18D36

MAXIMUM FIELD (MK. I)	20.5 KG
(MK. II)	22.0 KG
VOLTAGE (MK. I)	109 V
(MK. II)	95 V
CURRENT (MK. I)	2.9 Ka.
(MK. II)	3.0 Ka.
MEAN EFFECTIVE LENGTH	43.0 in.
GROSS WEIGHT	20 Tons
WATER CONSUMPTION (MK. I)	40 GPM
(MK. II)	33 GPM



* WATER CONN. ON UNDERSIDE OF MODIFIED MAGNET.

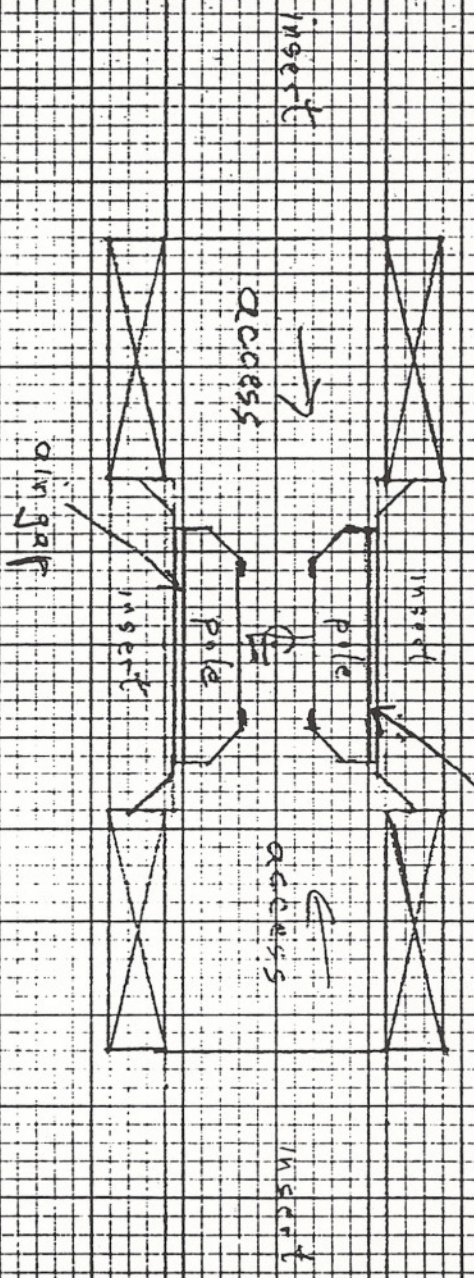
5644

G-2 Poles - (Modelled at 0.5644 X seals)

24" gap (0.5644 x seals)
Length = 26" (8 x gap)

Top holder

air gap



ULTRAPRECISE MAGNET DESIGN AND SHIMMING*

G.T. Danby and J.W. Jackson
 AGS Department, Brookhaven National Laboratory,
 Upton, Long Island, New York 11973

Abstract

Computer studies of pole design and magnet shimming techniques are discussed for a very precise 14.72 GeV iron core storage ring magnet to be used for the proposed measurement of the muon anomalous magnetic moment. The experiment requires knowledge of the field in the 7m radius storage ring dipole to approximately 0.1 ppm (1×10^{-7}). The goal is to produce field uniformity of approximately 1 ppm. Practical and mathematical limitations prevent obtaining such accuracy directly with a computer code such as POISSON, which is used in this study. However, this precision can be obtained for perturbations of the magnetic field. Results are presented on the internal consistency of the computations and on the reliability of computing perturbations produced by Fe shims. Shimming techniques for very precise field modification and control are presented.

I. Introduction

This report, limited in its scope to computer studies by the authors, discusses a part of the ongoing design effort for an ultraprecise 3 GeV/c storage ring. The g-2 experiment proposal¹ has been approved as part of the future physics program at the high intensity, post-Booster, Alternating Gradient Synchrotron (AGS). An international collaboration is involved in detailed design of the storage ring and detection apparatus.

The computer studies are of general interest because of the precision required. Most accelerator magnets perform at a $\Delta B/B_0 > 1 \times 10^{-4}$ field uniformity, for which the computer codes--in this instance POISSON² can, if carefully used, reliably predict the field within the beam aperture. For example, the AGS Booster dipoles agreed with computations to $\Delta B/B \sim 1 \times 10^{-4}$ over the "good field" aperture. High field superconducting magnets designed by the authors had similar agreement.

The experiment and the storage ring design are solidly based on a highly successful CERN design.³ The third of a series of muon g-2 experiments, it resulted in a knowledge of the magnetic field integral appropriately averaged over the muon orbits to $\Delta B/B_0 = 1$ to 2×10^{-6} . This, plus other smaller systematic errors were less than the statistical uncertainty of 7 PPM obtained in the experiment. The result stands as the state of the art.

Operation at 5×10^{13} protons in the AGS using the Booster, should permit a statistical uncertainty of 0.3 PPM in the new experiment, assuming the same pion decay injection technique as at CERN. Other injection possibilities might further reduce this error. To carry out this very fundamental measurement, it is desirable that systematic errors be < 0.1 PPM. These are dominated by magnetic field uncertainty, which involves the error in knowledge of the magnetic field, averaged over space and time in relation to the muon distribution. Figure 1 taken from the 1986 update⁴ of the proposal shows the general layout of the experiment. Figures 2 and 3 show the magnet cross section.

The improvements in precision anticipated for the new experiment come from several areas.
 (i) The gap increase from 14 to 18 cm allows more elaborate field monitoring and feedback. For CERN the

- principal error³ was control of each of the 40 magnet sections by correction coils. These used feedback from a single point NMR measurement in each section. With extra space much more elaborate control can be used.
- (ii) A "trolley" capable of moving around the circumference inside the beam aperture carrying a matrix of NMR probes is being constructed. This can be "parked" out of the way without breaking vacuum. This "on-line" albeit intermittently, coexistence of complete mapping and physics running is a new feature.
- (iii) The "end effects" of the CERN 40 magnet blocks, although continuous at the pole, contributed significant field and measurement errors between blocks. The new ring will be constructed with 45° sectors machined to be close fitting at their ends to approximate a continuous ring.
- (iv) More elaborate use of field shimming by adjustment to the iron cross section remote from the pole faces is planned. A large air gap between the poles and the return yoke will be used as part of this strategy.
- (v) Superconducting coils improve B_0 stability and reduce the need for magnet cycling. (Power saving.)

The goal of the computer simulations has been to develop techniques to control the dipole field and lower order multipoles so that $\Delta B/B_0 < 1 \times 10^{-5}$ over the necessary "good field" 9 cm diameter can be relatively easily obtained. The error would be reduced to $< 1 \times 10^{-6}$ by special local static shimming or active current control such as pole face windings. The final factor of 10 to $\Delta B/B_0 < 1 \times 10^{-7}$ would come from measurements, i.e., knowledge of the field adequate to compute the orbits over the muon distribution.

The calculations have already produced a good precision pole profile, although not final. An experimental program will model the polar region in exact scale. Specialty steels will be tested, the impact of inclusions or voids, and grinding or polishing to increase pole surface planarity.

SOURCE	COMMENTS	FRONTS (ppm)
MAGNETIC FIELD	Includes absolute calibration of the poles and averaging over space, time, and muon distribution.	0.07
ELECTRIC FIELD CORRECTION	0.7 ppm correction	0.05
PITCH CORRECTION	0.8 ppm correction	0.02
PARTICLE LASSES		0.08
TRIMMING POLES		0.02
	TOTAL	0.09

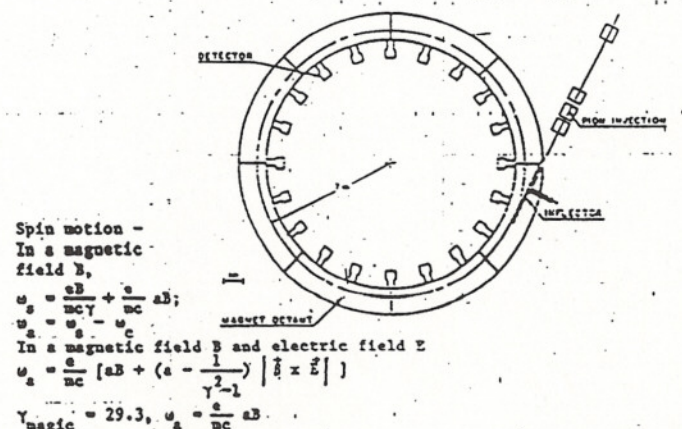


Fig. 1. AGS Muon g-2 Experiment.

* Work performed under the auspices of the U.S. Dept. of Energy.

II. Design Optimization

During 1986 the computer calculations were used to reduce the cross section and weight of the magnet to 2/3 that in the Proposal.¹ The use of 1 cm "air" gaps between each pole and return yoke facilitated this, since the flux return reluctance is significantly decoupled from the behavior of the poles. (Table I.)

TABLE I: Multipole Change with Air Gap and Weight Reduction. $B_0 = 14.7$ kG

	I Base* (W=65cm)	II W=55cm	III W=55cm +4 corners off	IV W=55cm +10 cm off
ANI/NI(base)	0	+2.16%	+2.40%	+4.30%
$\Delta B_n/B_0$ (Normalized)				
n=1 (quad)	0	-1.3 PPM	-2.6PPM	-2.6PPM
2 (sext)	0	-.6	-.5	-.7
3	0	-.1	-.1	-.1
4	0	0	0	0
5	0	0	0	0
6	0	0	0	0
7	0	0	0	0
8	0	0	0	0

Col. I: the 1985 Proposal Magnet Cross Section, with 1 cm air gap behind each pole.

Col. II: for a 10 cm (18%) reduction in width of the return yoke block, centered on the horizontal midplane.

Col. III: also cut four corners off magnet.

Col. IV: also reduced thickness of top and bottom yoke member by 10 cm. (This increased reluctance by ~2%.)

In all cases in this Report, multipoles are expressed at $R = 4.5$ cm, $y = 0$; $B_0 = 14.7$ kG.

The result of very large weight (and cost) reduction is an appreciable increase in reluctance and ampere-turns requirement, but no significant change in multipole field errors. The magnetic and dimensional tolerances of the yoke flux return are not unusually tight and are relevant mainly to the dipolar term. For example, scaling from Col. II, a 0.65mm change in width of the HMP block would produce dipolar change of 1.4×10^{-4} : equivalent to a 25 μ m change in the 18cm gap.

Consider the effect of raising the central field by 1% in two cases, the geometry of Col. I and of the Col. IV in Table I. This result is shown in Table II.

TABLE II: Change for B_0 increased by 1% to 14.847 kG.

	I (Base, 1985) 1% + 0.16%	II (light weight) 1% + 0.58%
ANI/NI (base)		
$\Delta B_n/B_0$ (4.5 cm)		
n = 1 (quad)	-14.2 PPM	-14.7 PPM
n = 2 (sext)	-6.6	-6.8
n = 3	-.2	-0.2
n = 4	-.3	-0.3
n = 5	0	0
n = 6	0	0
n = 7	0	0
n = 8	0	0

Note the effect on the multipoles of raising B_0 by 1% is almost independent of the very large changes in yoke geometry. The quadrupole is due to C-magnet yoke asymmetry. The 1% higher field reduces the permeability in the vicinity of the air gaps. The reduced permeability in the poles also affects the sextupole. Table II can also be used to establish tolerances on magnetization properties in the pole steel. A 1% change in saturation magnetization would produce roughly the change in Table II. The storage ring central field will always operate at 14.72 kG.

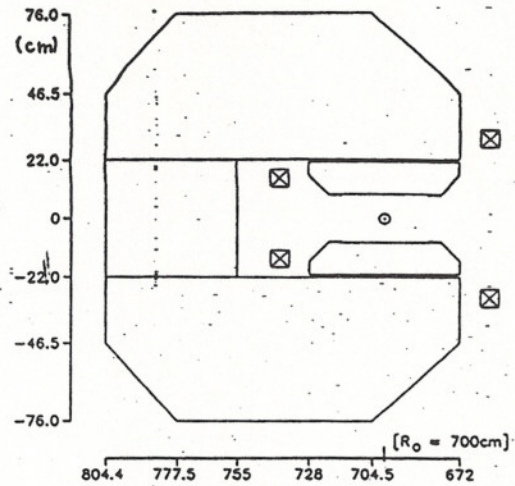


Fig. 2. Magnet cross section.

The C-magnet return produces a very large systematic gradient. Three perturbations have been explored: (i) tilt the pole faces, (ii) larger bumps on the inside pole edges than on the outside, (iii) shim in the air gap at the rear of the poles to induce more flux on the inside. While (i) and (ii) are possible for refined shimming, they are too local to the "good field" aperture and generate significant octupole. Method (iii) can give a large almost pure quadrupole so the magnet can start off with the systematic C-magnet gradient removed. See Table III.

TABLE III. Perturbing Air Gap Behind Pole to Remove Quadrupole.

$\Delta B_n/B_0$ (4.5 cm)	I "Standard" Case	II Pole gap Slope ± 0.40 cm	III Effect of "wedge" gap
n=1(quad)	-204.6 PPM	+ 3.4 PPM	+208 PPM
n=2(sext)	- 38.9	-32.8	+ 6.1
3	+ 1.7	- 1.1	- 2.8
4	- 0.2	- 0.5	- 0.3
5	+ 0.2	+ 0.2	0
6	- 1.3	- 1.3	0
7	- 0.2	- 0.2	0
8	- 0.2	- 0.2	0

Col. I: standard case (see Fig. 2) 1 cm air gap.
Col. II: base of pole wedged so that air gap varies from 1.4 cm at $R = +28$ cm to 0.6 cm at $R = -28$ cm. This effect can be accomplished also by moving the center of gravity of shims in the parallel air gap.
Col. III is the difference between II and I.

Note the almost pure quadrupole, with only 1% octupole contribution. Because of the very large radial asymmetry being corrected, a small sextupole change occurs in the baseline gradient sextupole magnet.

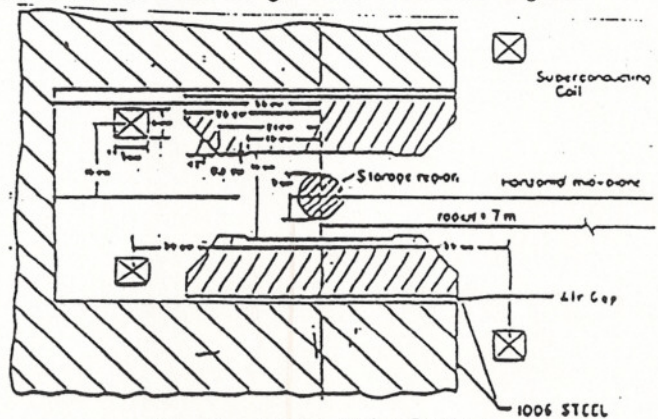


Fig. 3. Magnet Polar Region.

The effect of the coil motion is shown in Table IV.

TABLE IV: Coil Position Tolerance

	Multipole (4.5 cm)	Outer Coil Up 1 mm.	Outer Coil Inward 1 mm.
0	Dipole	- 24.1 PPM	+ 7.56 PPM
1	Quadrupole	+ 0.60	+ 0.38
2	Sextupole	- 0.09	- 0.12
3	Octupole	+ 0.02	+ 0.04
4	Decapole	- 0.01	- 0.02

Notes:

- Outer coils are located at R=739 cm, y=±15 cm (Fig. 2 and Fig. 3.)
- Inner coil not tabulated but sensitivity less.
- All multipole terms < 1 PPM, except for dipole.

III. Shimming Perturbations

The approach of the g-2 design is to produce pole surfaces as flat as economically practical by machining plus possibly grinding or polishing the surface of sections to minimize "hill and dale" errors. Very homogeneous material will be used to minimize "pot holes."

For reference, consider simplified 0.001" (25 μm) errors in the gap and the parallelism of the pole surfaces: (i) a .001" systematic gap error gives 141 PPM dipole change, (ii) a .001" side-to-side tilt gives a quadruple of 11 PPM at R = 4.5 cm, (iii) a .001 symmetric variation: the gap at the center .001" different than at the pole edges, gives ~ 3.6 PPM sextupole. These illustrate the incentive to make the dipole ΔB/B very small around the azimuth by shimming the reluctance or possibly by current loops remote from the pole surfaces. The present state of the design is shown in Col. II of Table III. A slight change to the metric pole profile will remove the 33 PPM sextupole. Touchup of radial asymmetry can take care of drupole and octupole in the computed magnet. The perturbation studies at this sensitivity illustrate techniques for optimization: the magnet as first constructed will have larger errors.

Next to the pole faces themselves, the most sensitive perturbations are the bumps on the edges of the pole fences. In the present design these are 0.5 cm thick and 6 cm wide, starting at R = ± 15 cm. Their tolerances and their utility for perturbations are shown in Table V.

TABLE V. Perturbation of Bumps on Pole Face Edges.

B _n /B ₀ (4.5)cm	I	II	III	IV
	Add .02 cm to inner bumps	Add .02 cm to outer bumps	Predicted Sum	Computed Sum
n=1(quad)	+18.0	+18.4	- 0.4	+ 0.7
2(sext)	+14.9	+15.1	+30.0	+30.1
3(oct)	+ 7.9	- 7.7	+ 0.2	+ 0.1
4	+ 2.9	- 2.9	5.8	5.8
5	+ 0.8	+ 0.8	0	0
	+ 0.2	+ 0.2	+ 0.4	+ 0.4

In Col. I and II, the field has been computed for the thickness of the two bumps increased at the inner and outer radius respectively. Col. III is the analytic sum of I and II. Col. IV is the computed sum.

Note that Col. IV shows symmetric perturbation and gives only symmetric terms. The ratio of 10 pole to sextupole is 20%. This bump perturbation should be used in combination with more remote perturbation to suppress both sextupole and (n=4) 10 pole simultaneously. Col. I and II show that if equal and opposite sign changes (I-II) were made on the inside and outside radius, the sextupole would not change, only quadrupole and other odd terms. This is a good way to reduce octupole, with residual gradient done by other means.

DO NOT TYPE BELOW THIS LINE

Table V permits estimating .001" (25 μm) rms bumps height errors: 2 PPM sextupole and 2 PPM quadrupole occur, with everything else smaller. Skew moments (not computed) will be comparable. Three tests are used for the internal consistency of the computations. The magnetic fields as computed and the magnetic multipole fit agree in the 9 cm "good field" region to 1 PPM (See Fig. 4.) Next, a change in the geometry of an iron portion of the magnet is made and the difference in the multipole content computed. The amplitude of this change is varied. A linear relationship for the multipole content of the change is observed for reasonable perturbations lending itself to extrapolation. Finally the computed field is tested based on symmetries. An iron bump is added to one of the four corners of the poles and the change computed. By symmetry, the multipoles resulting from this perturbation will also be produced by similar bumps in the other 3 quadrants, with predictable phase changes. This permits prediction of any combination of up to 4 bumps. The computations confirm the prediction for modest size perturbations. Note this process involves generation of the mesh for each geometry, iterative calculation of the field everywhere in the iron and air, and generation of the field multipoles.

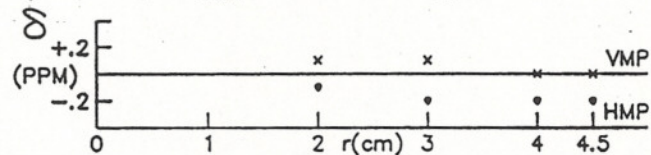


Fig. 4. Difference δ =Field-Multipole Reconstruction.

The computations need only be credible to perform perturbations at the PPM level, i.e. to predict the necessary correction for the residual error measured in the magnet. The magnet will have both cylindrically symmetric and azimuthally varying field errors due to geometrical factors, magnetic forces, magnetization in iron, temperature control, etc. (Note that 1 PPM=0.18 μm gap tolerance.) Careful operating control plus shimming perturbations can correct anything except the most local pole surface defects. A fundamental limit is the temporal stability and reproducibility of the magnet. Active feedback must be used beyond this limit. Dynamic and possibly also static corrections will be made with current loops applied in sections, possibly 1 meter long. Such coil corrections are analytically straightforward to compute, but should be small at least on pole surfaces. In addition to taking space and generating heat coils have "lumpy" current distributions which generate higher multipole errors as they correct. This will impact on the final < 0.1 PPM knowledge of the field.

References

- AGS Proposal. A new Precision Measurement of the Muon g-2 Value at the Level of 0.35 PPM. V.W. Hughes et al. September 1985.
- R. Holsinger (LANL), private communication, 1976.
- Final Report of the CERN Muon Storage Ring. J. Bailey et al. Nuclear Physics B150 (1979) 1-75.
- AGS Proposal 821, September 15, 1986 (Same title).